UNIVERSITEIT
STELLENBOSCH
UNIVERSITY

The mid-crustal architecture of a continental arc - a transect through the South Central Zone of the Pan-African Damara Belt, Namibia

by

Christoffel Jasper Anthonissen

Thesis presented in partial fulfilment of the requirements for the degree of

Master of Science

at the University of Stellenbosch
2009

Supervised by Prof. Alex Kisters

Co-supervised by Prof. Gary Stevens

trending fabric can be interpreted to be a S_2 regional foliation. S_2 shows moderate to steeply dips (45°-75°) towards the SE (Fig 4.2.6).

In the area between the main Mon Repos diorite exposure and the AMC inlier, DSG rocks lie exposed as a shallow dipping sheet (of mostly Karibib Formation marble) with a shallow foliation in these recrystallized rocks.

The Habis granite

The "Habis granite" is typically strongly gneissose and contains a number of overprinting structural fabrics (Fig 4.2.7 & Fig 4.2.8).

1. An early magmatic fabric is defined by the alignment of large (2-5cm), mostly euhedral K-feldspar (Fig 4.2.7.A).
2. The dominant fabric in this granite is a solid-state foliation that overprints the magmatic fabrics. The solid-state fabric is defined by the alignment of matrix minerals, mainly biotite and quartz ribbons that wrap around the feldspar megacrysts. K-feldpar-phenocrysts are often marginally recrystallized and flattened in the foliation plane, resulting in augen textures. This foliation is steep to subvertical and sub-parallel with the contact of the enveloping of the DSG, being consistently parallel to $S_0/S_1/S_2$ in the supracrustals sequence (Fig 4.2.7 & Fig 4.2.8).
3. Additional shear bands can occasionally be seen cross-cutting the main foliation, resulting in crenulations of the dominant solid state fabric.

The fabric intensity increases towards the margins of the granite, resulting in a mylonitic solid state fabric at the DSG/Habis contact. Proto-mylonitic textures occur over a width of at least 100-300 meters parallel to the contact between the pluton and the DSG. Thin, 10-20cm wide ultramylonites occur parallel to and spaced between the protomylonitic foliation (Fig 4.2.8).

A consistently sinistral shear sense (in plan view) is indicated by S-C fabrics in the biotite-quartz matrix and recrystallized feldspar phenocrysts forming a stair-stepping geometry and the development of sigma-clasts (Fig 4.2.7). On surface outcrop a lineation could not be observed.

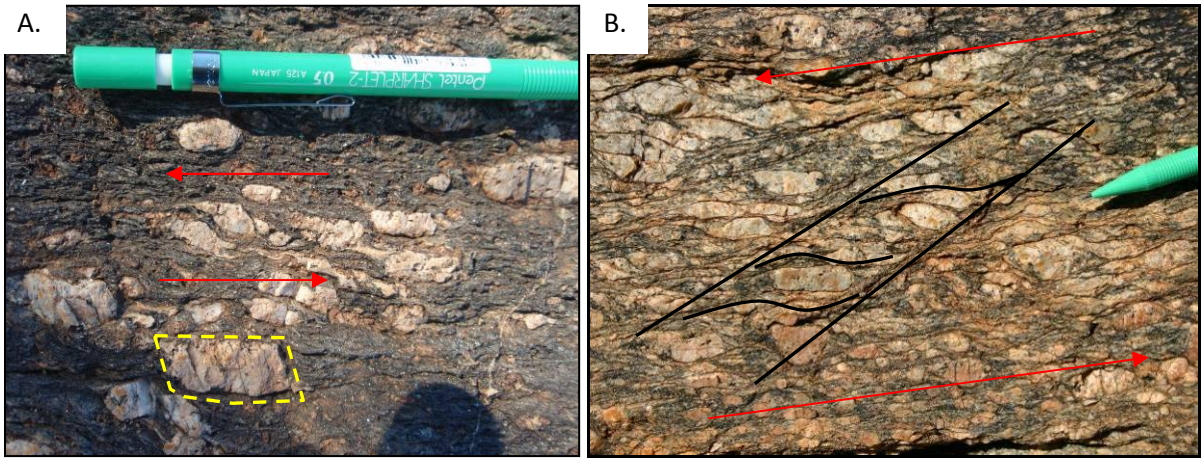

Fig 4.2.7: Mylonitic and proto-mylonitic fabrics developed within the Habis granite suite. A Mylonitic fabric is developed along the southern contact with the overlying DSG at 22°5'31.5"S; 15°49'34.2"E. **(A)** Commonly euhedral K-feldspars (annotated by yellow dashed line) are aligned parallel to a strong solid-state fabric, where the marginal recrystallization of feldspars into sigma-clasts indicate a sinistral displacement (red arrows). **B.)** A proto-mylonitic section of Habis granite shows this foliation expressed in the alignment of large feldspar phenocrysts.

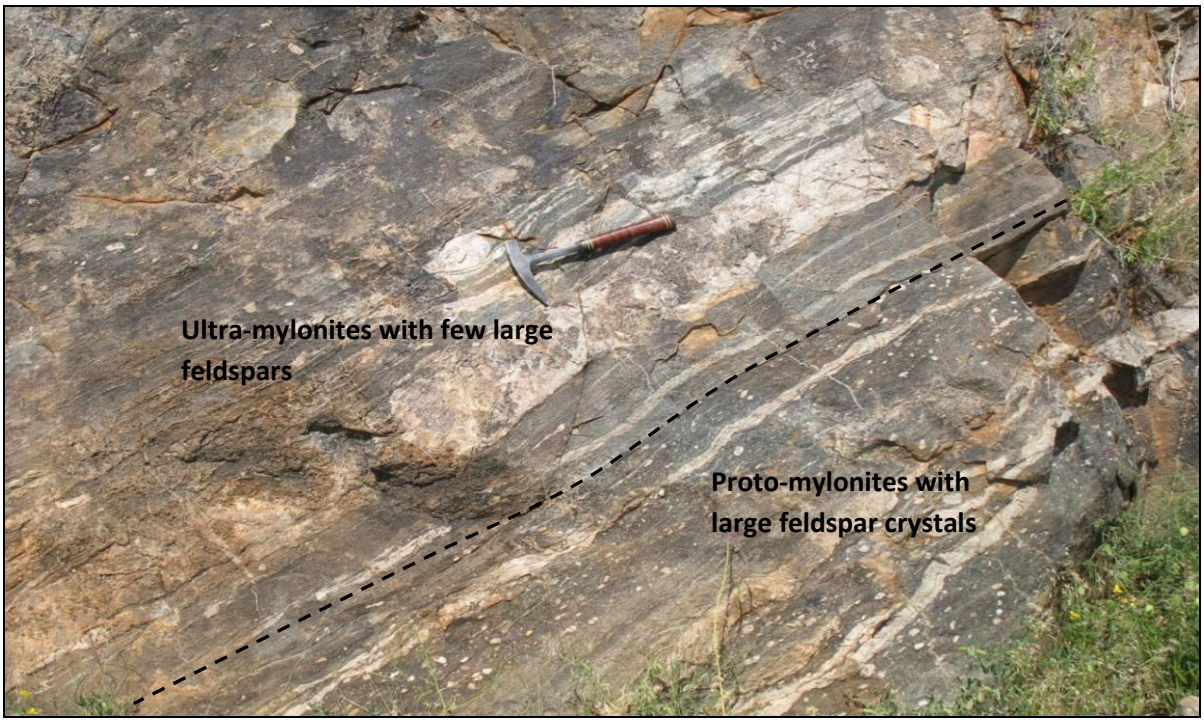

Fig 4.2.8: Layering in the Habis granite is made evident by (a) compositional layering between biotite-rich and leucocratic bands and (b) alternating, layer-parallel bands of of protomylonites and ultra-mylonites. This photo was taken at 22°5'28"S; 15°48'52"E, ca. 260m from the contact with the DSG

Retrogression of the biotite-rich granite is common towards the marginal zones of the granite (primarily its southern margin), where shear bands and cataclasites are defined by chlorite and small-scale breccias (Fig 4.2.7.B). The retrograde mylonites and cataclasites also show a sinistral sense of apparent displacement.

Towards its western margin, the Habis granite has a gradational contact with rocks of the AMC, characterized by a decrease in phenocrysts and an increase in mica in the Habis granite across the contact into biotite-muscovite schists of the AMC (22° 4'50.14"S; 15°49'4.45"E). No intrusive relationship can be identified as most of this contact is overlain by surficial cover. The contact between the Habis granite and the overlying rocks of the DSG is sharp with foliations in the DSG and Habis granite being sub-parallel to each other (Fig 4.2.9). Although the contact between the DSG and the Habis granite might have originally have been a intrusive one, the lack of any alteration along the sharp contact as wel the mylonite textures in the granite suggests that this is a tectonic contact.

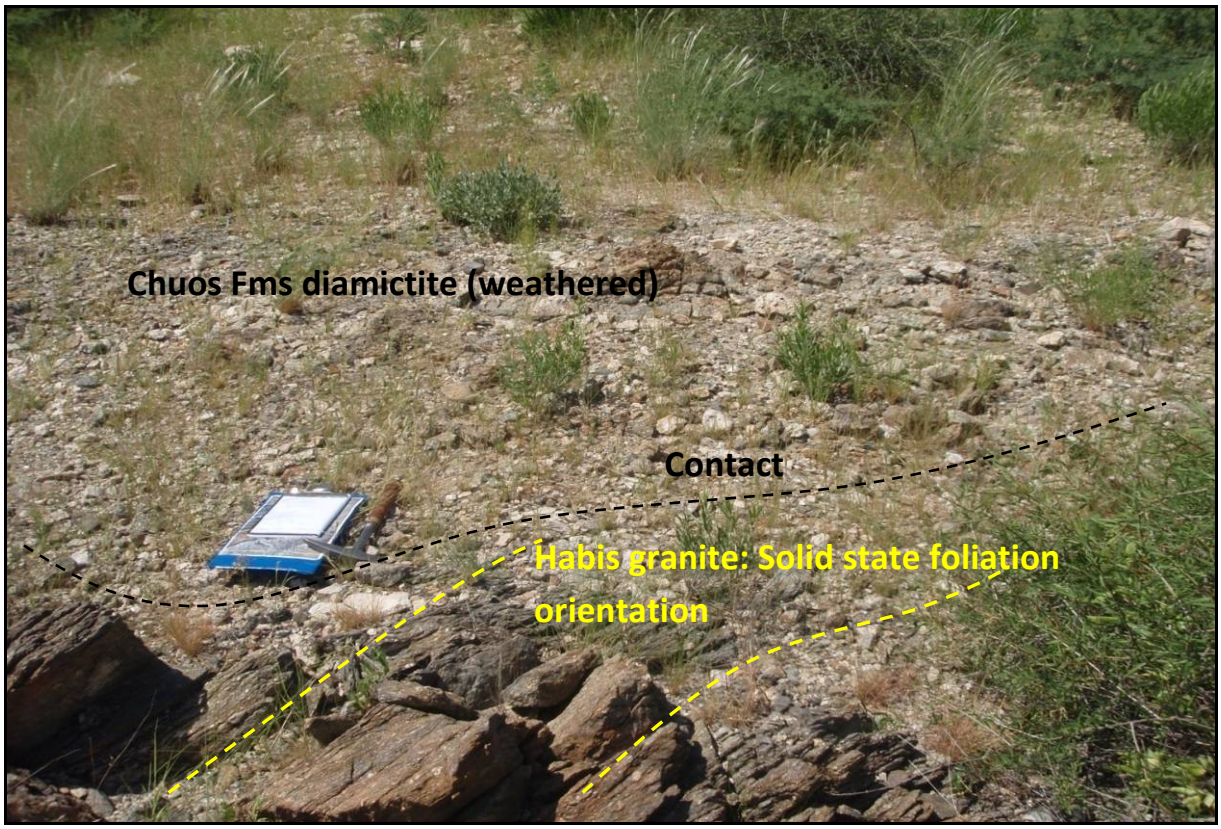

Fig 4.2.9: The sharp contact between the Habis granite and the overlying rocks of the Chuos Formation diamictite. Looking SSE at 22° 5'28.77"S; 22° 5'28.77"S. The contact between the Habis granite is nowhere well exposed and is often weathered. The strong foliation within the Habis granite suite is consistently sub-parallel to the contact with overlying formations.

The solid-state foliation within the Habis granite has a consistent SE dip, but it is important to note that most outcrop is found along the SSE limb of the large 2nd order fold (Fig 4.2.6, sub-domain C). Here the foliation shows predominantly SE dips (average 122/60), parallel to the regional S_2 foliation in the DSG (Fig 4.2.6 & Fig 4.2.10). Protomylonites and mylonites in this area show a consistent sinistral sense of apparent displacement (Fig 4.2.7). Elsewhere in the Habis granite, the solid-state

foliation is sub-parallel to the contact with the overlying DSG, also turning around the core of a 2nd-order fold (Fig 4.2.1). No obvious linear fabrics were developed in the granite.

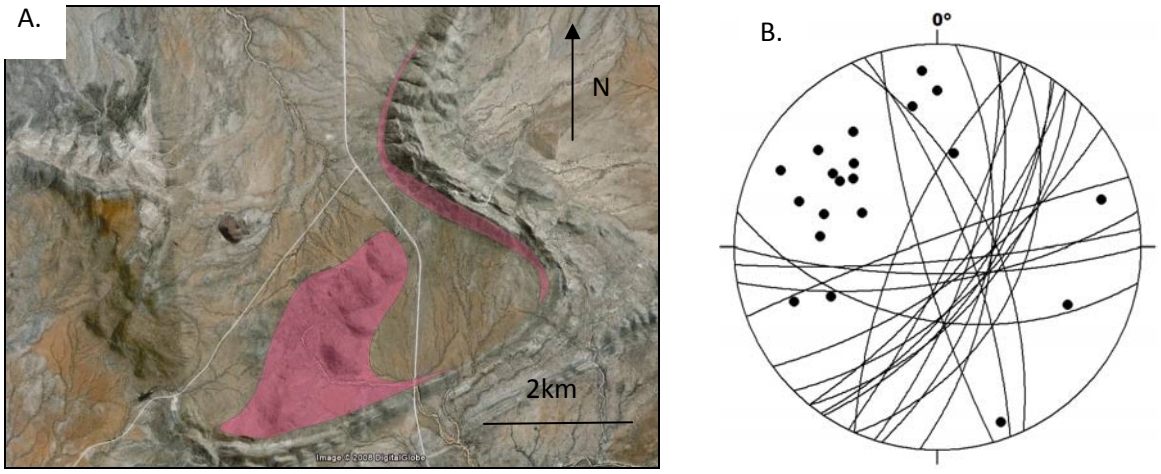

Fig 4.2.10: A.) The Habis granite shows the best outcrop in the S of the Etusis mapping domain, where it is exposed as large pavements and boulders. Most measurements of the Habis' foliation are from this area. **B.)** Great circles and poles to foliations of the solid-state fabric in the Habis granite, showing predominantly SE dips. The spread of dips indicates contact-parallel dips of the foliation from subdomains A and B (see Fig 4.2.6) along the eastern contact of the granite. The aerial photoraph taken from Google earth.

The Mon Repos diorite

The Mon Repos diorite lies directly N and NW of the DSG, AMC and Habis granite suite in this domain. The apparently sharp, though not very well exposed, contact between the AMC and the Mon Repos diorite is directly overlain by white recrystallized marbles of the Karibib Formation.

An isolated erosional klippe in the centre of the AMC/Habis granite inlier (at 22°03'54"S; 15°48'37"E) exposes an up to 40 m thick sheet of Mon Repos diorite sandwiched between AMC basement in the footwall (of shear zone) and white-re-crystallized marbles of the Karibib Formation in the hangingwall (Fig 4.2.5). This klippe exposes a much thicker wedge of marble than those found as slivers between the DSG and the AMC near the Habib mountain (Fig 4.2.5). The diorites crop out over an area of about 700m in diameter, topped by a small outcrop (70 m in diameter) of marbles. A very similar relationship between underlying diorite and overlying marble units is exposed some 4km to the N on the farm Mon Repos (at 22°01'55"S; 15°48'49"E). Here, a prominent, E-W trending ridge is made up of marbles in the top 25m, surrounded and underlain by rocks of the Mon Repos granodiorite (Fig 4.2.2 - Marble hill). This suggests that the diorite represents a thin (40-50 m), but laterally extensive sheet between the Karibib Formation marbles and the AMC. The Mon Repos diorite N of the basement at its type locality has a very pronounced solid- state foliation defined by the preferred orientation of biotite and horneblende within the rock matrix (Fig 4.2.11.A). This fabric is consistently dipping to the SE at an average of approximately 143/70 (Fig 4.2.11.B).

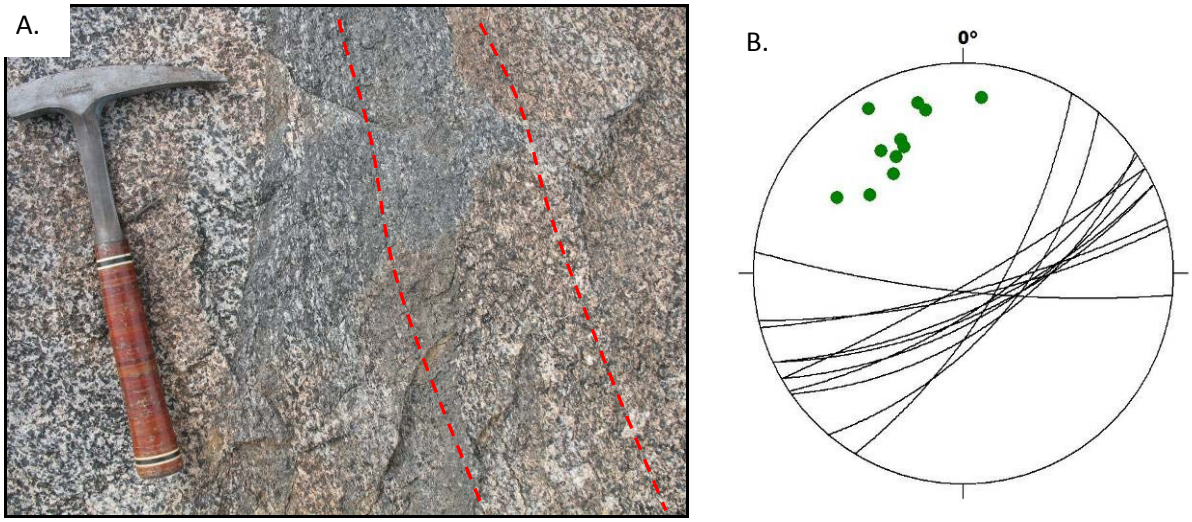

Fig 4.2.11: The Mon Repos diorite suite. **A.)** A well developed foliation (Red dashed lines) is often visible in the diorites and granodiorites of the Mon Repos suite. This is defined by the prefered orientation of hornblende crystals in the matrix. **B.)** This foliation dips consistently steeply towards the SE at ~143/70.

Folding and minor faulting

In its E parts, the Etusis domain is dominated by a large NNE verging overturned 2nd order antiformal fold. The fold structure is mainly defined by rocks of the Karibib Formation and cored, in the W, by rocks of the Habis granite (Fig 4.2.12.A).

The fold has a NNE vergence, indicated by the steep to overturned nature of the northern limb, where Habis granite overlies rocks of the Karibib Formation. The fold geometry varies from E to W and along the axial trace. The fold half-wavelength is ca. 6km in the far W, where the granites form the core of the fold, decreasing to 2km in the E in rocks of the Karibib Formation. This fold plunges ca. 105/50 (Fig 4.2.12.B).

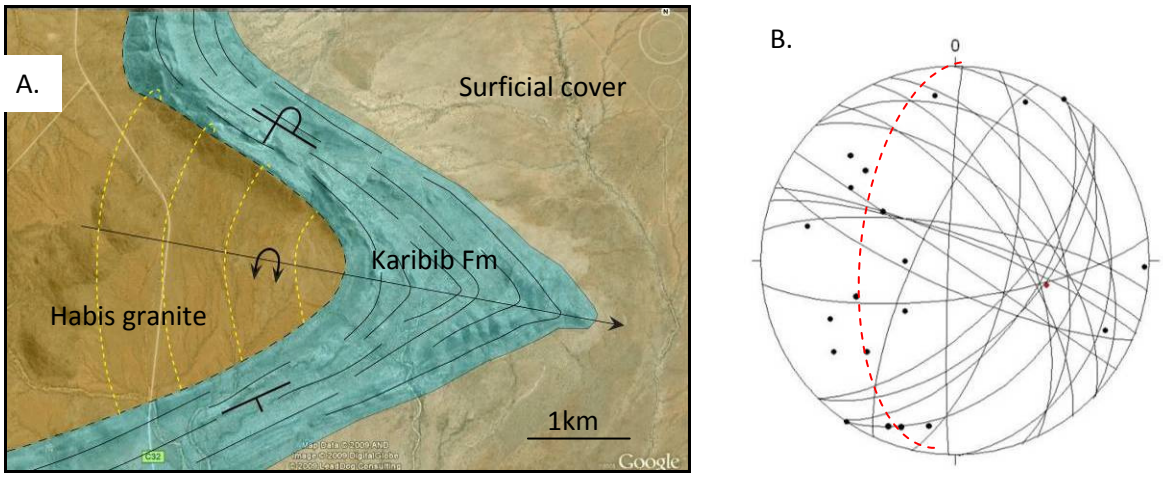

Fig 4.2.12: A.) Large antiform plunging 105/50, poles and great circles on stereonet **(B.)** indicates the orientation of bedding around the fold hinge. The NE limb of the fold is steeply overturned, with central Habis granite overlying marbles of the Karibib Formation on the NNE limb of the fold.

A second regional-scale fold structure exists at 22°3'50.70"S; 15°48'0.39"E. This fold is a N trending open synform that only exists for some 500m's before flattening out into sub-horizontal bedding exposed in the Habib mountains along the N strike of the axial trace. This syncline is cored by the Karibib Formation and underlain by Ghaub Formation and AMC gneisses. This fold has a half-wavelength of approximately 300m (Fig 4.2.13).

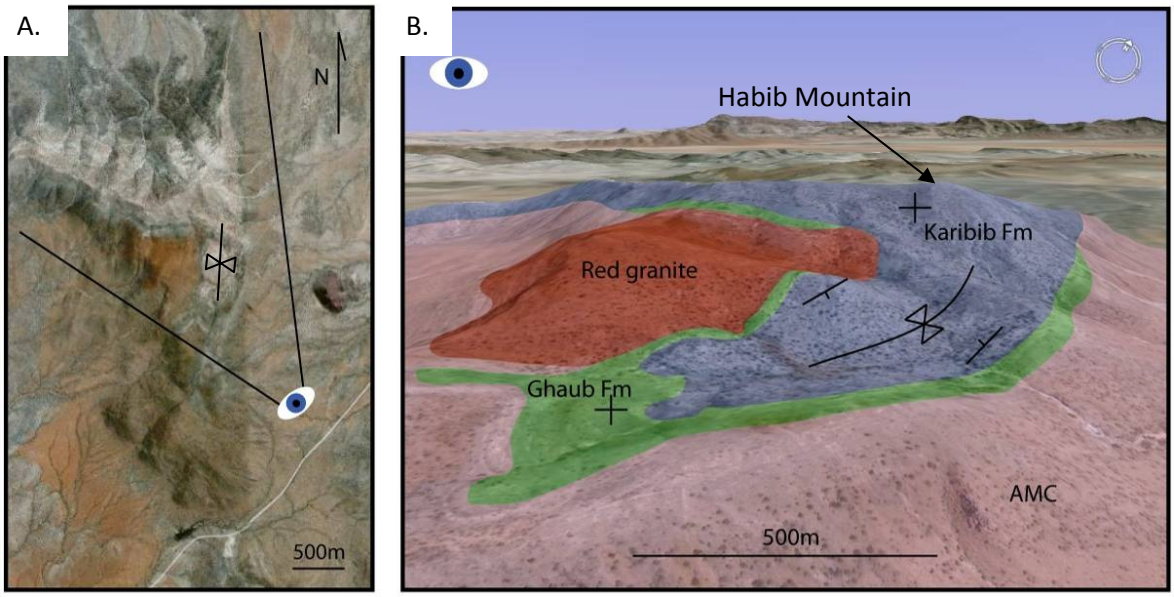

Fig 4.2.13: An 2nd order synform with a N trending axial plane. This fold has a subhorizontal hinge and is only developed for about ~500m (it opens and flattens towards the N and S). **Figure A** gives an indication of the location of the fold and the location of the viewpoint for image **(B.). B.)** The fold is cored by marbles of the Karibib Formation (blue) and underlain by calc-silicate felses of Ghaub Formation (green) and schist and gneisses of the AMC (pink).

The only other fold structures preserved are 3rd and 4th order folds developed on a m- to cm- scale in the DSG. Their rather sporadic occurrence does not allow for any conclusive structural analysis of these folds Fold plunges for the few measured folds range between 230-330/40-60.

A number of S-N trending, km-scale faults exist in this domain (Fig 4.2.1) and can be identified where lithologies have been offset form each other. The most notable of these faults occurs where the Ghaub Formation is at its thickest (22°5'47.4"S; 15°48'24.3"), about 5 km S of the Habib mountain (Fig 4.2.2). This fault is associated with fine-grained red granites that have been intruded between basement rocks and Karibib Formation marbles (Fig 4.2.1).

Faults are 3-4 km in length and cross cut all earlier ductile and penetrative fabrics and formations, suggesting a later formation than the main Damaran structures indicating a much younger deformational event (Fig.4.2.1).

Summary

Fabric and strain intensities in the Etusis domain are highest along the southern contact between the central Habis granite/AMC with the overlying DSG. The basal marble units of the Karibib Formation display strong fabric intensities, indicated by the pervasive recrystallization of the marbles and obliteration of primary sedimentary features and compositional variations. Mylonites in the Habis granite along the marble-granite contact are common. Magmatic and solid state fabrics within the Habis granite suite and the DSG are sub-parallel to each other and to the contact between these two units. A S_1 foliation is seen following the limbs of a central overturned fold and a S_2 foliation is found to dip towards the SE and/or the NW. In contrast, the wedge-shaped formations of the DSG below the Karibib Formation in the W parts of the Etusis mapping domain largely retain primary textures, showing markedly lower-strain intensities along the basement-cover contact. Rocks of the AMC show mainly angular fabric relationships with the overlying DSG, indicating the preservation of original unconformable contacts.

Diorites of the Mon Repos diorite suite are intermittently developed as subhorizontal sheets several tens of meters thick, between rocks of the AMC and overlain by marbles of the Karibib Formation. The lack of intrusive contacts with the overlying, commonly highly re-crystallized marbles and the strained nature of Habis granite imply shearing along this relatively shallow contact and the emplacement of the diorites as shallowly dipping sheets along this sheared basement-cover contact.

4.3 Dorneb domain

Domain description

The Dorneb mapping domain (Fig 4.3.1, Fig 4.3.2, Appendix II) is underlain by Salem-type granites covering an area of about 85km² in the central parts of this domain. The Salem-type granites are bound in the NW and SE by mainly biotite schists of the Kuiseb Formation. The SW and NE margins of the granites are bounded by rocks of the Gamikaub and Okongava diorite intrusions (Goas diorite suite), respectively (Fig 4.3.1 & Fig 4.3.2). Where exposed the contact between the Salem-type granites and the diorites is sharp.

A swarm of younger, mainly WNW trending pegmatite dykes were intruded into the northern and central parts of the granites (Fig 4.3.1).

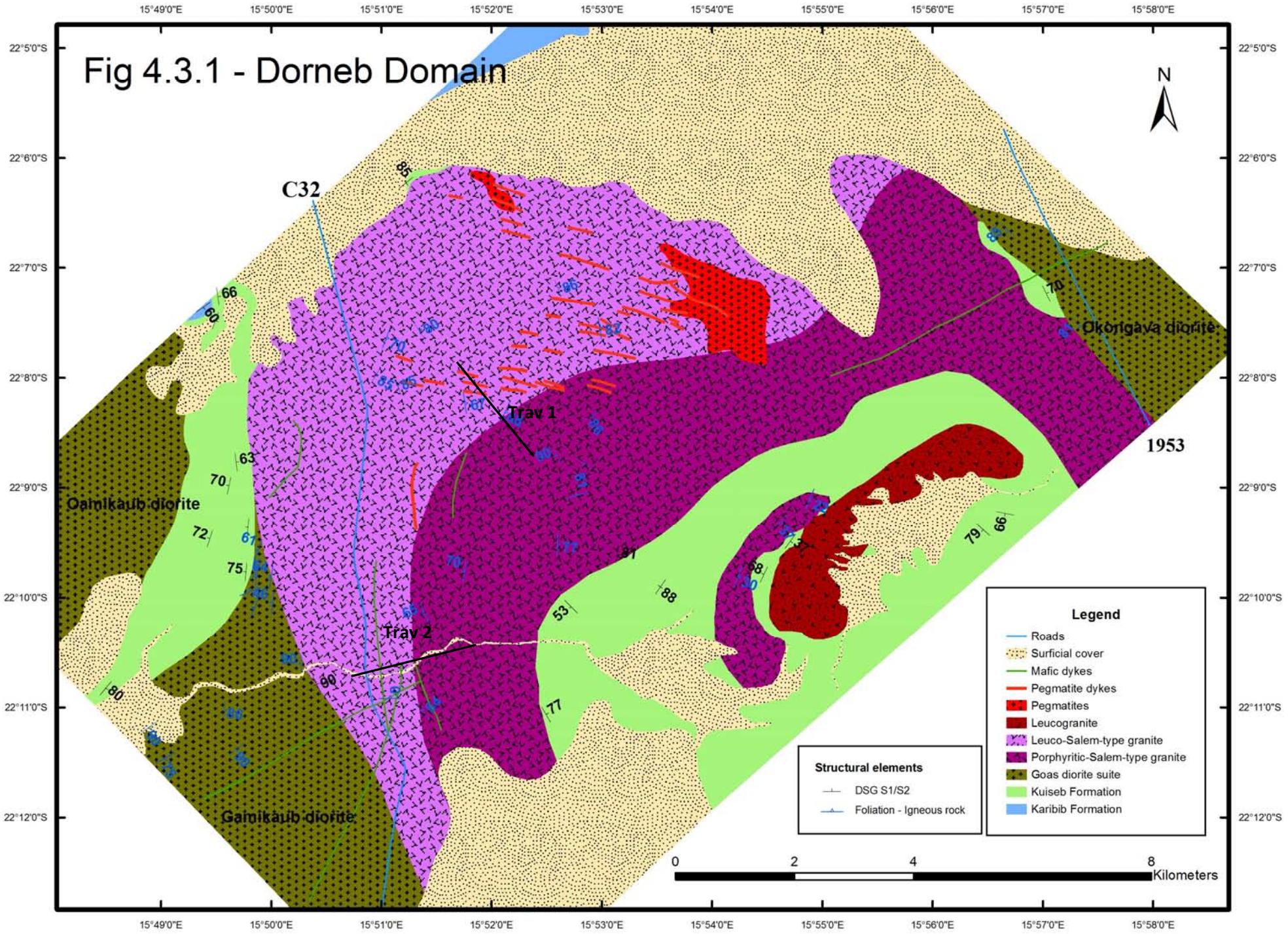

For a detailed version of this map, see Appendix II

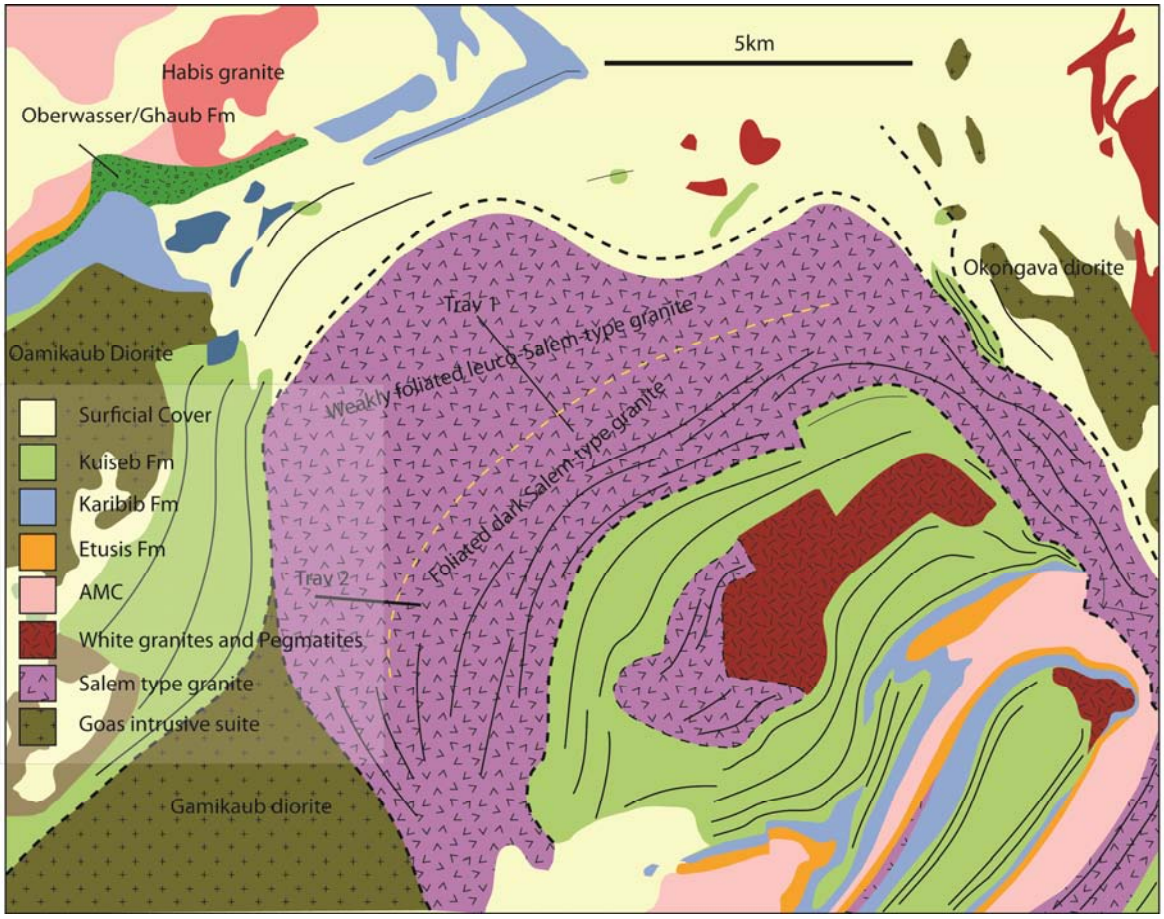

Fig 4.3.2: Simplified map of the Dorneb domain. The central feature of this mapping domain is the massive Salem-type granite intrusion. Form lines have been are indicated where a clear foliation exists. For clarity faults and mafic intrusions have been omitted. Intrusions of the Goas dioritic suite are named according to Miller, (2008). This map was modified after Smith, (1966).

The Salem-type granites

The large, central Salem-type granite plain consists of two distinct granite phases. The aerially most prominent phases are (1) leucocratic granites and (2) more melanocratic, biotite-hornblende-rich K-feldspar megacrystic granites (chapter 3.4). From N to S of this platform, there is a gradual compositional transition from leucocratic granite (at 22° 7'31.55"S; 15°52'31.43"E) to the darker megacrystic Salem-type granite (at 22° 9'0.42"S; 15°52'43.68"E) (Fig 4.3.3). A W to E traverse across the granites, however, exposes sharp sub-horizontal contacts between the leucocratic granite and the darker megacrystic variety. Good exposures of this contact occur at 22°10'36.12"S; 15°51'57.28"E, showing leucocratic granites underlying the darker Salem-type granites (Fig 4.3.3 & Fig 4.3.4). The same relationship is exposed in many of the low-lying hills showing structurally lower leucogranites capped by the darker megacrystic granite (Fig 4.3.4).

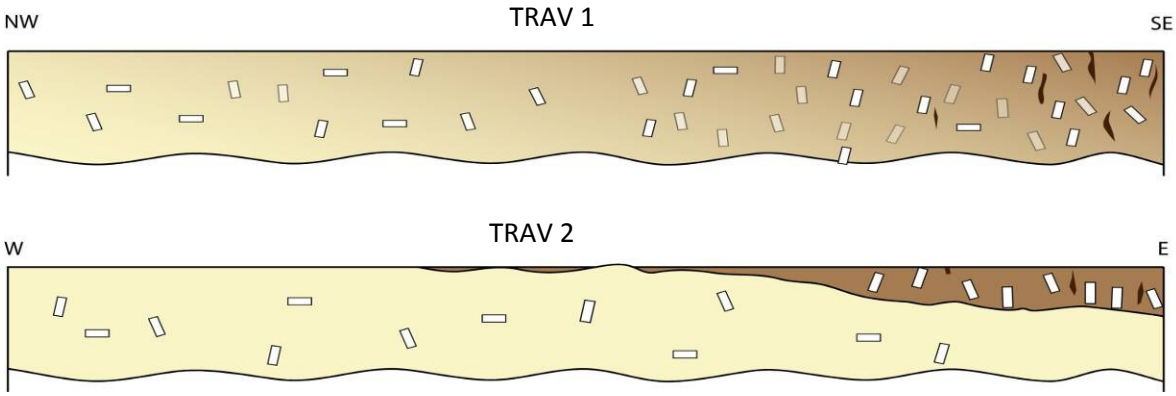

Fig 4.3.3: **Trav1** provides a schematic overview of the gradual transition form leucogranite to biotite-hornblende granite from NW to SE. **Trav2,** however, shows much sharper contacts and a distinctly darker granite variety shallowly overlie the leucogranite. The location of these 2 traverses is indicated on Fig 4.3.2.

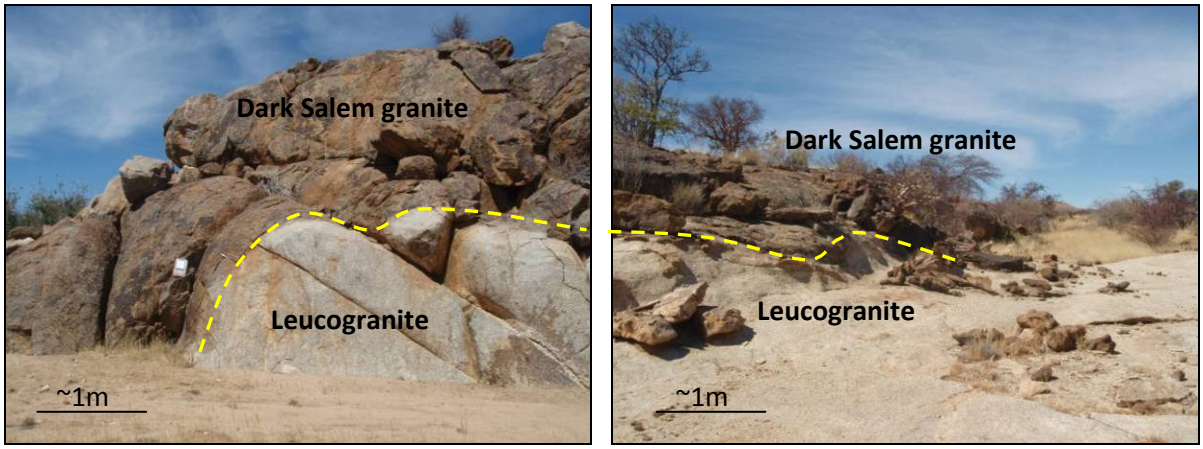

Fig 4.3.4: Outcrops of the dark biotite-hornblende-granite can be seen overlying the leucocratic granite. The shallow dip of the contact is shown in the right hand photo, where large granite exposures are capped by the darker variety. Both photos were taken at the transition/contact zone between these two granite varieties at co-ordinates, 22°10'36.12"S; 15°51'57.28"E.

The leucocratic Salem-type granites show distinct variations in fabric intensity. Leucogranites show, in general, weaker fabrics compared to the megacrystic varieties. A very weak planar fabric, defined by the alignment of large, euhedral K-feldspar phenocrysts is discernable in many of the granite platforms. The preferred orientation of euhedral magmatic phenocrysts, in the absence of any dynamic recrystallization features, suggests that this is a weak magmatic fabric (Fig 4.3.5). This foliation shows subvertical dips, but a rather random orientation throughout the leucogranites in plan view (Fig 4.3.8.B).

Fabrics are far more prominent in the darker megcrystic hornblende-biotite granites. Here, a solid- state foliation is defined by the preferred orientation of biotite parallel to the magmatic foliation defined by the alignment of K-feldspar phenocryst (Fig 4.3.6). The fabric is most pronounced parallel to the margins of the dark megacrystic granites and within several hundred meters of the contact zone with rocks of the Kuiseb Formation. This fabric becomes weaker and is progressively lost as rocks grade into the structurally lower leucogranites.

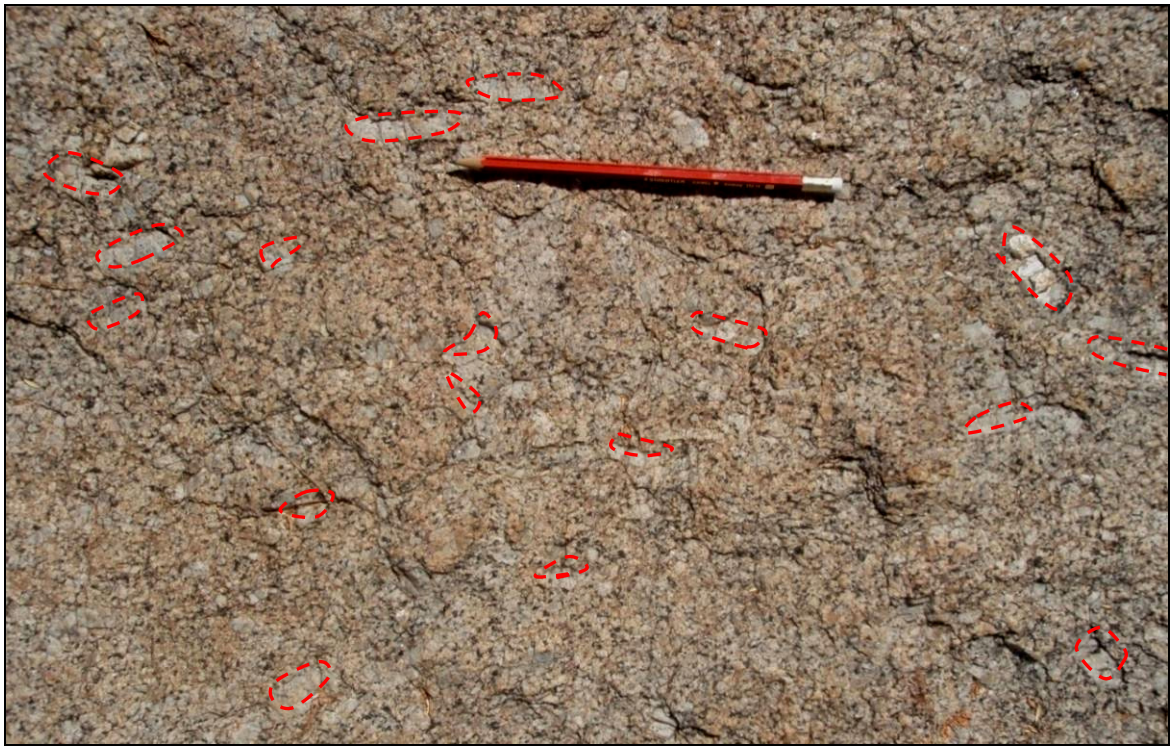

Fig 4.3.5: The leucogranitic variety of the Salem granite suite shows a weaker fabric than that found in the biotite-hornblende rich granite variety. Here a very weak magmatic fabric is defined by the alignment of K-feldspar phenocrysts. This photo was taken at 22°08'28"S; 15°50'34"E looking down in plan view with the top towards the W.

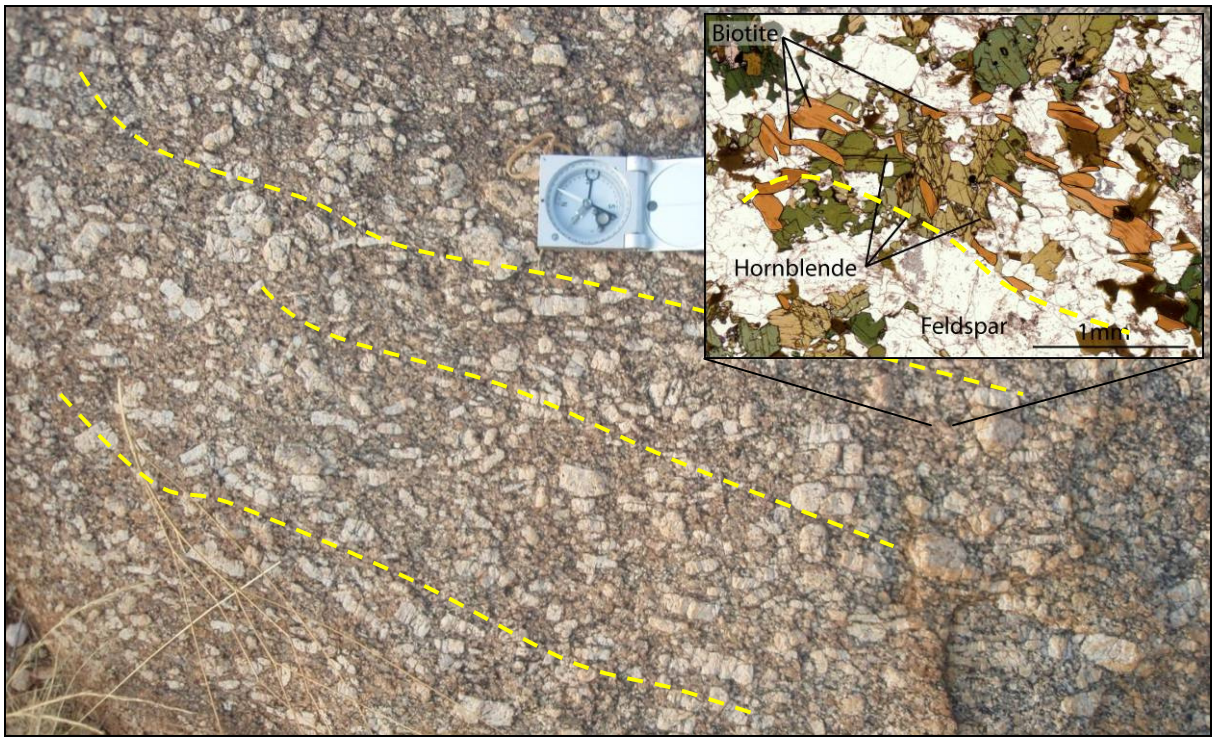

Fig 4.3.6: A typical dark hornblende-biotite Salem-type granite showing the alignment of K-feldspar phenocrysts in a dark biotite-hornblend rich matrix. Yellow lines show fabric orientation, trending in this case, at ca. 015°. Photo was taken in plan view at 22°8'09"S; 15°57'16"E. In thin-section a magmatic foliation is defined by the partial alignment of biotite in the rock matrix. The foliation is easier to observe in hand sample then in thin-section.

Intrusive contact relationships of Salem-type granites

The leucocratic Salem-type granite is in contact with schists of the Kuiseb Formation along its NW margin. This contact is locally discordant and is exposed on the farm Etusis (22°8'11" S; 15°49'43"E). Here the leucogranites have a sharp contact with Kuiseb schists, the latter showing no apparent strain or thermal aureole. Granite apophyses and veinlets protruding from the pluton into the schist units are, however, commonly folded, suggesting an, at least, late-tectonic (D2) timing of emplacement (Fig 4.3.7). On a regional scale the granite/schist contact is semi-concordant to the foliation in the schist of the Kuiseb Formation. Although the granite does not show a regionally consistent foliation, a S_1 foliation in the Kuiseb Formation curves around the margin of the Salem granite batholith and trends between 170° and 050° (Fig 4.3.2).

The SE contact of the dark megacrystic Salem-type granites with the Kuiseb Formation schists is largely concordant and developed as an up to 1.2 km wide lit-par-lit type intrusion zone in which the biotite schists of the Kuiseb Formation are intruded by bedding and foliation (S_1) parallel granite lenses and sills ranging from several 10's of m to a few cm's in width.

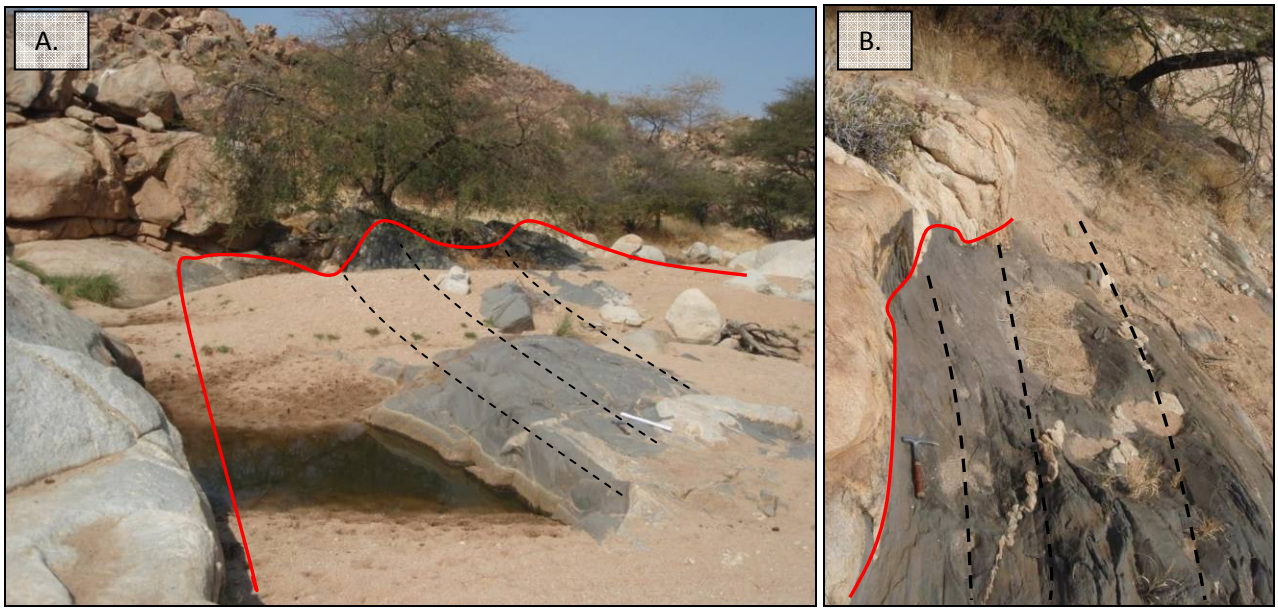

Fig 4.3.7: Intrusion of the Salem leucogranite into the schist of the Kuiseb Formations at the NW contact of the Salem-type granite intrusion. Locally, this intrusive contact (red line) is discordant with the granite cross-cutting the foliation (dashed lines) in the Kuiseb schist. B.) A number of small granite veinlets are folded indicating late-tectonic emplacement. Photos were taken at 22°8'11" S; 15°49'43"E.

The granite contact is sub-vertical, showing dips of between 60° and 90°. This steep contact zone assumes progressively shallower dips towards the SE, where the domain is increasingly dominated by schist of the Kuiseb Formation, with dips of 130/40 at the SE border of the mapping domain. A foliation (most likely S_1) in homogeneous schist NW and SE of the central Salem granite platform

curves in a U-shape around the contacts, dipping moderately to steeply to the SSE in the middle of this mapping domain (Fig 4.3.2 & Fig 4.3.8).

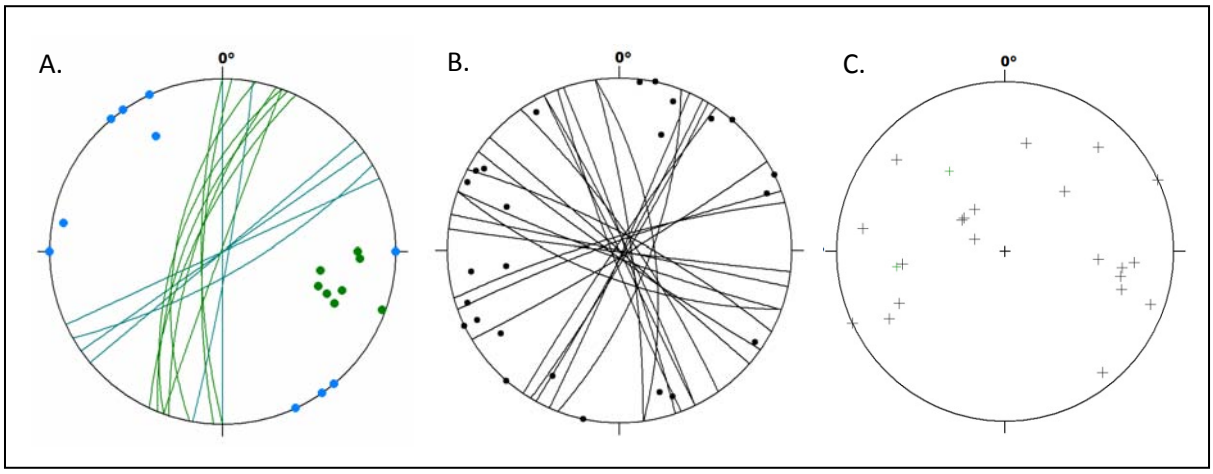

Fig 4.3.8: Foliations in the **Gamikaub diorite (A.)**, **Central Salem-type granites (B.)**and **Kuiseb schist in and around the Salem-type granites (C.)**. **A.)** The Gamikaub diorite shows a steep N-S trending foliation (green grade circles and their poles) in the wedge between the Salem-type granites (to the E) and the Kuiseb Formation (to the W). A upright NE trending folaition is developed in the middle of this pluton (light blue grade circles and it's poles). **B.)** Leucogranitic Salem-type granites in the NW and central part of this mapping domain show no consistent trend, but what is generally a weak magmatic fabric is consistently upright. **C.)** The foliation within schist (indicated by black poles to the foliation) in and around the margin of the porphyritic Salem-type granite. This foliation is moderately SE dipping in the middle of the mapping domain and wraps around the pluton and the Audawib fold complex.

Towards the centre of the mapping domain, the amount of megacrystic granite gradually increases. Here xenoliths of schist only occur as small fragments within the granite. The foliation and long axis of wall-rock xenoliths are aligned parallel to a magmatic fabric and, in fact, define the magmatic fabric together with the preferred orientation of K-feldspar megacrysts (Fig 4.3.9)**.** Large xenoliths of the Kuiseb Formation (up to 10 m in width) occur as much as 1km from the main lit-par-lit contact zone. Significantly, xenoliths of the Kuiseb Formation are only found within the dark biotite-hornblende Salem-type granite, whereas leucogranites are devoid of country-rock xenoliths (Fig 4.3.9).

Schists of the Kuiseb Formation SE of the central Salem-type granite body have, in many places been intruded by a very homogenous, fine-grained, quartz-K-Feldspar leucogranite, that is compositionally and texturally distinct from the Salem granite suite (chapter 3.4). These leucogranites are devoid of any structural fabrics and are quite common throughout the field area and particularly near the contact zones between the Salem-type granites and the Kuiseb Formation, representing somewhat of a marginal contact phase being intrusive into the Kuiseb Formation. A large hill (5.5km²) consisting almost entirely of this type of granite lies in the middle of the schists SE of the Salem-type granite (Fig 4.3.1 & Fig 4.3.2).

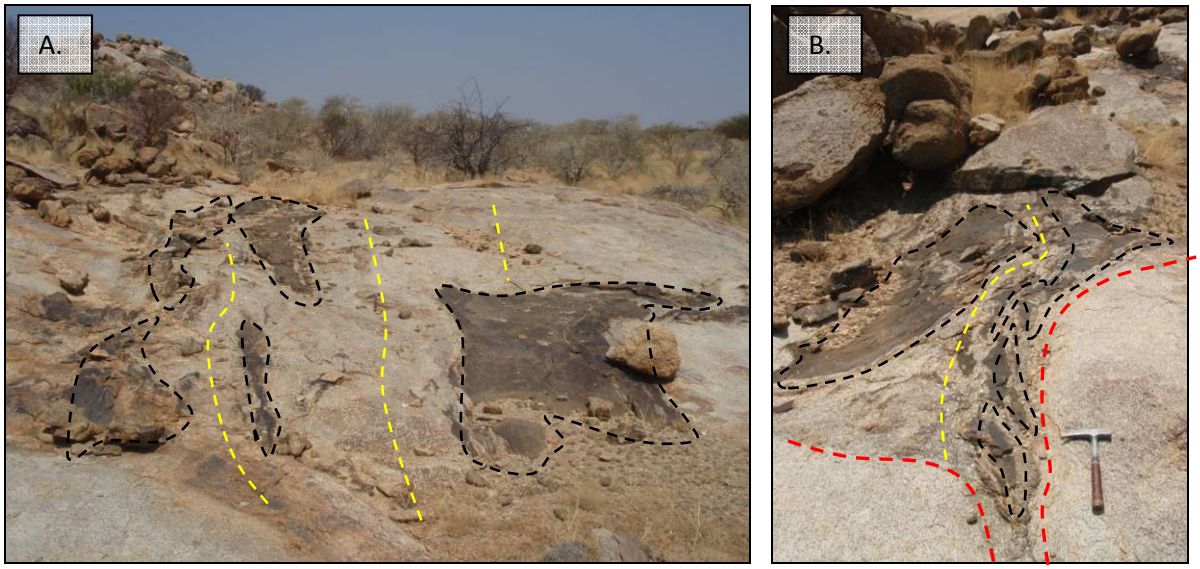

Fig 4.3.9: Elongate xenoliths of schist of the Kuiseb Formation (dark brown) within Salem-type granite are aligned to form an upright foliation with the granite. A.) A number of schist blocks (dark, annotated) are lined up in the lit-par-lit contact zone. B.) Schist xenoliths (black dashed lines) are found within hornblende-biotite rich Salem-type granite (inside the red dashed line) isolated within a much more leucocratic granite phase. Yellow dashed lines indicate the foliation orientation within darker megacrystic Salem-type granites, these are parallel to the long axis of schist xenoliths. These photos were taken at the contact zone between Salem-type granite and Kuiseb Formation schists at 22° 9'42.24"S; 15°51'46.94"E.

The Salem-type granite and the diorite contacts are sharp where exposed, but mainly covered by alluvium and calcrete. An exposure of the contact between the Salem-type granite and the Gamikaub diorite (at 22°10'43"S; 15°50'14"E) and aerial photography indicate an overall sharp, NNW trending contact. Where the Gamikaub diorite pinches out between the Kuiseb Formation in the W and the Salem-type granites in the E (NE) the Gamikaub diorite has a foliation sub-parallel to that diorite/schist contact. This foliation becomes ever weaker towards the centre of the Gamikaub pluton becoming upright and NE trending (Fig 4.3.8.A). This contact can be traced for approximately 9 km along strike. The contact between the Okangava diorite and the Salem-type granite is not well exposed, but aerial photography suggest that this contact too is sharp, and NNW trending. A large schist xenoliths is wedged in this contact at 22°07'14"S; 15°56'14"E, the orientation of this xenoliths also suggests the contact trends 340°.

Folding, faulting and pegmatite intrusion

The lower parts of the Kuiseb Formation are exposed along the NW and SE margin of the Dorneb domain, bordering against central Salem-type granites and the lower formations of the Swakop Group (Karibib Formation) NW and SE of the Dorneb domain. The preservation of the Kuiseb Formation in this area, i.e. the uppermost formation of the DSG, suggests that the Dorneb domain is underlain by a large (10 km halfwavelength) 1st order syncline cored by the Kuiseb Formation and intruded in its central trough by the Salem-type granites.

The only observable and mappable folds are a minor, cm to dm scale 3rd or 4th order folds with no clear consistent orientation. The lack of marker horizons in schist and a bad weathering profile make larger folds impossible to observe.

Low relief and the lack of marker lithologies in the Dorneb mapping domain also complicates any identification of faults. A single NW trending fault could be identified by the offset of a large schist unit by about 20 m in the fine-grained leucogranites. This fault is at least about 100 m in length, but much of it is overlain by surficial cover. This feature cross cuts all geologic formations and post-dates granite intrusion.

Summary

The Dorneb domain is underlain by a areally extensive Salem-type granites that are intruded into schist of the Kuiseb Formation and emplaced between the Gamikaub and Okangava diorites towards their SW and NE margins respectively. Intrusive relationships suggest that the earlier intrusive phase of dark, hornblende-biotite-rich Salem granite was intruded syntectonically as sills into a steep foliation in the Kuiseb Formation SE of the main granite pluton. The curved nature of the schist foliation against the Salem type granite suggest that this is an earlier (possibly S_1) refolded foliation. Weakly foliated leucocratic Salem-type granites towards the NW of the domain intruded into both schist and darker foliated horneblende-biotite-rich Salem-type granite. Salem-type leucogranites were intruded later then the darker variety and the cross cutting nature of this granite into schist as well as a lack of strong fabrics suggest a late- to post-tectonic intrusion. This mapping domain is cored by schists and Salem-type granites bound in the NW and SE by lower formations of the DSG in a overall 1st order synform.

4.4 Audawib Domain

Domain description

Metasedimentary rocks of the DSG and pink gneisses of the AMC are exposed on the farm Audawib centred around the Kuduberg (Fig 4.4.1 & Fig 4.4.2), forming a NE-SW trending structure, ca. 18 km in length and 5 km in width. The main structure, the Audawib fold complex consists of a succession of doubly-plunging synforms and antiforms. Rocks of the DSG are well exposed and allow for a relatively unambiguous lithostratigraphic correlation. The rocks of the AMC are particularly well exposed on the topographically high-lying areas of e.g. the Kuduberg (Fig 4.4.2) where the gneisses are structurally underlain by rocks of the DSG. The Audawib fold complex is surrounded by Salem-type granites to the NE, NW and SE (Fig 4.4.1)

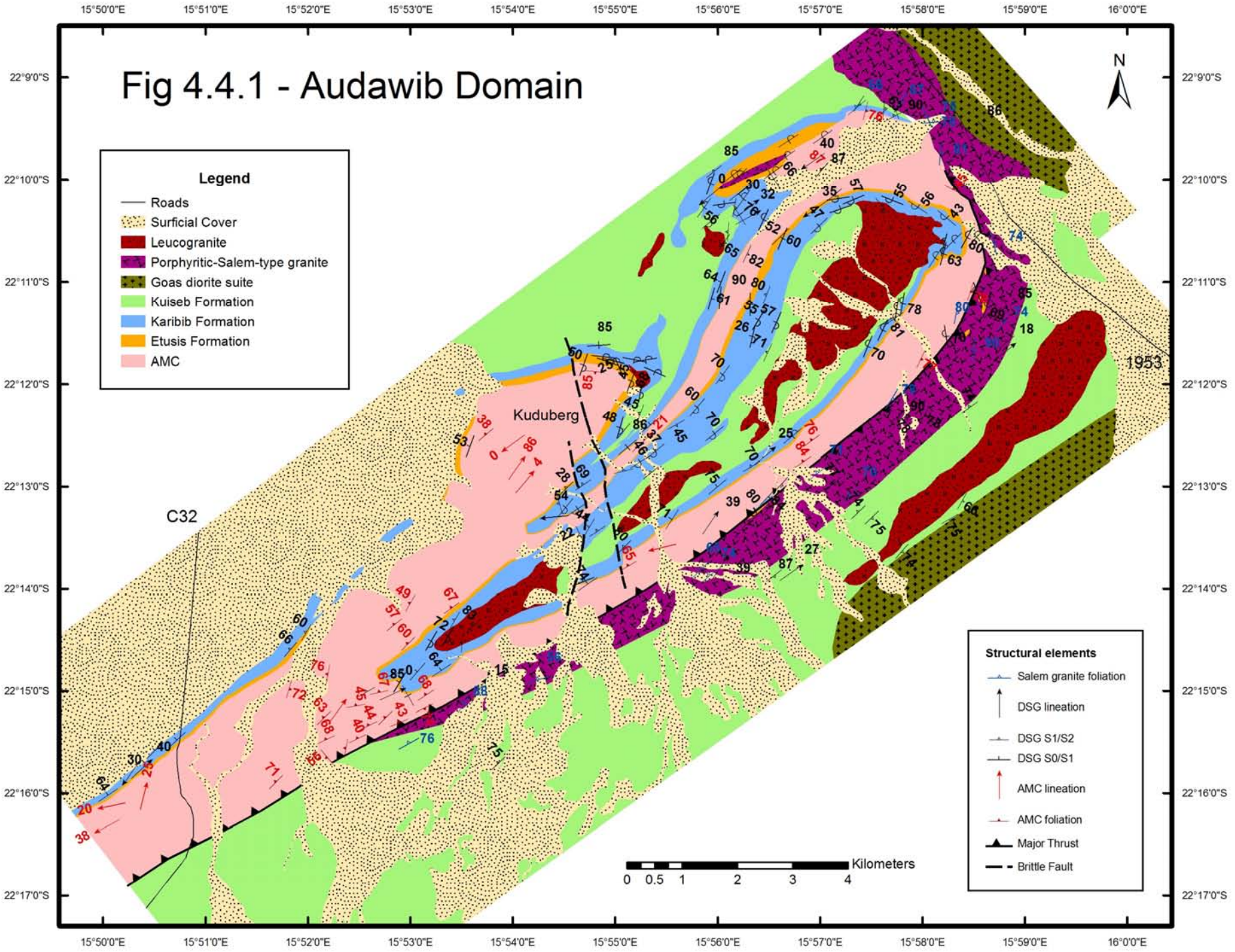

For a detailed version of this map see Appendix III

Structural fabrics

A pervasive S_1/S_2 planar fabric is developed in rocks of the DSG (Fig 4.4.2 & Fig 4.4.4), rocks of the structurally overlying AMC (Fig 4.4.2 & Fig 4.4.3) and the surrounding Salem-type granite platform (Fig 4.4.2 & Fig 4.4.5). A magmatic foliation in the Salem-type granite is defined by the preferred alignment of K-feldspar megacrysts. While the Salem-type granites do not show any obvious linear fabrics, mineral lineations (L_2m) are, in places, developed in the rocks of the DSG. Crenulations and mineral lineation (L_2m/L_2c) are both common in the AMC (Fig. 4.4.3).

Planar fabrics in all rocks trend mainly NE-SW, parallel to the strike of the Audawib fold complex. A clear distinction between S_1 and S_2 is only possible in the hinges of folds, where the two foliations are developed at high angles. The S_1 foliation is refolded by the folds, whereas the S_2 is axial planar to folds (F2). For the most part, however, S_1 and S_2 are parallel to each other, particularly along the NE trending limbs of the Audawib fold complex. The S_2 foliation dips, on average, 321/75 in the SW parts of the Audawib fold complex and 141/74 in the NE part of the domain. This foliation is developed throughout rocks of the AMC, the DSG and the Salem-type granites (Fig 4.4.2).

Stratigraphic inversion

The most notable feature of this domain is that all lithologies appear overturned in the Audawib fold complex. This inverted stratigraphic succession is developed across the entire fold complex. Rocks of the AMC are structurally the highest unit, forming the topographic high of the Kuduberg. The mainly pink feldspathic gneisses are successively underlain by rocks of the Etusis, Karibib and Kuiseb Formations (Fig 4.4.6 & Fig 4.4.7). This is the case in all folds of the combined Audawib fold complex, so that anticlines show synformal geometries (Fig 4.4.7) and synclines antiformal geometries (Fig 4.4.6).

Thus the AMC is the uppermost member and the Kuiseb Formation is the lowermost unit (Fig 4.4.6 & Fig.4.4.7), this inversion is present even where fold shapes are open indicating that the stratigraphic inversion is not merely the result of a locally overturned limb of e.g. a verging fold, but that the entire stratigraphy is inverted.

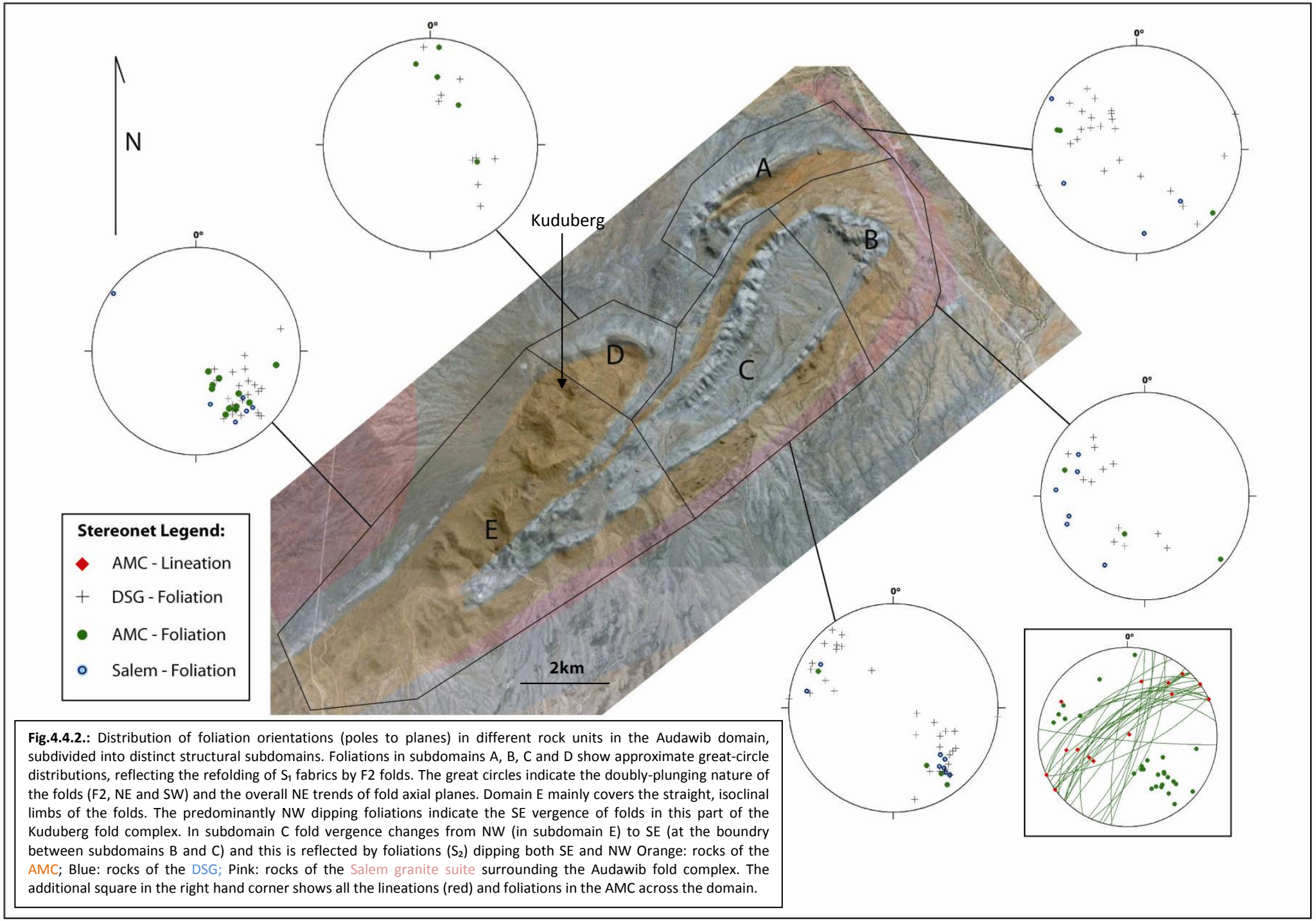

Fig.4.4.2.: Distribution of foliation orientations (poles to planes) in different rock units in the Audawib domain, subdivided into distinct structural subdomains. Foliations in subdomains A, B, C and D show approximate great-circle distributions, reflecting the refolding of S_1 fabrics by F2 folds. The great circles indicate the doubly-plunging nature of the folds (F2, NE and SW) and the overall NE trends of fold axial planes. Domain E mainly covers the straight, isoclinal limbs of the folds. The predominantly NW dipping foliations indicate the SE vergence of folds in this part of the Kuduberg fold complex. In subdomain C fold vergence changes from NW (in subdomain E) to SE (at the boundry between subdomains B and C) and this is reflected by foliations (S_2) dipping both SE and NW Orange: rocks of the AMC; Blue: rocks of the DSG; Pink: rocks of the Salem granite suite surrounding the Audawib fold complex. The additional square in the right hand corner shows all the lineations (red) and foliations in the AMC across the domain.

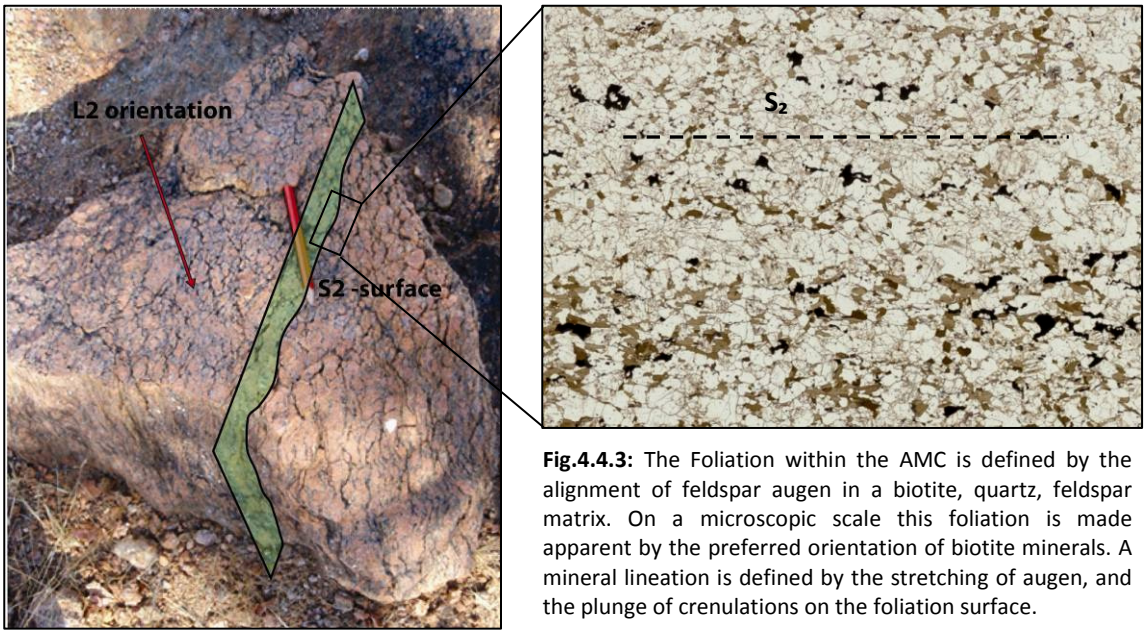

Fig.4.4.3: The Foliation within the AMC is defined by the alignment of feldspar augen in a biotite, quartz, feldspar matrix. On a microscopic scale this foliation is made apparent by the preferred orientation of biotite minerals. A mineral lineation is defined by the stretching of augen, and the plunge of crenulations on the foliation surface.

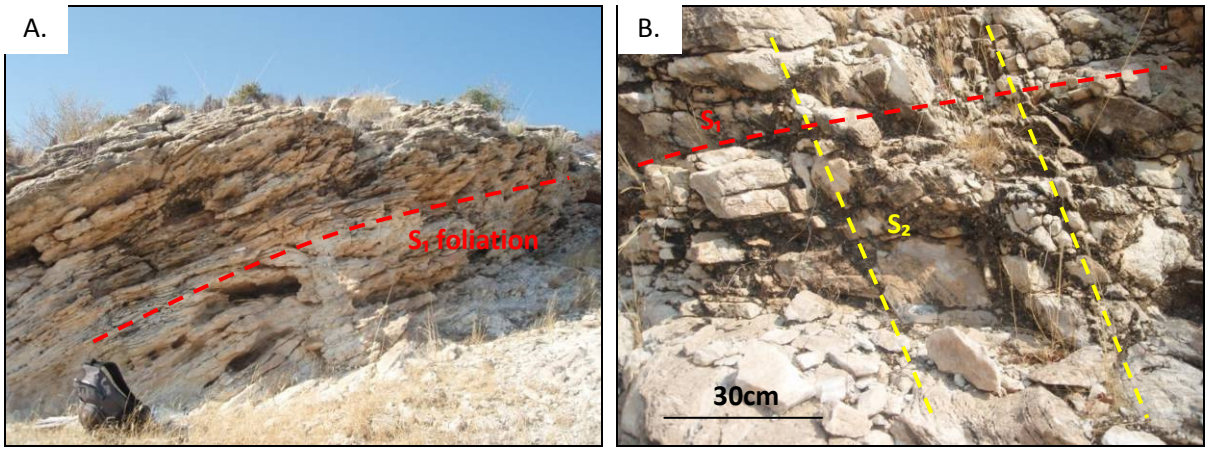

Fig 4.4.4: A.) Pervasive shallowly dipping fabric (S_1) in marbles of the Karibib Formation. Primary features (S_0) are largely overprinted. **B.)** A steep, widely spaced cleavage (321/76) in recrystallized white marble is interpreted to represent an axial-planar S_2 foliation. Photos were taken at 22°12'41.9"S; 15°55'16.7"E looking SW.

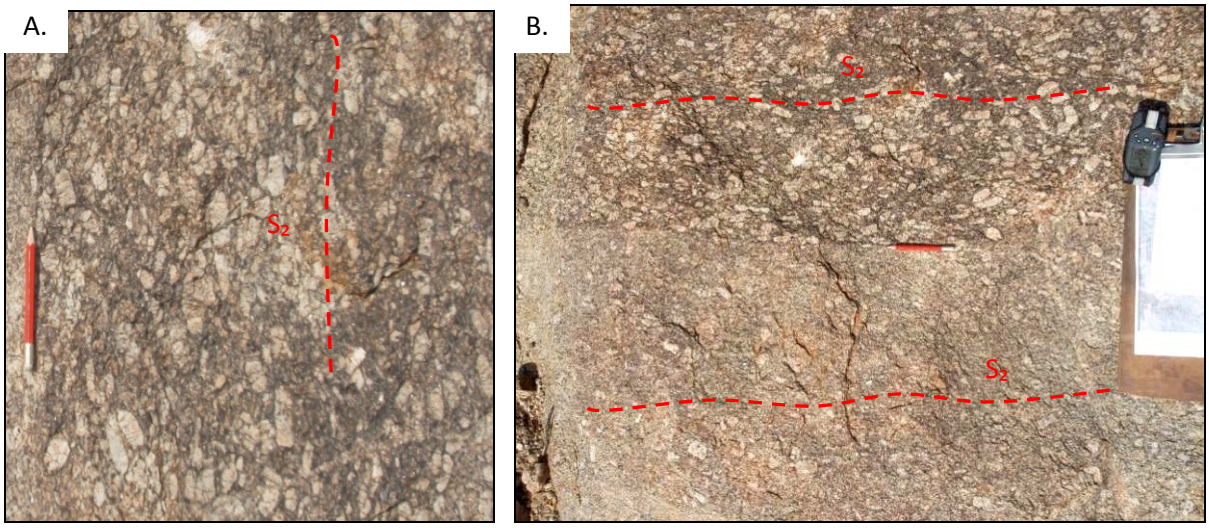

Fig 4.4.5: A.) S_2-parallel magmatic foliation in megacrystic biotite-rich Salem granite south of the Audawib fold complex defined by the preferred alignment of euhedral K-feldspar megacrysts **B.)** The magmatic foliation is concordant with the contact between sheets of Salem-type granite of slightly varying composition, also highlighting the sheeted nature of the granite.

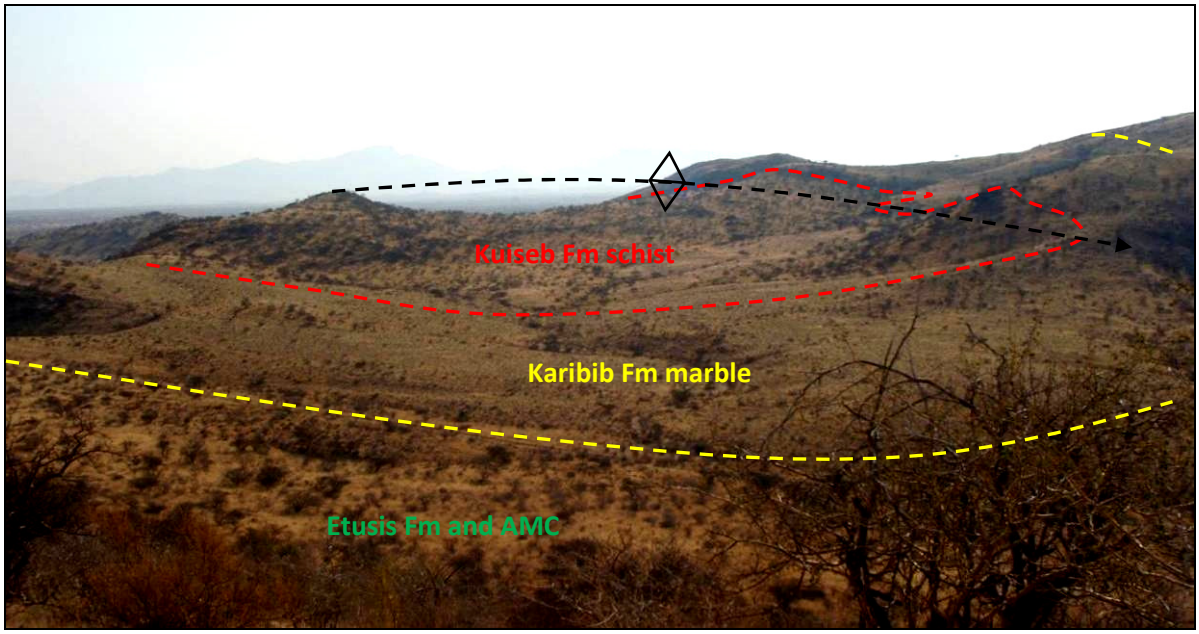

Fig 4.4.6: The Kuiseb Formation lies in the centre of an antiform, making it the lowermost formation, in this case overlain by marbles of the Karibib Formation. This photo looks westward at a 2nd order antiform (syncline) from a prominent hill of quartzite (Etusis Formation) at 22°10'34.3"S; 15°56'38.2"E.

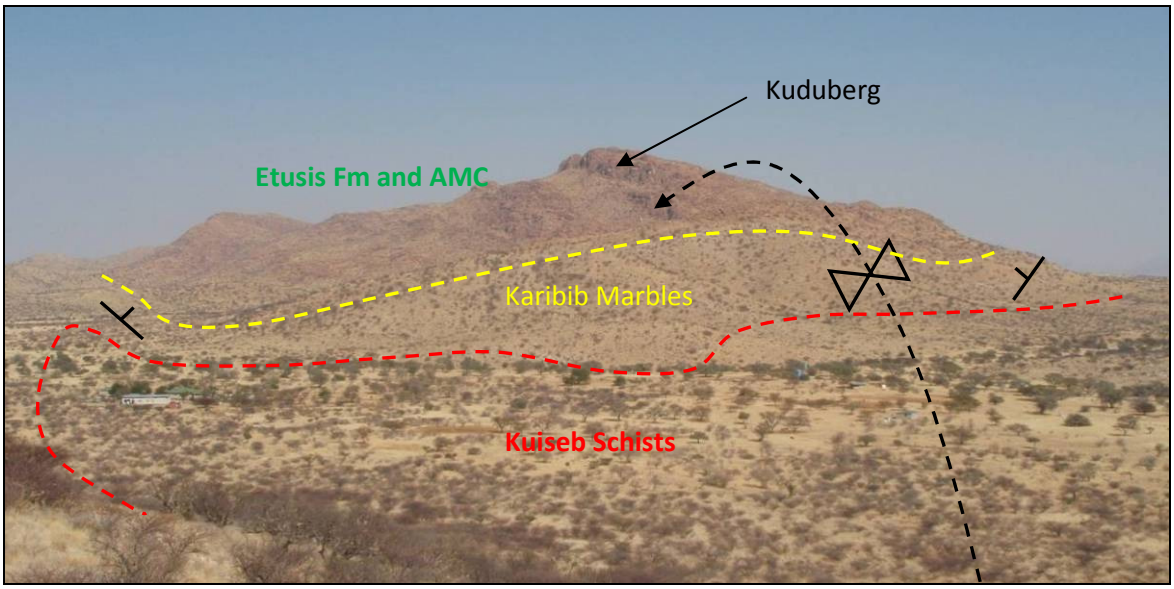

Fig 4.4.7: An inverted sequence is once more illustrated in a 2nd order syn-form (anticline) cored by gneisses of the AMC. Here the AMC rocks form the topographically high Kuduberg; these rocks are underlain by the Etusis Formation, the Karibib Formation and the Kuiseb Formation. This photo was taken looking SW at the Kuduberg from 22°11'57"S; 15°55'58.6"E.

Fold geometry

The Audawib fold complex is made up of four km-scale NE-trending 2nd order folds. Folding has affected lithological contacts and, as such, bedding (S_o) and the bedding parallel foliation (S_1). These four folds, labelled I to IV from S to N, are all doubly plunging towards the SW and NE, giving the overall structure a dome-like appearance. The S_2 foliation across this domain is axial planar to the folds. However, dips of S_2 vary systematically from NW in the SW to SE in the NE of the Audawib fold complex, resulting in the bi-vergent nature of the folds (Fig 4.4.8).

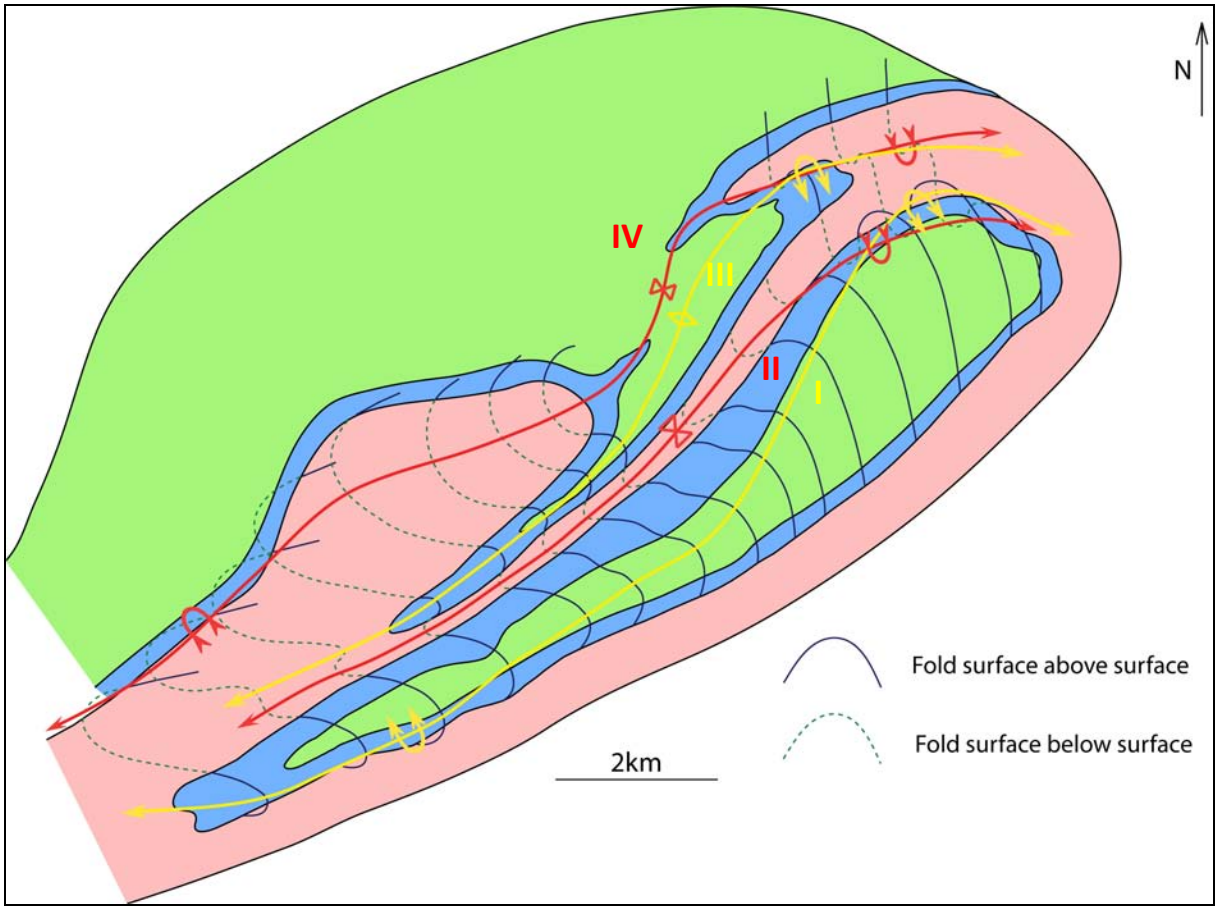

Fig 4.4.8: The Audawib fold complex. Four doubly-plunging 2nd order, NE-SW trending folds can be seen (I-IV, fold hinge lines annotated; yellow: antiformal syncline; red: synformal anticline). All folds in the NE part of the domain verge NW whereas the same folds verge SE in the SW part of the domain. The Kuiseb Formation is illustrated in green, the Karbib Formation in beige and the AMC and Etusis Formation in orange.

The largest of these four folds is the SE antiformal syncline, fold I. The fold is cored by schists of the Kuiseb Formation and associated leucogranites (Fig 4.4.8). The doubly-plunging (and bi-vergent), non-cylindrical fold can be followed for ca. 10 km along its axial trace, and reaches a wavelength of ca. 4 km in the NE. The hinges of fold I plunge towards ca. 300/60 (NW) in the SW and towards 060/50 in the NE, defining its doubly-plunging geometry (Fig 4.4.9). The hinge line curvature of > 90° defines an almost sheath-fold geometry.

Interlimb angles vary from open to tight and isoclinal. The bivergent geometry seen in all of the four 2nd order folds (I-IV) means these folds verge towards both the NW and SE (Fig 4.4.8), parallel to the S_2 foliations.

Fold I is followed to the NW by fold II, a smaller synformal anticline. This tight fold has a wavelength of ca. 1km and the homogenous nature of the gneisses in the core of the fold hampers the identification of any fold closure. The repetition of lithologies along the limbs,

however, indicates the presence of a fold. The vergence of fold II fold conforms to that of fold I and the axial-planar S_2 foliations parallel to its axial surface (Fig 4.4.2 & Fig 4.4.8).

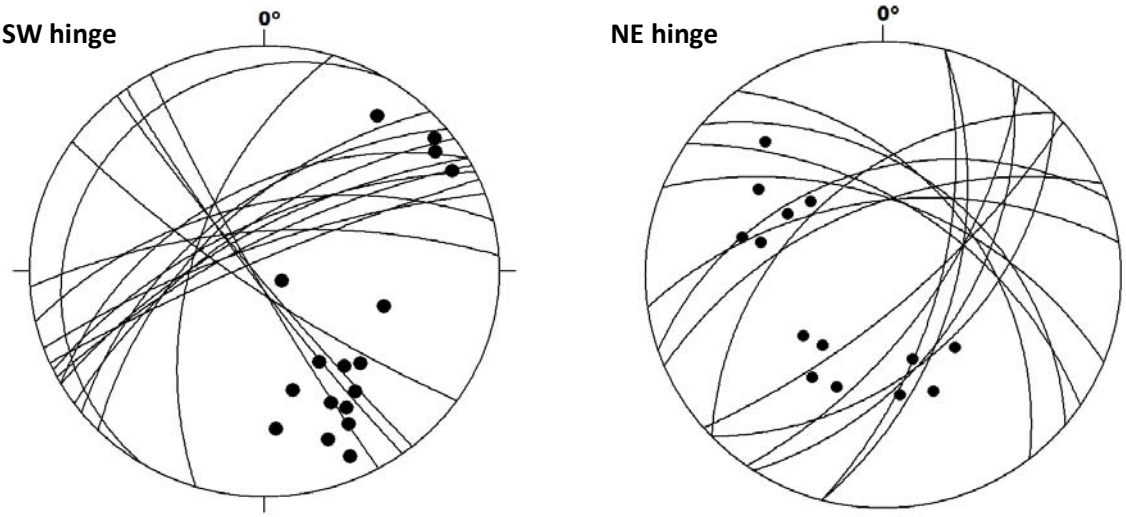

Fig 4.4.9: Stereonets of foliations around the fold hinges of Fold I. Great circles and pole to planes of bedding contacts (S_0/S_1) along the SW and NE fold hinge of the largest 2nd order fold, Fold I, illustrating the doubly plunging nature of the folds across this domain.

The Etusis Formation on the limb between fold II and III is very thin reaching, in places, no more than 5m in thickness. Here, the quartzites of the Etusis Formation seem much more homogenous and highly recrystallized, with no visible S_o banding preserved. Thinning of and high-strain textures in the quartzites are likely to be the result of shearing along this limb.

To the NW of fold II follows a second antiform-synform pair (antiform- fold III; synform – fold IV). This fold pair has a wavelength of between 1 and 2.5km, with the longest wavelength at the SW closure and the shortests wavelength at the folds' NE closure. Lithologies in the hinge of fold IV are all well developed giving no indication of shearing (out) of the lithologies.

3rd and 4th order folds

The hinges of the km-scale 2nd order folds are clearly visible on a regional scale and can be seen in the field. Smaller 3rd order folds are more difficult to identify and a more localized repetition of lithologies of, for example, the Kuiseb Formation within marbles of the Karibib Formation (Fig 4.4.10) near the fold hinges of 2nd order folds indicates the presence of 3rd order parasitic folds. These folds typically have wavelengths of between 50 and 100 m.

Even smaller 4th order folds are scarce, and can only be identified where S_o layering is preserved in marbles of the Karibib Formation. These folds have wavelengths of between 1 and 10 m (Fig 4.4.11) and also follow the regional NE-SW trend.

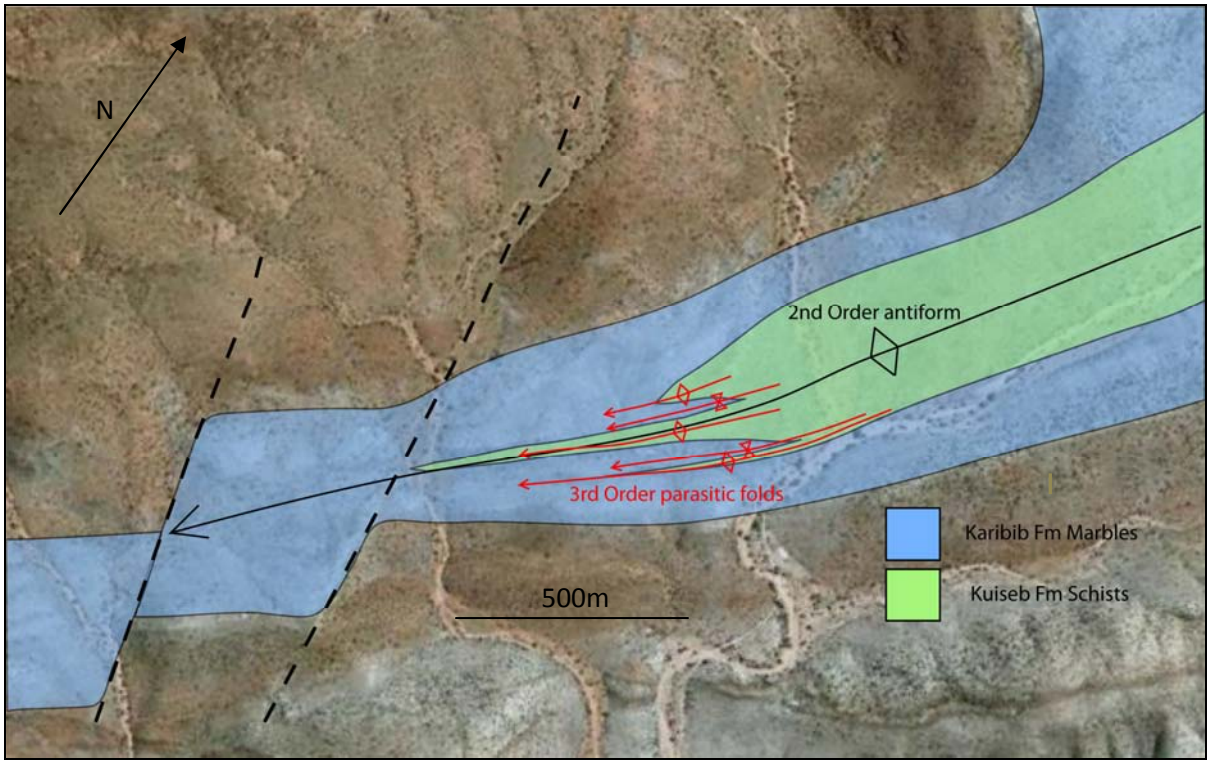

Fig 4.4.10: 3rd order folds occur as parasitic folds within larger 2nd order structures. These folds trend NE-SW parallel to 2nd order structures and the S_1/S_2 foliation. This figure is of the SW hinge of fold III.

Fig 4.4.11: 4th order folding in rocks of the Etusis Formation quartzites **(A)** and Karibib Formation marbles **(B).** Folds axial planes are aligned NE-SW **(A)** and NNE-SSW (**B)**, parallel and sub parallel to F2 folds. Photos were taken at 22°15'41"S; 15°50'30"E and 22°14'30"S; 15°53'26"E.

Several traverses were done across the Audawib fold complex with the goal of determining the overall geometry of the fold complex, from these traverses several cross-sections could be compiled (Fig 4.4.12). These cross sections show the change of vergence of the fold complex from the SW to the NE, and the inverted stratigraphy in the Audawib fold complex. As will be discussed in chapter 6, the overall structure of the Audawib fold complex is that of a Km-scale, recumbent, refolded nappe (Fig 4.4.12). The thicknesses of units are variable and this is likely the result of secondary 2nd and 3rd order folding as well as a shearing along some of the fold limbs.

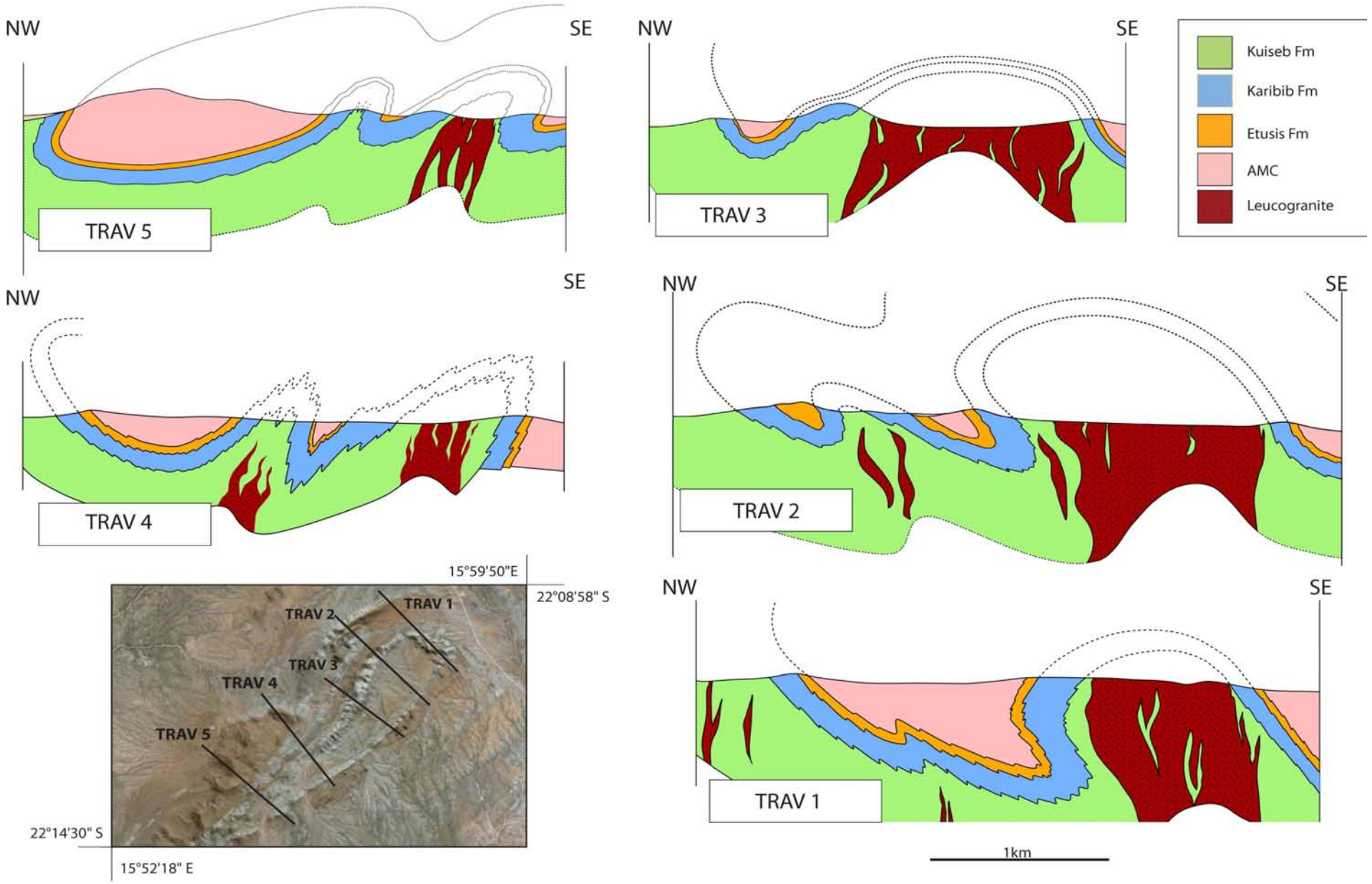

Fig 4.4.12: 5 Cross-sections illustrating the shape of the Audawib fold complex. Traverse 1 crosses the NE part of the mapping domain, where 2nd order folds verge towards the NW. Traverse 3 in the middle of the Audawib fold complex and shows upright folding. The SW traverse, traverse 5 indicates folding verging towards the SE. Antiforms are cored by schists that have been almost completely intruded by leucogranite. Synforms are cored by AMC gneisses. Fold vergence changes along strike of the fold complex.

Salem-type granites and intrusive relationships

The Salam-type granite occurs to the NE and SE of the Audawib fold complex. Along the SE boundary Salem-type granites form a ca. 1 km wide tongue of granite between AMC gneisses in the Audawib fold complex to the NW and Kuiseb schists immediately SE of the granite intrusion. This strip of Salem-type granite pinches out towards the SW, leaving AMC gneisses of the Audawib fold complex in direct contact with schist of the Kuiseb Formation to its SE (Fig 4.4.1).

The contact between the Salem granite and AMC gneisses is very sharp and straight and can be followed for 10 km's along its ENE strike. The foliation in rocks of the AMC is parallel to foliations in the Salem-type granite (Fig 4.4.2, Sub-domain C) and both foliations are sub-parallel to the contact. Moreover, isolated, sheared slivers of marbles and quartzites were observed along this contact. The largest of these slivers is a package of typical Etusis Formation quartzite and marble, presumably of the Karibib Formation caught between the AMC and the Salem-type granite (22°13'7.8"S; 15°56'28.9', Fig 4.4.13). This isolated, exotic block is about 1 km long, parallel to the AMC/Salem contact, and up to 80 m wide. The foliation in this sliver dips steeply to the NNW (ca. 340/80 (S_o-S_1)) and the marbles overlie the Etusis Formation quartzites that are directly in contact with Salem-type granites. Several smaller isolated marble slivers also occur along this contact and, in places, primary bedding may be preserved in these blocks. These smaller slivers are between 2 and 10 m in length and no more than 2 m wide (Fig 4.4.13.C)

Near the NE hinge of the Audawib fold complex, numerous large blocks of sheared feldspathic-quartzite are found as xenoliths within Salem-type granites along the AMC contact. These blocks of feldspathic-quartzite show clear compositional banding (Fig 4.4.14) and probably represent xenoliths of the Etusis Formation. Intense folding and shearing of the quartzites, defined by the strong grain-shape preferred orientation of quartz-feldspar aggregates, results in a penetrative fabric in the xenoliths. This type of fabric intensity is not recorded anywhere else in rocks of the Etusis Formation exposed in the study area.

The sharp contact between the AMC gneisses of the Audawib fold complex and Salem-type granites as well as the numerous, slivers of highly strained DSG rocks along this contact imply that this is a tectonic contact and has been marked as such on the geologic map (Fig 4.4.1 & Appendix III).

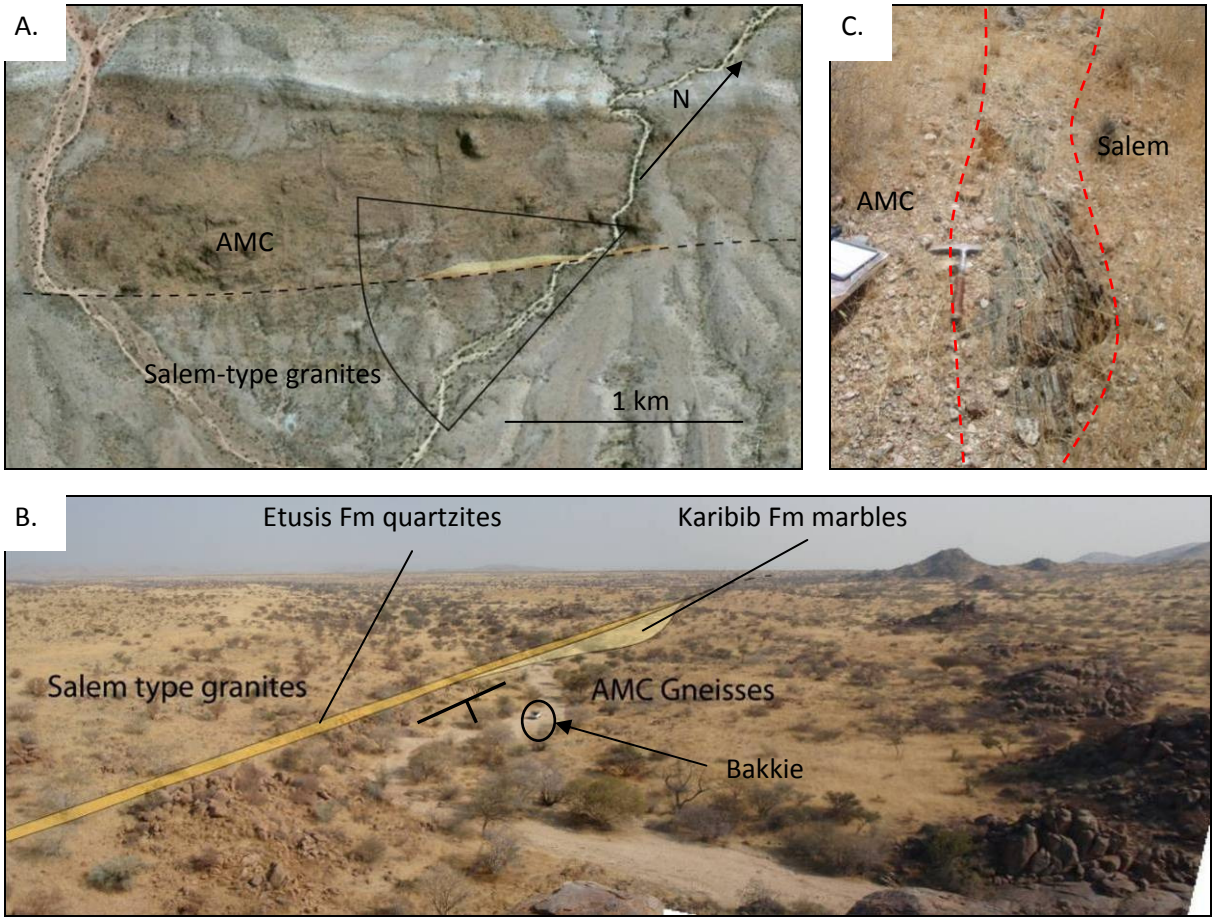

Fig 4.4.13: Slivers of Etusis Formation quartzites and Karibib Formation marbles are often found between the contact of the Salem-type granite platform and the gneisses of the AMC. The largest of these is a long sliver of quartzite and marble **(B.).** Photos **A and B** show this sliver as it is found in the field, quartzite in orange and marbles in white. Photo **C** was taken from 22°12'56"S; 15°56'36.7"E looking SW and is shown in aerial photo **A.** (Google earth image) **C.)** Smaller marble slivers along the AMC\Salem-type granite contact, are common and scattered.

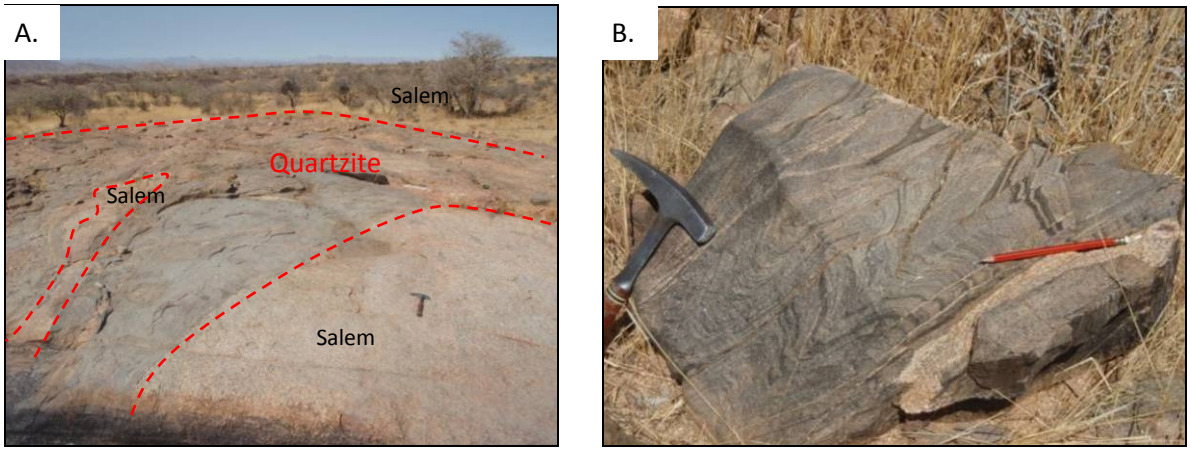

Fig 4.4.14: Large xenoliths of quartzite within the Salem-type granite occurs near the NW AMC/Salem contact. **(A.)** Xenoliths can occur as large isolated blocks of as much as 400m² in extent. **(B)** The quartzites show compositional banding similar to that in the Etusis Formation. These bands have however been highly transposed and sheared. These photos were taken at 22°11'34"S; 15°58'34"E adjacent to the AMC/Salem contact.

The SE boundary of the Salem-type granite with Kuiseb Formation schist is an up to 70 m wide zone of lit-par-lit intrusion. At this contact, the extensive cm- to dm-scale interfingering between schist and Salem-type granites has almost resulted in hybrid and seemingly assimilated rock types in which K-feldspar megacrysts occur in a biotite-rich, schist-like matrix (Fig 4.4.15). K-feldspar and biotite define a strong NE trending foliation (Fig 4.4.15)

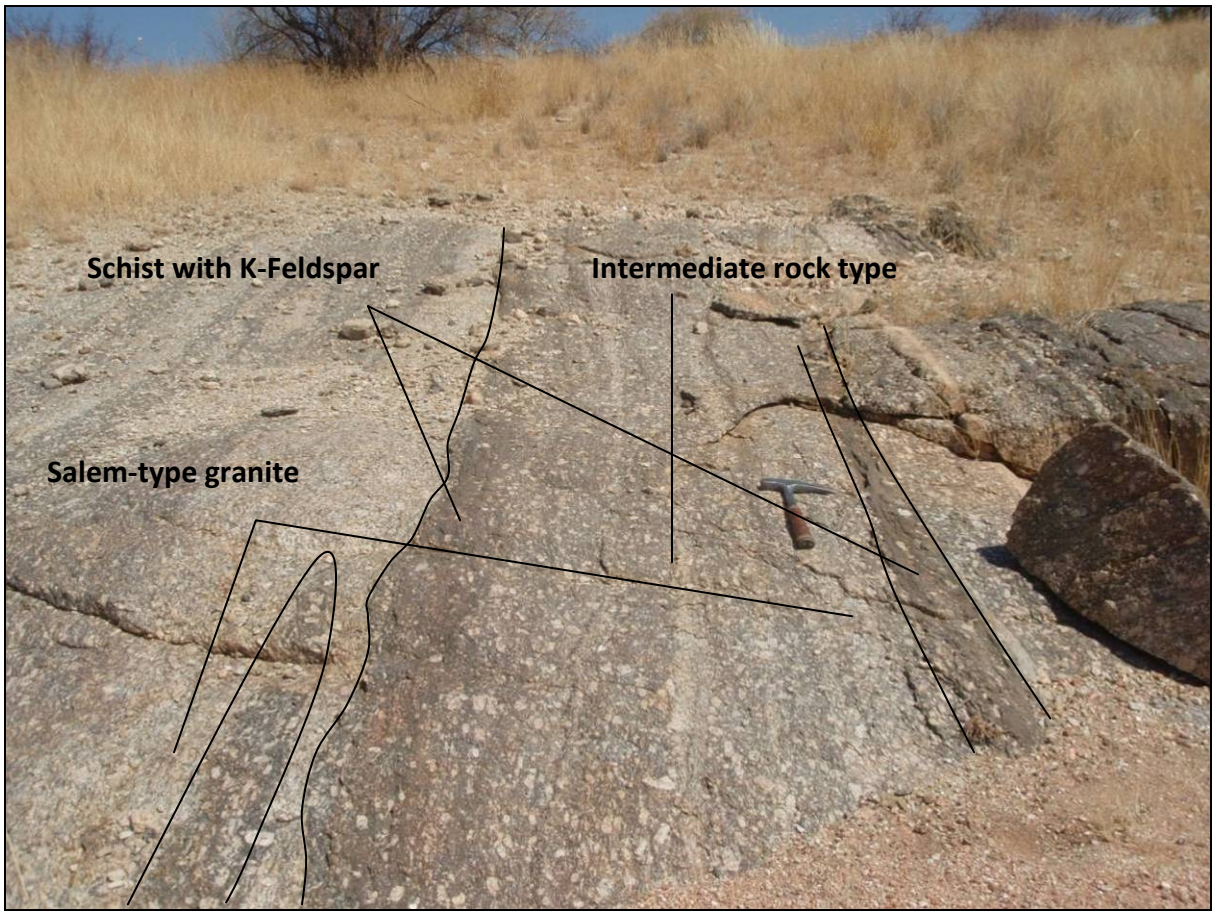

Fig 4.4.15: The contact between the Salem-type granite and the Kuiseb Formation schist towards the SE is a lit-par-lit type contact zone. Biotite-rich, foliated layers with large K-feldspar megacrysts give the impression of partial assimilation of the wall-rock schists by the granites. The compositional layering is parallel to both the granite foliations defined by K-feldspar megacrysts and the contact. This type of layering is interspersed with thicker (up to 5m thick) homogenous bands of alternating schists and Salem-type granites. This photo was taken at 22°14'51.7"S; 15°54'17.2"E, looking SW.

Summary:

The main feature of this mapping domain is the central Audawib fold complex underlain by schist at its NW margin and surrounded by Salem-type granites at its NE and SE contacts. The lithological sequence (AMC through to the DSG) in this domain is inverted with the Kuiseb Formations being the basal formation and the AMC gneisses being the uppermost unit. Stratigraphic inversion is likely to be the result of complex folding and nappe formation. The Audawib fold complex consists of several SW-NE trending, bivergent (SE and NW) doubly plunging (SW and NE) folds. Doubly plunging folds give this central complex a dome like appearance typical of folds in the SCZ, in fact, hinge line curvatures of up to

110° point to sheath-like geometries closing to the NW. Stratigraphic inversion was likely the result of 1st order F1 recumbent folding. This was subsequently followed by F2 folding to give this complex its bivergent doubly plunging geometry and resulting in a type 3 refolded fold interference pattern (Fig 4.4.8 & Fig 4.4.12). All lithologies have been affected by this folding and the AMC, DSG and Salem-type granite suite all show structural fabrics co-axial with these fold trends. The SE contact between the Salem type granites and the AMC gneiss along the SE boundary of the fold complex is sharp, strongly foliated and numerous allochthonous slivers indicate the existence of a shear zone along this contact.

This structure is further analysed in the discussion in chapter 5.

4.5 Otjimbingwe mapping domain

Domain description

The upper formations of the DSG, namely the Kuiseb Formation and Tinkas Formation, underlie the Otjimbingwe townlands, SE of the Audawib mapping domain. Marble units of the Karibib Formation are subordinate and are succeeded by inter-layered schists, marbles and calc-silicate felses of the Tinkas Formation. The Tinkas Formation is thought to occupy a stratigraphic position alongside the Kuiseb Formation schists and represents a lateral basinward facies variation of the Kuiseb and Karibib Formations (chapter 2). All lithologies strike approximately SW-NE (Fig 4.5.1). Fabric intensities show a progressive increase from NW to SE and closer to the Donkerhuk batholith at the SE border of this domain. This southernmost part of the Otjimbingwe domain forms part of the OLZ. Based on differences in its structural and lithostratigraphic inventory, the Otjimbingwe domain has been subdivided into a NW and a SE sub-domain (Fig 4.5.2).

The NW sub-domain occupies the S and SW portion of the Otjimbingwe domain and stretches from the boundary of the Audawib fold complex (chapter 4.4) to the Erekere mountains and the Audawib river in the SE. This domain has an across-strike width of up to 8 km and is almost entirely underlain by biotite- and biotite-cordierite schists intermittently exposed between extensive calcrete terraces. Quartzites of the Etusis Formation form an isolated, NE trending, ca. 4.3 km long and up to 1 km wide ridge in the central parts of the sub-domain. Towards the SE, rocks of the Kuiseb Formation grade into the Tinkas Formation and are intruded by progressively more abundant leucogranite sills.

The SE sub-domain starts where the schist of the Kuiseb Formation show an increase in intercalated marbles and calc-silicate felses that characterize the gradual transition into the Tinkas Formation. This coincides with a change in deformational style and increase in fabric intensities. This area is the OLZ defined by previous workers (e.g. Sawyer, 1981; Miller, 1983).

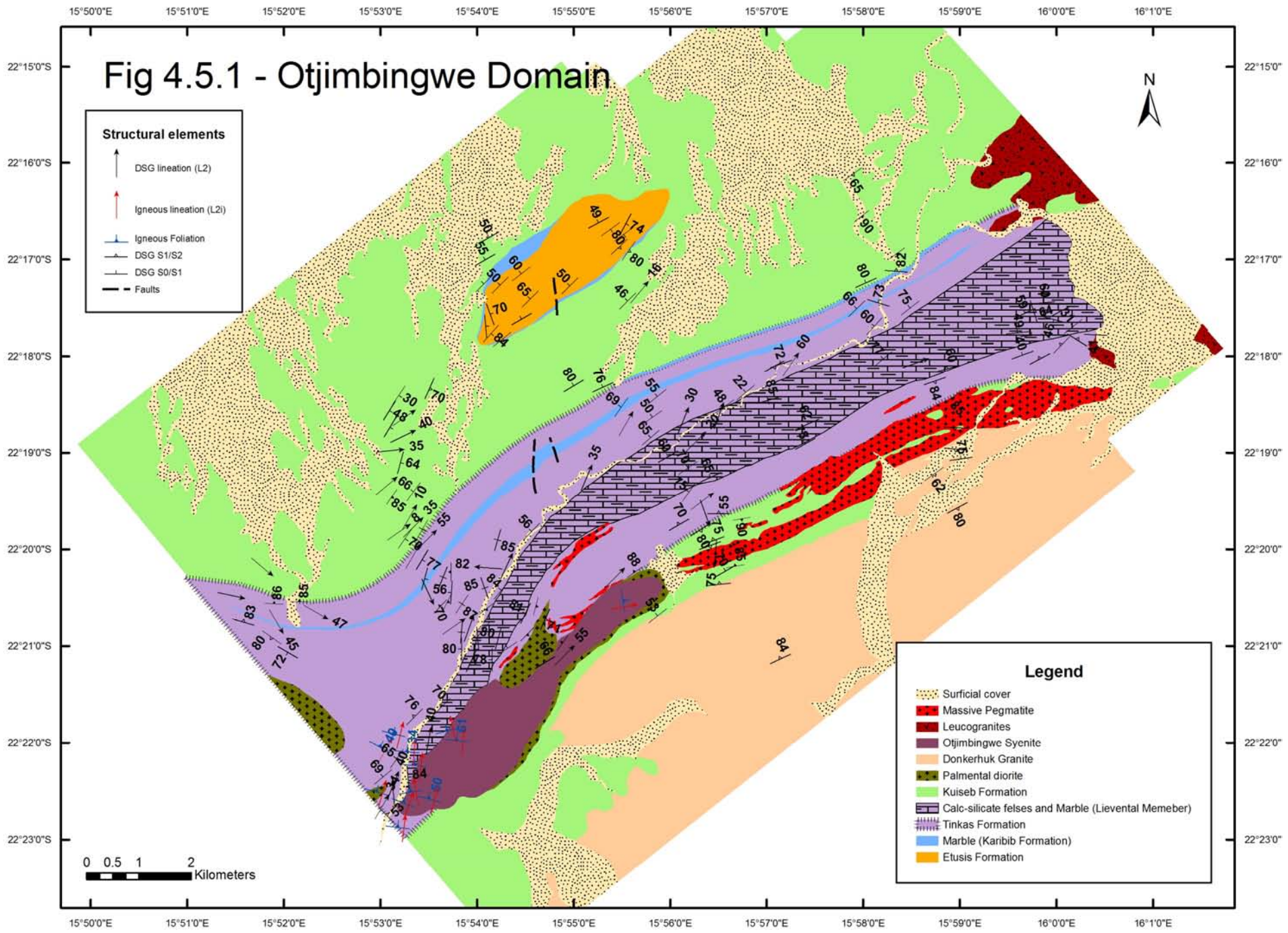

For a detailed version of this map, see Appendix IV

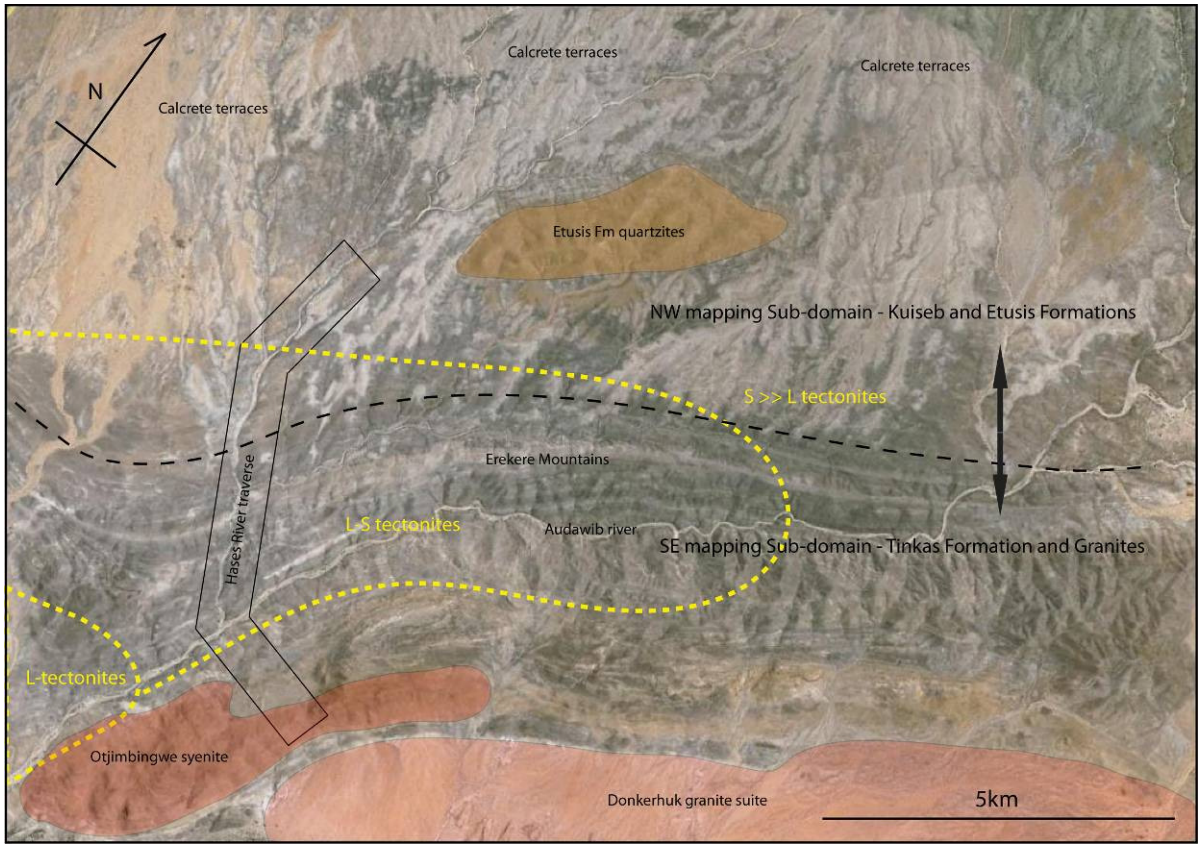

Fig 4.5.2: Overview of the Otjimbingwe mapping domain, delineating a NW from a SE sub-domain (black dashed line). The SE sub-domain coincides with the Okahandja Lineament Zone, identified by previous workers as a major structural lineament (e.g. Sawyer, 1981.) The boundary of the two sub-domains is close to the transition of the Kuiseb Formation in the NW to the Tinkas Formation in the SE. The yellow dashed line demarcates broad zones of different fabric development showing along-strike variations from flattening-type fabrics (S tectonites) to constrictional-type fabrics (L-tectonites).

NW sub-domain

Much of the low-lying areas in this domain are covered by calcrete, but a large (4x1 km) NE trending, central ridge of reddish, well-foliated and commonly crenulated Etusis Formation quartzite offers good exposure (Fig 4.5.2 & Fig 4.5.2.A). While rocks of the Etusis Formation commonly retain well-developed sedimentary features (e.g. in the Etusis mapping domain), the quartzites and arkosic quartzites in these outcrops invariably contain a foliation and appear sheared (Fig 4.5.3.B). The foliation is defined by the grain-shape preferred orientation of quartz discs and quartz-feldspar aggregates and biotite bands. This steeply-dipping NE trending foliation is parallel to tightly folded S_0/S_1 banding, where present (Fig 4.5.3.B). A cream-coloured marble unit, presumably belonging to the Karibib Formation, structurally overlies the quartzites along the NW flanks of the Etusis Formation ridge, but underlies the quartzites in the SE, where it is only developed as a very thin (< 10-15 m) pervasively recrystallized horizon. This marble seems to be absent in both the SW and NE terminations of the ridge of Etusis Formation quartzites.

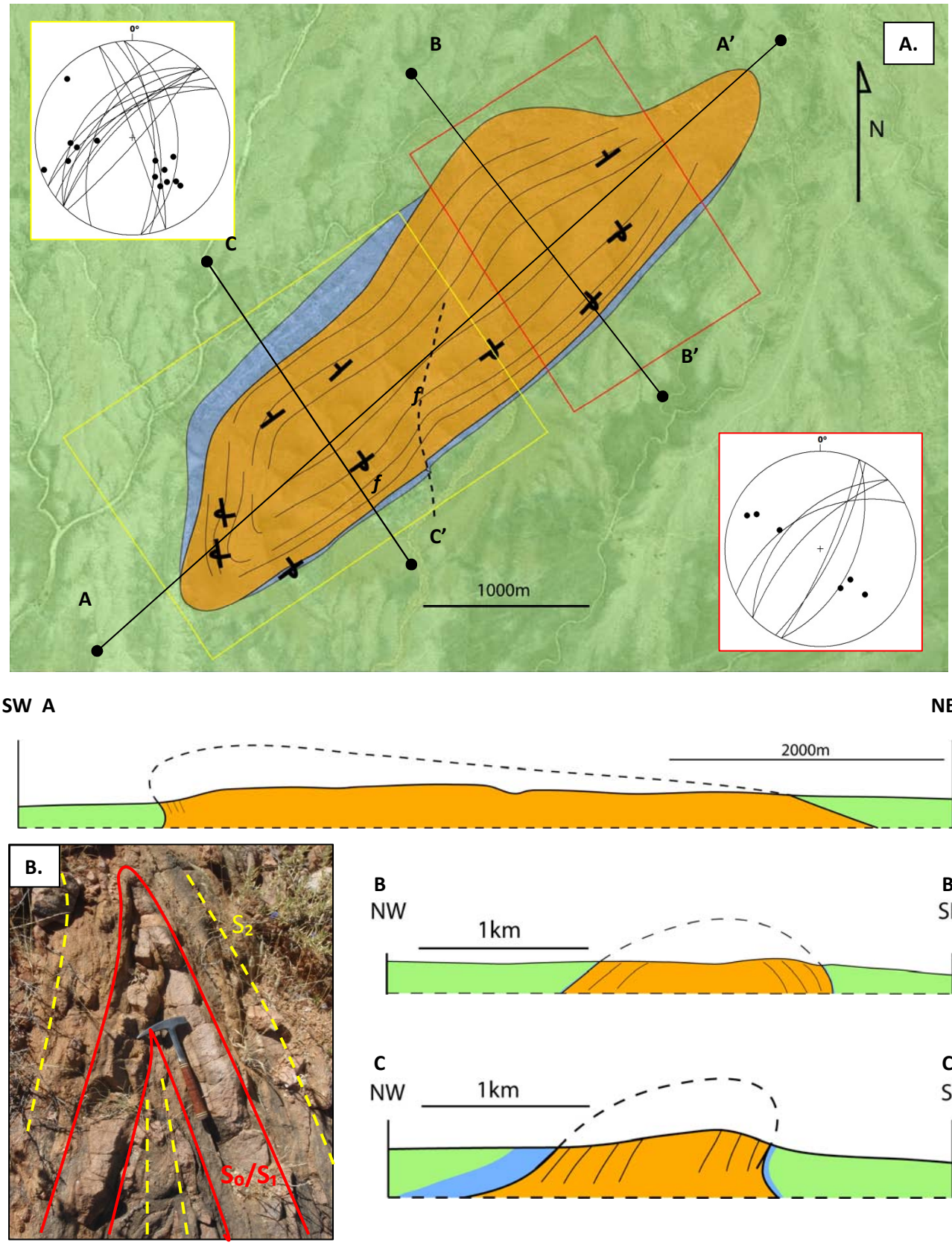

Fig. 4.5.3: A.) Simplified geological map of the central ridge of Etusis Fm quartzites. Stereonets (inserts) show the poles and great circles of the main S_2 foliation for the NE and SW portions of the ridge, respectively. This foliation dips towards the NW throughout the exposure, except for the SE and NW termination of the quartzites. From these orientations it is possible to deduce a sheath like geometry, displayed in 2 cross-sections (B-B' & C-C') and a longitudinal section (A-A'). This hill lies at the co-ordinates: 22°16'58" S; 15°54'58" E and is surrounded by a thin band of marbles and a large schist plateau. **B.)** This hill is made entirely of foliated quartzites. The foliation is axial planar to small F2 folds (NE-SW trending) suggesting a S_2 foliation parallel to the 1st order sheath fold structure.

Both the foliation in the Etusis Formation as well as the marble-quartzite contacts outline a km-scale NE-trending antiformal fold structure underlying the ridge of quartzites. Along the slopes of the central ridge, the marble-quartzite contacts and foliation dip consistently towards the NW. SE and E dips point to the presence of a fold closure in the SW termination of the ridge. Foliation dips are to the NW again on the SE side of the ridge. These beds are considered to be overturned to the NW, given that the thin marble unit in the SE structurally underlies the quartzites of the Etusis Formation. The overall structure of the Etusis ridge is depicted in a longitudinal section (Fig 4.5.3. A-A') and two cross sections (Fig 4.5.3. B-B' and C-C'). The cross sections point to the upright to SE vergence of the fold structure. The longitudinal section suggests steep NE plunges for both the SW fold closure as well as the NE termination; a fold closure for the NE termination of the Etusis ridge could not be identified with certainty. The resulting geometry of the Etusis Formation ridge is that of a SE verging, strongly non-cylindrical fold with a, possibly, sheath geometry and SW closing fold (Fig 4.5.3).

A consistently NE trending foliation is developed in the surrounding biotite- and biotite-cordierite of the Kuiseb Formation. The dip of this foliation, though quite variable, tends to be close to vertical (135/90). The orientation of this foliation is, thus, axial planar to the fold in the Etusis ridge, but compositional banding (S_o) that would allow to identify similar folds in these metapelites are only rarely preserved and cannot be traced over larger distances. Where exposed, S_o in the schists shows overall NE trends, ranging from subhorizontal to subvertical, which may point to the presence of similar folds in the Kuiseb Formation.

The structure of the Kuiseb Formation in this NW sub-domain is best exposed along the Hases River that offers a superb cross-section through the otherwise homogeneous schist units (see Fig 4.5.2 for location). A detailed section was mapped between coordinates 22°18'15"S; 15°53'15"E to 22°20'56"S; 15°53'56"E, where the Hases River converges with the Audawib River (Fig 4.5.4).

The rocks show a well-developed bedding-parallel foliation (S_1). S_o/S_1 are folded and tight- to isoclinal, NE-trending upright F2 folds alternate with areas of open, NE-trending, upright F2 folding over an across-strike distance of approximately 800m. Open folds have wavelengths of up to 50m and amplitudes of only about 3 m (Fig 4.5.5.C). The folds are non-cylindrical and commonly subhorizontal, but doubly plunging to the NE and SW. An axial-planar foliation (S_2) is well developed in the hinges of the folds (Fig 4.5.5.B) and commonly expressed by pressure solution seams and the concentration of biotite. Fold shapes tighten over a distance of 100-150 m and although folding is well exposed in the river section, individual beds cannot be traced between adjacent folds due to the lack of any marker layers. With further tightening of the folds, fold shapes are tight- to isoclinal and actual fold hinges are difficult to identify since the hinge-lines are parallel to both S_1 and S_2 surfaces and fold closures

become nearly impossible to observe (Fig 4.5.5.A). High strain fabrics also provide evidence of localised shearing along S_2 (Fig 4.5.5.A). In zones of isoclinal folding, hinges have, in many cases, been sheared out, leading to complete bedding transposition (of S_o/S_1) into S_2. These zones merely show an upright layering, pervasive foliation development and folding is only evidenced by the occasional preservation of isoclinal, rootless folds in the schist. Here the axial planar foliation is parallel to a S_1 foliation with the result that S_1 and S_2 are indistinguishable. It is only in areas of open folding that fold hinges become apparent and that S_1 can be distinguished from the upright to NW-dipping S_2 foliation (Fig 4.5.5).

Fig 4.5.4 & Fig 4.5.5 illustrates the change in fold expression along this river traverse. Supporting orientation data indicates how all layering and folding become progressively rotated into a upright orientation further down (S to SE) the Hases river and towards the OLZ.

In the SE of the Hases river schists of the Kuiseb Formation contain gradually more calc-silicate and marble layers and this is the transition into the Tinkas Formation. Here, bedding is subvertical and, where exposed, bedding transposition of layering can be clearly seen by e.g. the isoclinal folding of calc-silicate felses in marbles and the boudinage of competent layers (Fig 4.5.5.E). A L_2m lineation is commonly developed on S_2 surfaces in the schist units. The lineation is expressed by the preferred orientation of sillimanite in metapelites, hornblende in feldspathic, felsic intrusive (L_2i) units and the stretching of cordierite crystals in schist (Fig 4.5.10). This lineation is weak in the NW portion of Hases river traverse, but becomes very pronounced SE towards the Audawib river and the OLZ consistently plunging towards the NE direction (35/60). This linear fabric is discussed in more detail later in the chapter.

SE sub-domain (Into the OLZ)

The SE subdomain stretches from the Erekere mountains to the Donkerhuk granite batholith (chapter 2). The transition from the Kuiseb into the Tinkas Formation coincides with the S boundary of the SCZ and its transition into the OLZ (chapter 2). It represents a continuation of the structural pattern of upright- to SE-verging, tight- to isoclinal F2 folds and pervasive S_2 foliation recorded to the immediate NW, although fabric intensities are higher and bedding transposition is pervasive. Moreover, the rocks have been intruded by numerous granitoids, including leucogranite sheets, rocks of the Palmental diorite suite and the Otjimbingwe syenite. Tight to isoclinal F2 folding is ubiquitous along this part of OLZ, forming a strongly overprinting S_2 fabric and giving rocks a subvertical layered appearance. F2 folds range in half-wavelength from a few cm to 100s of m. The F2 folds completely transpose the S_o/S_1 fabrics so that bedding in the subvertical sequences is parallel to S_2 (Fig 4.5.6).

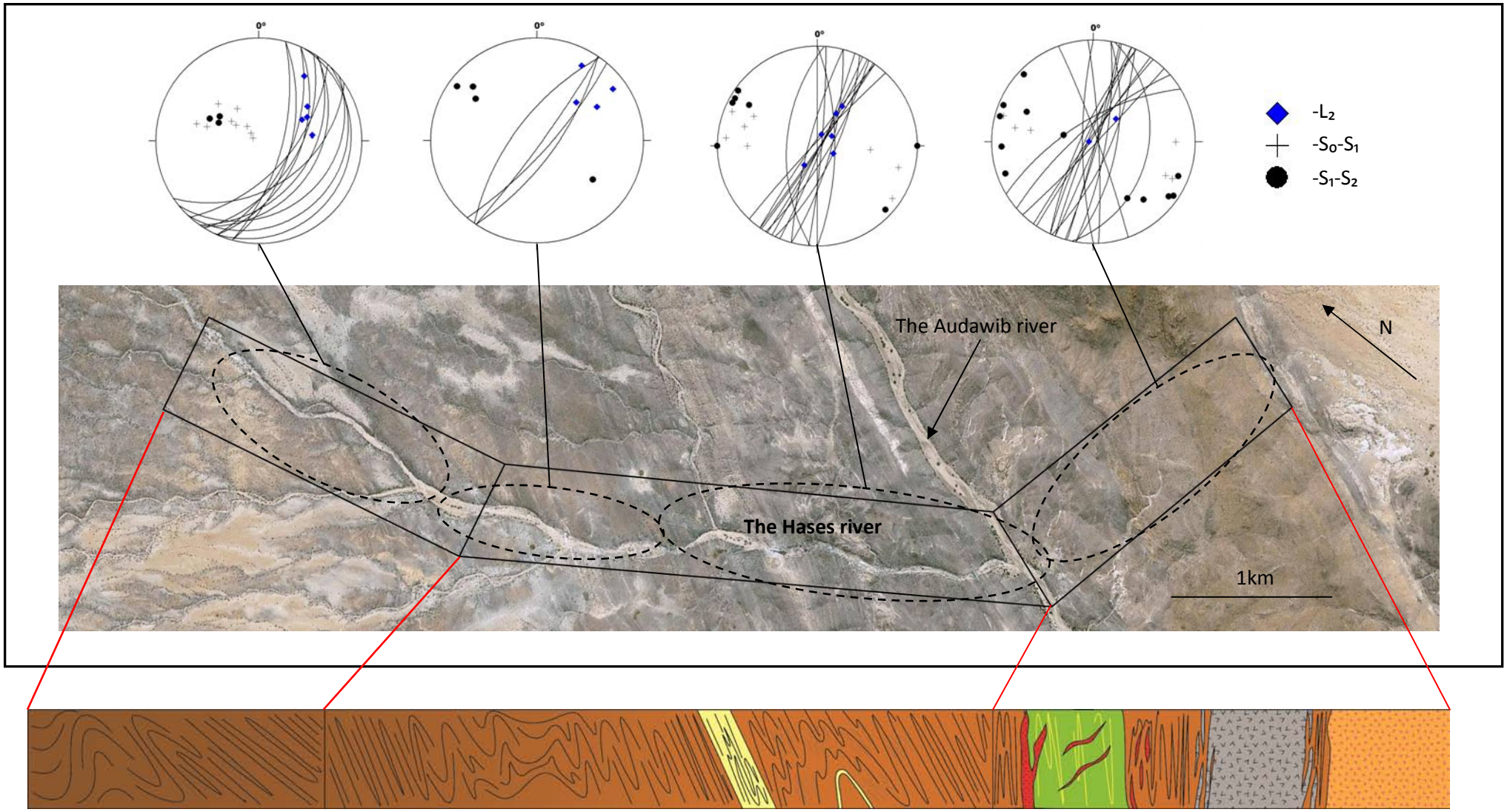

Fig. 4.5.4: A traverse across the Hases river exposes the progressive steepening of fabrics ($S_0/S_1/S_2$). A steep NE-plunging mineral lineation is consistently developed along this traverse, as well as a consistent upright NNE trending S_2 foliation. For the most part, S_1 and S_2 are parallel and indistinguishable in the mainly upright, tight- to isoclinal folds and only discernable in open folds. Note the general steepening of the L_2 stretching lineation from shallow- to moderate NE plunges (left-hand diagrams) to steep and subvertical plunges in the increasingly transposed areas to the SE (stereographic projections on the right-hand side).

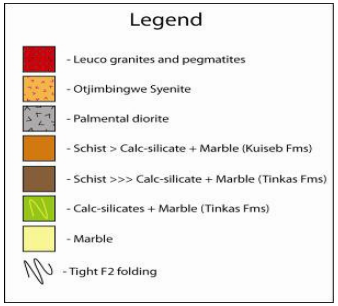

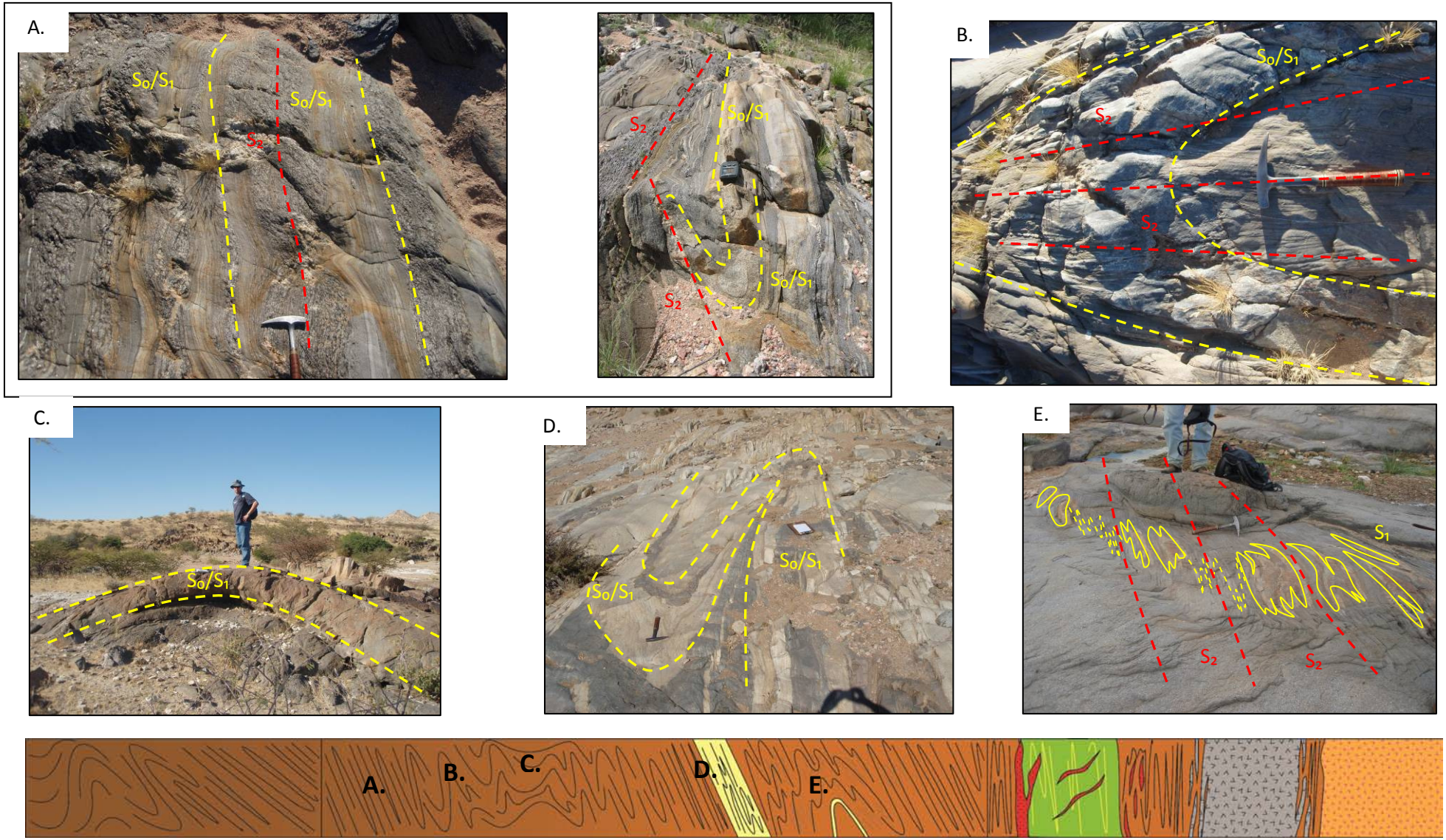

Fig. 4.5.5: The appearance of the outcrop as well as the fold characteristics change along the Hases river traverse. There is a alternation between areas of open folding and tight upright folding. **A.)** What appears to be simple straight compositional banding across much of the traverse is, in fact, the result of lithological repetition due to upright folding. Here S_1 and S_2 are sub-parallel and fold hinges can only be seen when exposed in sections. **B.)** Larger folds (m scale wavelengths) gradually appear on surface and it becomes possible to distinguish S_1 and S_2 in fold hinges. **C)** Shallow, open folds (tens of meters in wavelength) in the NW part of the traverse. **D.)** Close to a central marble horizon, the composition contrast between marbles schist and calc-silicates as resulted in the exposure of isoclinally folded layers with amplitudes of up to 20 meters. Protracted deformation has in many cases led to folding and subsequent boudinage of many layers. This is most evident where Calc-silicate felses that have been folded in schists. **E.)** Boudins contain a very strong S_2 overprint. All tight folds as well as foliations trend SW-NE. Isoclinal and transposed folding persists up to the margin of the Otjimbingwe syenite.

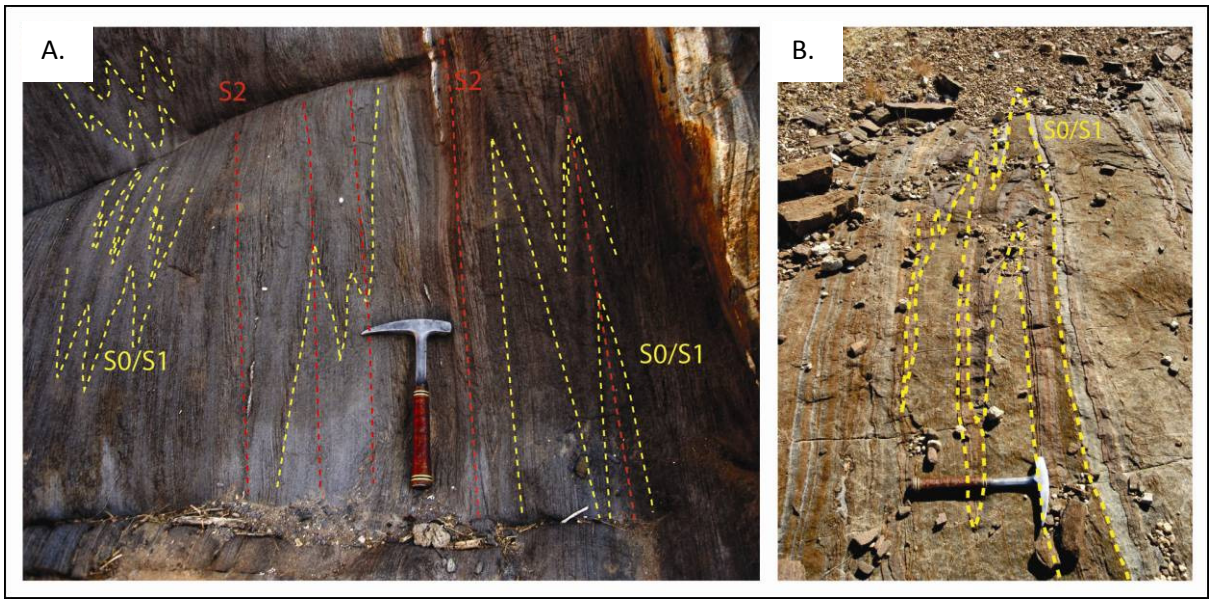

Fig 4.5.6: Extreme transposition of layers is common in rocks of the Tinkas Formation. Transposition can be difficult to observe in schists, and is most pronounced where slightly different lithologies occur, such as calc-silicate felses interlayered with marbles **(B.). A.)** Transposed foliations in schists in the Audawib river. S_o/S_1 (yellow dashed lines) is only visibly due to slight colour (compositional) differences in the schists. S_o/S_1 has been overprinted by a strong upright S_2 foliation (red dashed lines). **B.)** Transposed bedding defined by calc-silicate felses and marbles in the centre of the Tinkas Formation; S_o/S_1 annotated by yellow dashed line.

Fold plunges are highly variable and range from subhorizontal to subvertical. Bedding transposition is made evident by rootless, isoclinal folds, whereas limbs of e.g. calc-silicate felses or biotite schists in marble units undergo spectacular boudinage. Boudinage is often of a chocolate-tablet type, indicating a large component of layer-normal (NW-SE) shortening and extension in the plane of S_2 (Fig 4.5.7).

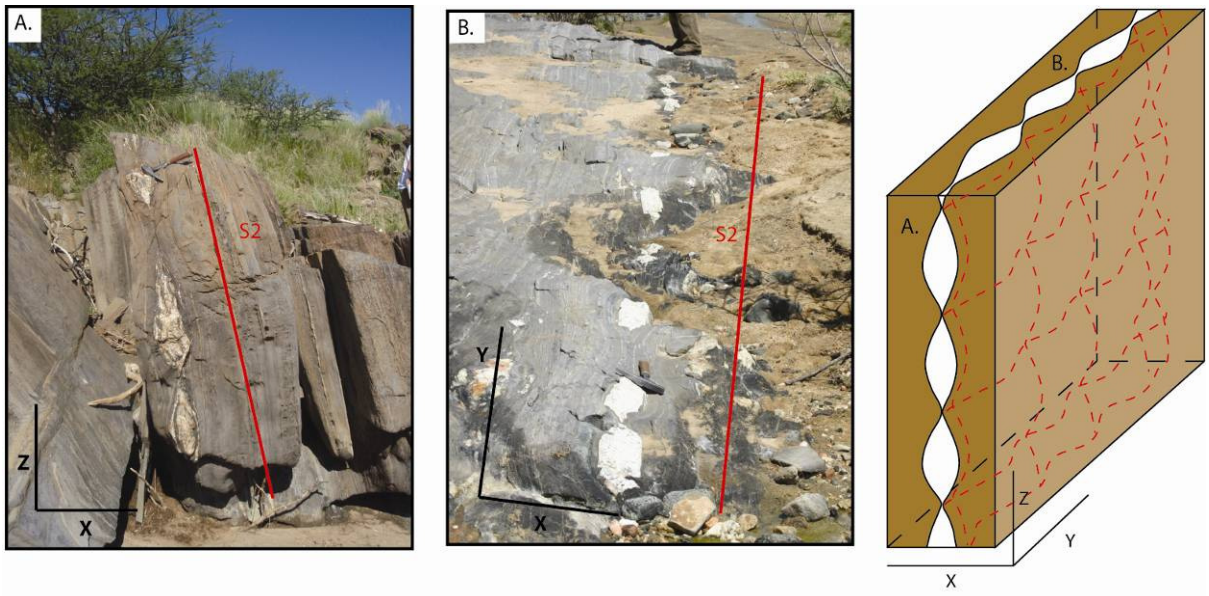

Fig 4.5.7 Boudinage of especially small granite sills in schist is very common in the SE part of the Audawib River. Boudinage is seen both in the vertical plane (A.) and the horizontal plane (B.). This implies a chocolate tablet geometry for many of the boudins in this domain. These photo were taken in the Audawib River at 22°17'26"S; 15°58'10"E, looking at a side view (A.) (looking SW) and top down plan view (B.).

In general, folding and boudinage is symmetrical (Fig 4.5.6 & Fig 4.5.7). Asymmetrical features and folding is only occasionally observed along the limbs of larger folds (with wavelengths > 50 m) but is rather uncommon. Moreover, the highly-transposed rocks are characterized by conjugate shear bands, also indicating the NW-SE directed bulk co-axial shortening strain (Fig 4.5.8.B) There are no reliable strain markers, but the rocks are S>L tectonites, although steep stretching lineations are developed on many S_2 foliation planes.

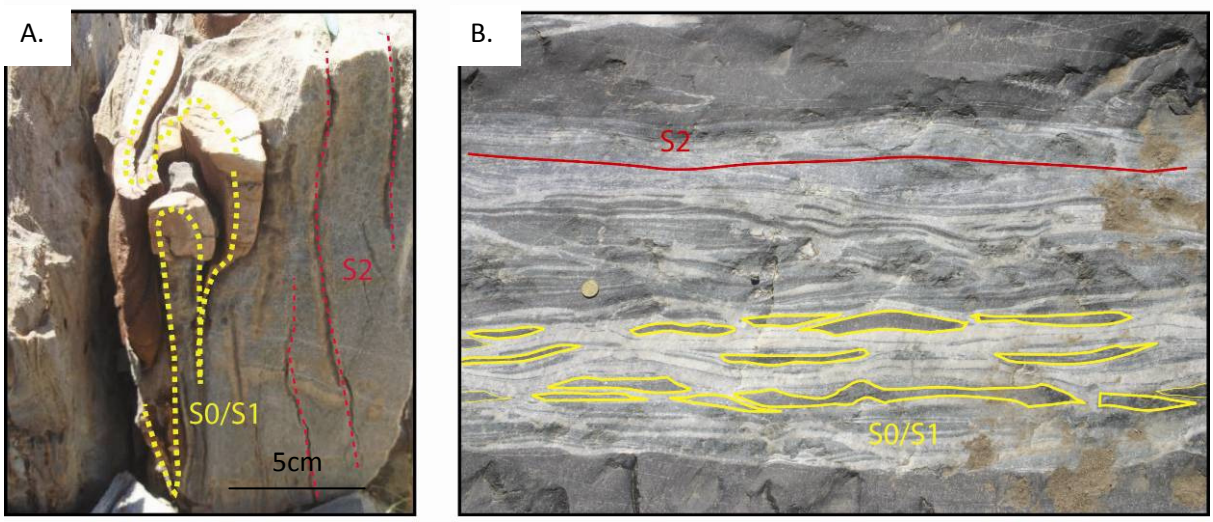

Fig 4.5.8: A.) Folding of calc-silicates in marbles show no prefered shear direction, and folding can be seen in both vertical and horizontal planes, with vertical as well as horizontal trending fold axis developed in small scale folds. (4^{th} or 5^{th} order). This photo was taken at 22°21'40"S; 15°53'22"E in the Tinkas Formations. **B.)** Conjugate shear bands in major banded marble units indicate bulk coaxial shortening of individual layers (S_o), showing no obvious shear sense. This photo was taken in the massive marble unit in the Hases river at 22°20'8'29"S; 15°53'33"E.

Overall, the most noteworthy features of deformation are (1) the pervasive development of high strain fabrics and bedding transposition, (2) the complete lack of non-coaxial fabrics and that strain appears to be of a pure-shear dominated flattening type.

Along strike of the OLZ and to the SW, there is a marked change in fabric development. In this zone, S> L tectonites give way to tectonites with rodded prolate textures (L>S) around the Palmental diorite in the SW corner of this subdomain. This change of fabrics is pronounced in an area of approximately 2-3 km in diameter around the the Palmental diorite (at 22°22'2"S; 15°53'10"E). Here, fabrics are dominated by L-tectonites and prolate fabrics. A strong mineral lineation is developed on almost all exposed S_2 surfaces. Lineations are defined by the preferred growth of sillimanite, stretched cordierite and quartz-feldspar aggregates. Intrusive sheets of Palmental diorite show a lineation (L_2i) defined by the preferred orientation of horneblende (Fig 4.5.11.B). This lineation is parallel to that in the DSG. Moreover, S_2 foliation planes appear crenulated and crenulation axes plunge parallel to the stretching lineations. Similarly, mesoscopic F2 fold axes show consistent

plunges to the NE parallel to the stretching lineations. In the Palmental diorite, wall-rock xenoliths are stretched showing, in 3 D, aspect ratios of, on average, 10-15:2-3:1 (Fig 4.5.9.B).

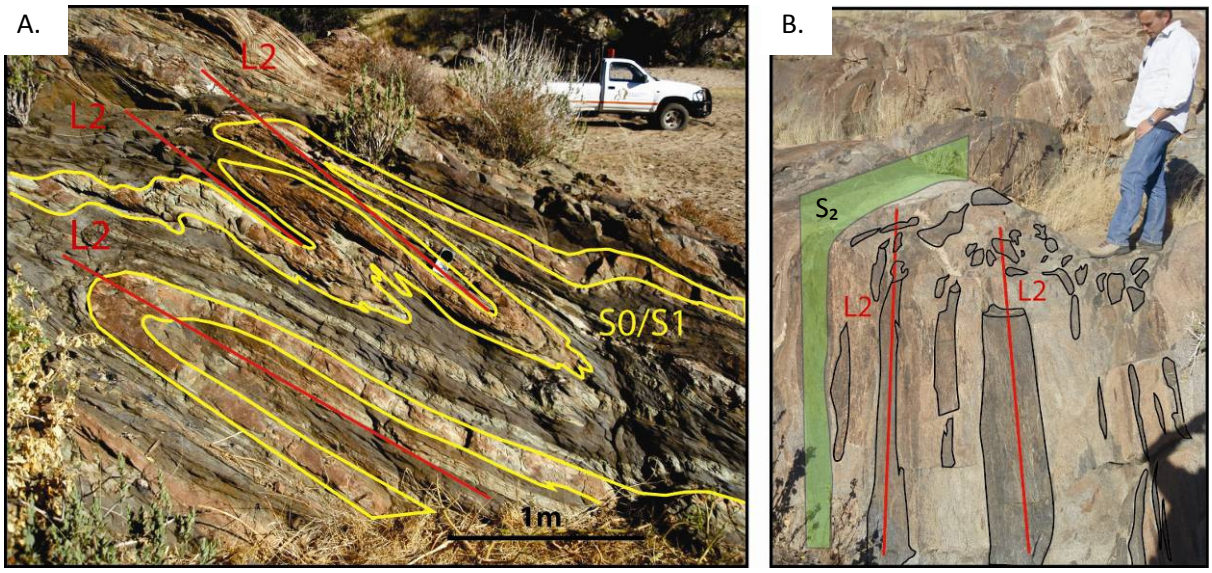

Fig 4.5.9: Prolate fabrics in the Audawib river in the SE of the mapping domain **A.)** Transposed calc-silicate felses, marbles and biotite schist have been tightly folded with axial planes being consistently parallel to each other and to a L_2 lineation in surrounding wall rocks. The traces of axial-planes in fold profiles define a NE plunging L_2C lineation. **B.)** Mafic enclaves in the Palmental diorite have been stretched, forming a very obvious prolate stretching fabric (L_2i). A less pronounced S_2 foliation can also be observed in these diorites.

The prolate fabric seen around the Palmental diorite becomes weaker towards the SE. Where the Hases river runs into the Audawib, prolate mesoscopic folding (Fig 4.5.9) of S_o/S_1 is no longer observed. Nevertheless, a strong mineral lineation (L_2m) and crenulations (L_2c) are found on S_2 cleavage surfaces (Fig 4.5.10 & Fig 4.5.11.A).

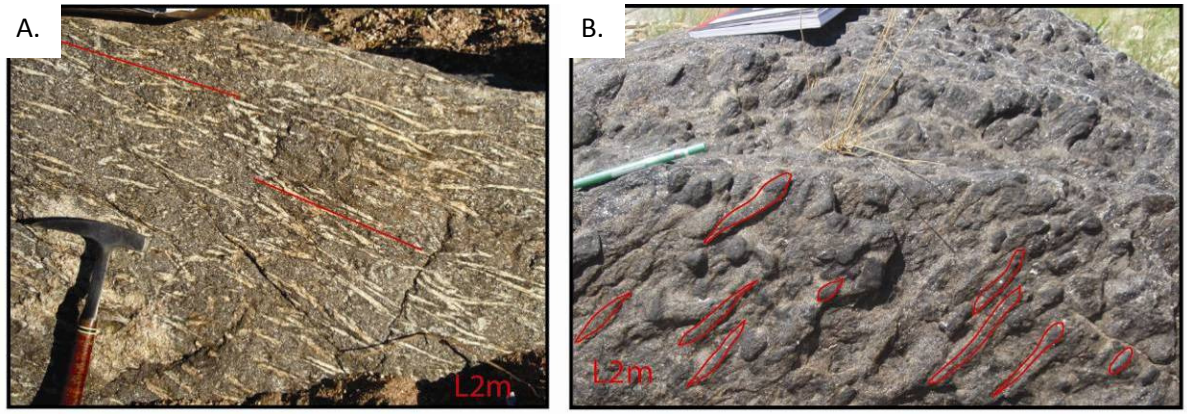

Fig 4.5.10: Mineral lineations (L_2m) in schist developed in foliation surfaces. **A.)** The preferred orientation of silimanite crystals on the S_2 surface defines a lineation.**B.)** A mineral stretching lineation is defined by stretched cordierite crystals on the S_2 surface. Photo A was taken in the Hases river at 22°19'26"S; 16°53'23"E looking NW. Photo B was taken in the Audawib river at 22°18'35"S; 15°56'26"E looking SE.

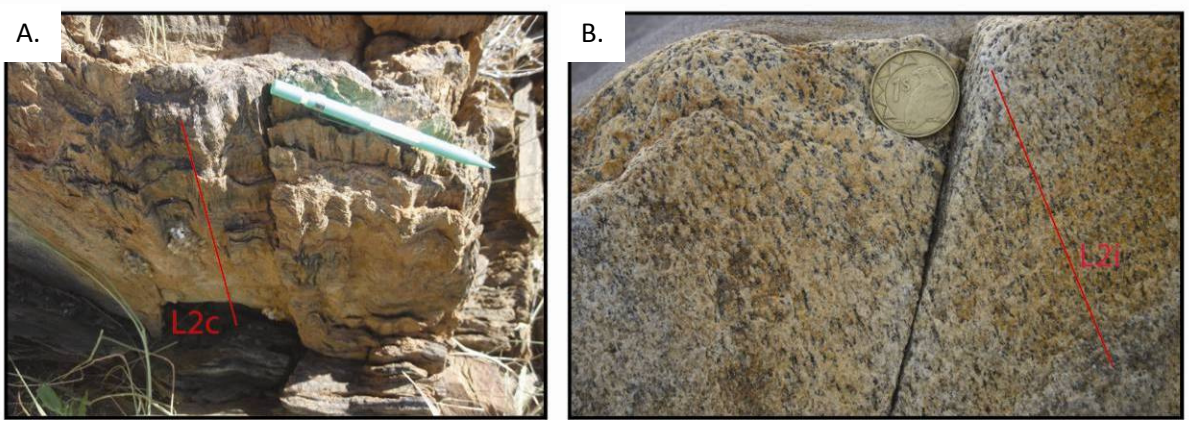

Fig 4.5.11: A.) A crenulation lineation (L_2c) is developed on the S_o/S_1 surface in schists of the Tinkas Formation, small crenulations are have wavelengths of about 15cm. 22°22'16"S; 15°53'19"E. **B.)** A mineral lineation is developed in Palmental diorites and is defined by the preferred orientation of dark horneblende crystals in the rock matrix. This L_2i foliation is developed on a less pronounced S_2 foliation surface in the diorites. This photo was taken at 22°21'52"S; 15°53'26"E looking onto the S_2 foliation surface.

In the NE parts of the Audawib river, linear fabrics are weaker. Here cordierite and sillimanite on S_2 planes only occasionally show a preferred mineral orientation. Boudinage is far more common here and a flattening (oblate) type of strain dominates the area.

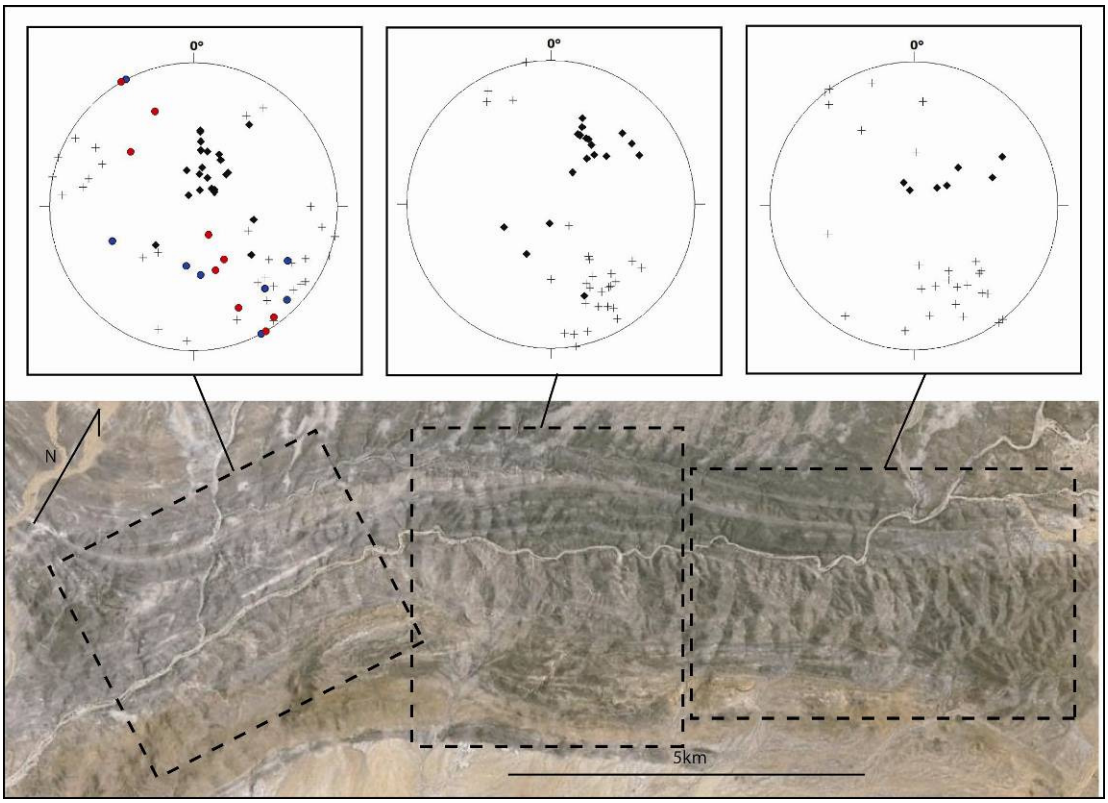

Fig 4.5.12: Foliation and lineation orientations across the SE portion of the Otjimbingwe mapping domain. Foliations are given as poles (+), lineations are represented by black diamonds. Red and blue circles are foliation poles of the Otjimbingwe syenite and Palmental diorite, repectively. All foliations have a roughly upright to SE verging orientation, even for the Otjimbingwe syenite and the Palmental diorite. All linear fabrics plunge steeply towards the NE, these linear fabrics becomes slightly shallower towards the ENE of the mapping domain. In the most NE section of the sub-domain, lineations are only scarcely developed.

In the SE subdomain the S_2 foliation in the DSG shows steep NW dips (ca. 320/75) and the pervasive L_2-fabric plunges, on average, 020/60 (F2 fold plunges, S_2 surface crenulations, mineral stretching lineations and rodded xenoliths) (Fig 4.5.12). The L_2 lineation not only becomes less pronounced NE of the Palmental diorite intrusion, but also becomes slightly shallower as it becomes weaker towards the NE. The L_2 orientation changes from about 020/60 to 030/40 in the middle of this mapping domain (Fig 4.5.12). S_2 stays relatively consistent along strike.

Granite Intrusions

Large parts of the OLZ are intruded by abundant granitoids. The granitoids are texturally and compositionally variable, but seem to be related to one of three main intrusive units, namely the Otjimbingwe syenite, the Palmental diorite and the Donkerhuk granite.

The Otjimbingwe syenite (chapter 3.4.5) forms a roughly oval pluton some 5km in length and 1km wide. The length of this pluton is parallel to the S_2 trending NE-SW. No associated veinlets or dykes are found in rocks of the DSG but the Otjimbingwe syenite shows a sharply cross-cutting, intrusive relationship with rocks of the DSG. The Otjimbingwe syenite contains a strong foliation and lineation (L_2i) defined by the preferred orientation of hornblende and K-feldspar crystals, particularly around its margins (Fig 4.5.13.A). This fabric within the Otjimbingwe syenite becomes weaker some 100 m away from its contact.

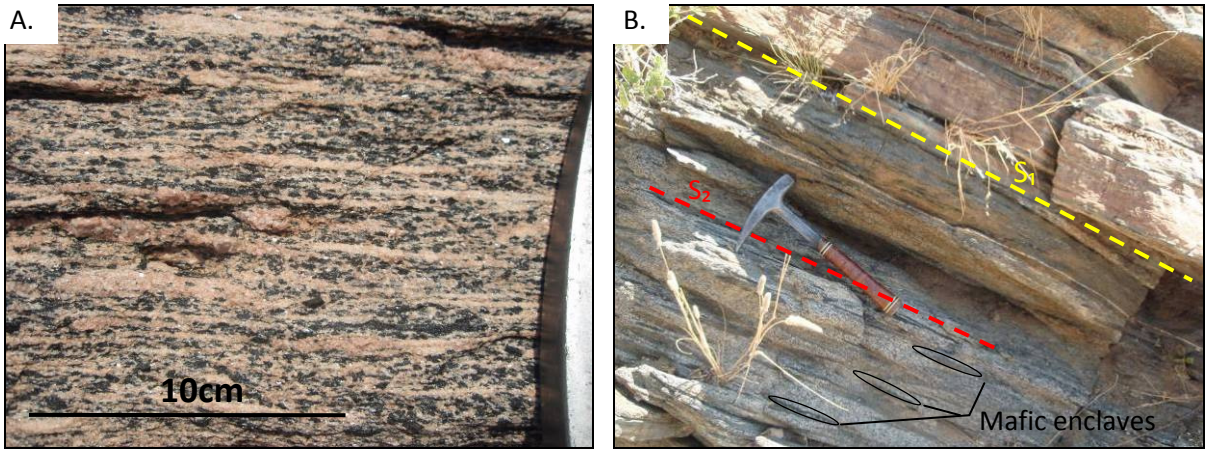

Fig 4.5.13: Linear and planar fabrics within the Otjimbingwe syenite **(A)** and Palmental diorite **(B)** respectively. **A.)** The Otjimbingwe syenite shows lineation (L_2i) defined by the preferred orientation of both K-feldspars (orange) and horneblende crystals (black). This photo was taken at 22°22"16'S; 15°53'19"E looking onto the S_2 foliation plane of the Otjimbingwe syenite. **B.)** The Palmental granite shows a notable S_2 foliation defined by the preferred orientation and flattening of mafic enclaves (red dashed line). Here S_2 foliation in the diorite is parallel to S_0/S_1 (yellow dashed line).This photo was taken at 22°22'9"S; 15°53'12'E looking E.

The foliation in the Otjimbingwe syenite is approximately parallel to that in the rocks of the DSG (Fig 4.5.12). Simairly the lineation in the Otjimbingwe syenite is roughly parallel to L_2 fabrics in the DSG plunging ca. 020/50.

The Palmental diorite is intruded into schist and calc-silicate felses of the Tinkas formation. The main body of this granitoid suite lies just SW of the mapping domain, but numerous smaller (several m wide) dioritic sills have been intruded into surrounding rocks of the Tinkas Formation (this is not the case for the Otjimbingwe syenite). Larger sheets has been intruded as several tens of meters wide sheets. This diorite along with a strong linear mineral fabric shows a less pronounced S_2 mineral foliation defined by preferred orientation of hornblende, subordinate biotite and mafic enclaves (Fig 4.5.13.B). Away from the diorite sills, prolate fabrics, well developed around the central Palmental intrusion, becomes subordinate. Fabrics of the Palmental diorite pluton are roughly similar to those found in the Otjimbingwe syenite (Fig 4.5.14).

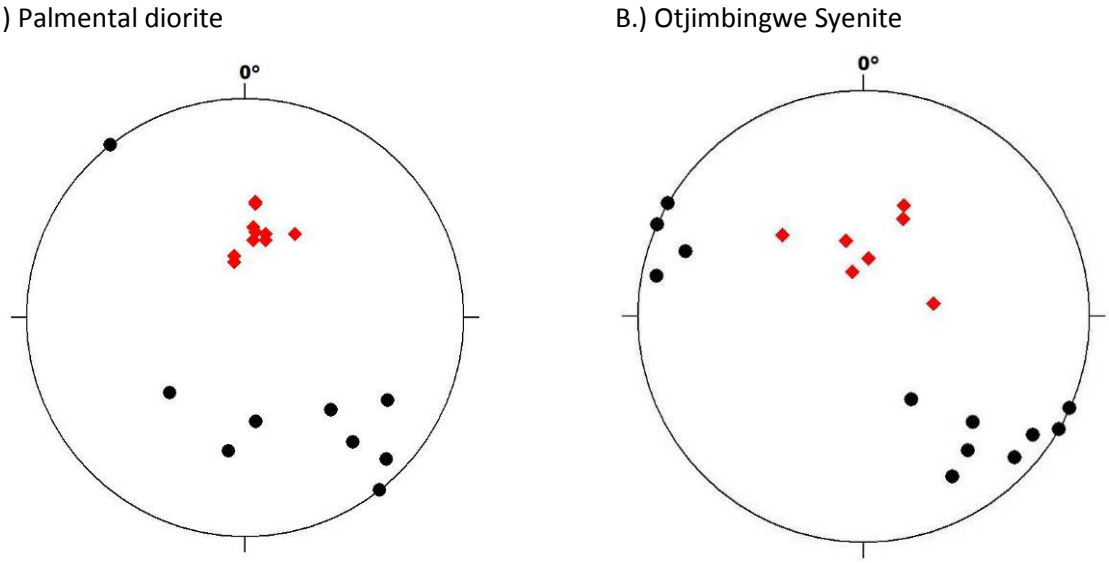

Fig 4.5.14: Structural fabrics within the Palmental diorite (A) and Otjimbingwe syenite (B). Black dots represent the poles to foliations in the granites. Red diamonds indicate the L_2i plunge defined by the aligment of minerals in the respective plutons. Both foliations and lineations in these two intrusive units are roughly concordant. S_2: 320/74; L_2i: 010/50.

Donkerhuk granite and associated granites

The Donkerhuk granite pluton (Chapter 3.4.3) intrudes along the SE boundary of this mapping domain, and shows a lit-par-lit type intrusive contact with schists of the Kuiseb Formation. (Gevers, 1963; Sawyer, 1981; Miller, 1983). Leucogranitic and pegmatoidal dyke/sills swarms of the Donkerhuk intrusion are thought to be intruded into the DSG forming the roof zone of the pluton. Associated with these dykes and sills are localised migmatites in schist within the Donkerhuk aureole (Sawyer, 1981; Miller, 2008)

The central batholith of the Donkerhuk pluton consists of fairly homogenous granites with few observable tectonic fabrics. Magmatic layering can be observed in the centre of this pluton (Fig 3.21).

The multitude of these sills and dykes associated with the Donkerhuk pluton extend outwards deep into the Kuiseb and Tinkas Formations adjacent to the Donkerhuk intrusion. Fine-grained Leucogranitic and pegmatiodal sills and dykes are found as far as 6km across strike away from the main contact between the Donkerhuk granite and the DSG (Fig 4.5.15).

Granites and pegmatites are intruded primarily as homogenous unfoliated sills into the upright S_2 foliation (Fig 4.5.16.A) and in some places into the S_1 foliation (Fig 4.5.17) in the Kuiseb and Tinkas Formations adjacent to contact zone. Large (mostly composite) granites sills can be up to 100m wide and up to 3km long. Sills are on average ca. 50 cm to 3 m wide extending for a few 100m along strike. Smaller granite veinlets (2mm-20cm wide) are quite common in schist and are often folded (Fig 4.5.16.B).

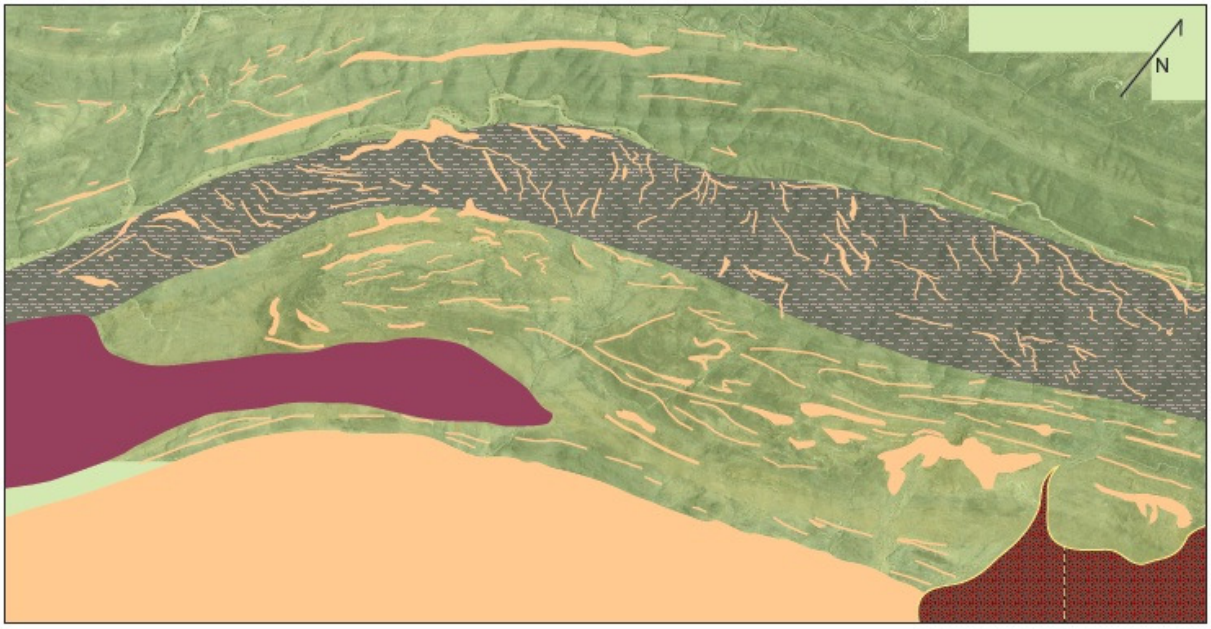

Fig 4.5.15: The "intrusive aureole" of the Donkerhuk granite. A great number of sills and dykes (annoted as pink lines) associated with the Donkerhuk granite have been intruded into rocks of the Tinkas and Kuiseb Formations. The majority of these intrusive units are sills. Dykes are more common in the crystalline calc-silicate fels and marble unit (green) in the centre of this figure. Sills are mostly intruded into the S_2 foliation in the DSG and thus trend roughly NE.

Many of the smaller veinlets especially those close to the Donkerhuk granite contact seem to show distinct leucosomes and melanosomes suggesting that veinlets might be the result of partial melting of schists (as suggested by Sawyer (1981) and Miller (2008)).

In the central calc-silicate fels and marble unit of the Tinkas Formation, granites typically cross cut the rocks as dykes, with only a few granites intruding as sills existing. The dyke-to-sill ratio in this rock unit is about 5:1.

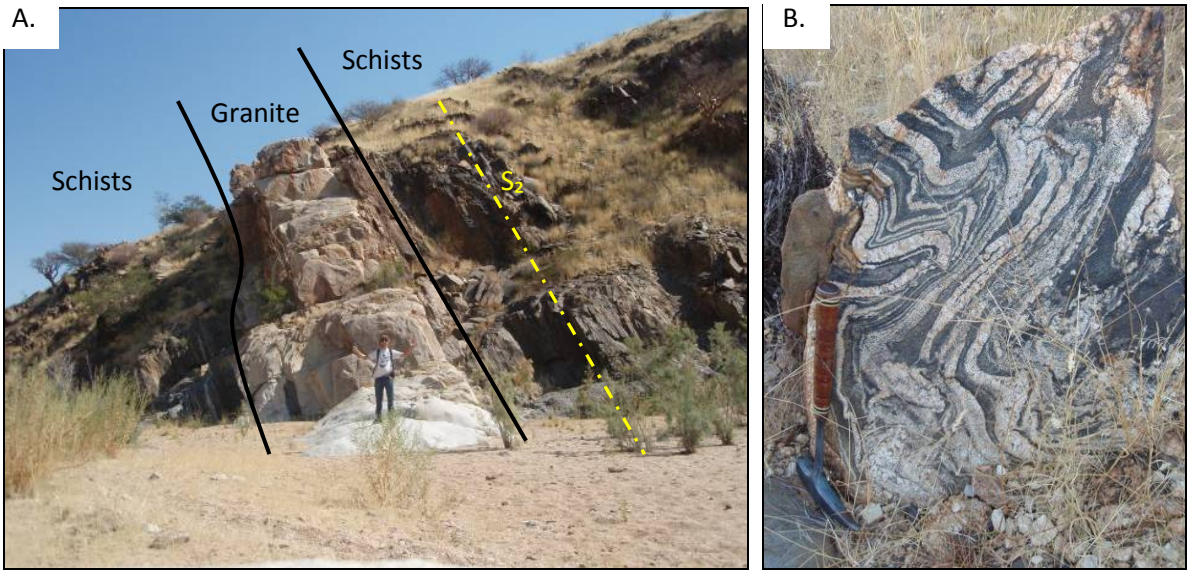

Fig 4.5.16: Leucogranitic sills intruded into the Tinkas Formation in the roof zone of the Donkerhuk batholith. A.) Large sills such as this one can be many meters wide. Such sills are typically undeformed and have intruded along the S_2 foliation. This sill dips steeply towards the NW. This photo was taken in the Audawib river at 22°18"9'S; 15°57'6"E, looking SW. B.) Smaller sills/veinlets are also found alongside larger sills in schists of the Tinkas and Kuiseb Formations. Granite veinlets are often only a few mm wide. A rheology contrast between schists and granite veinlets often results in tight folding.

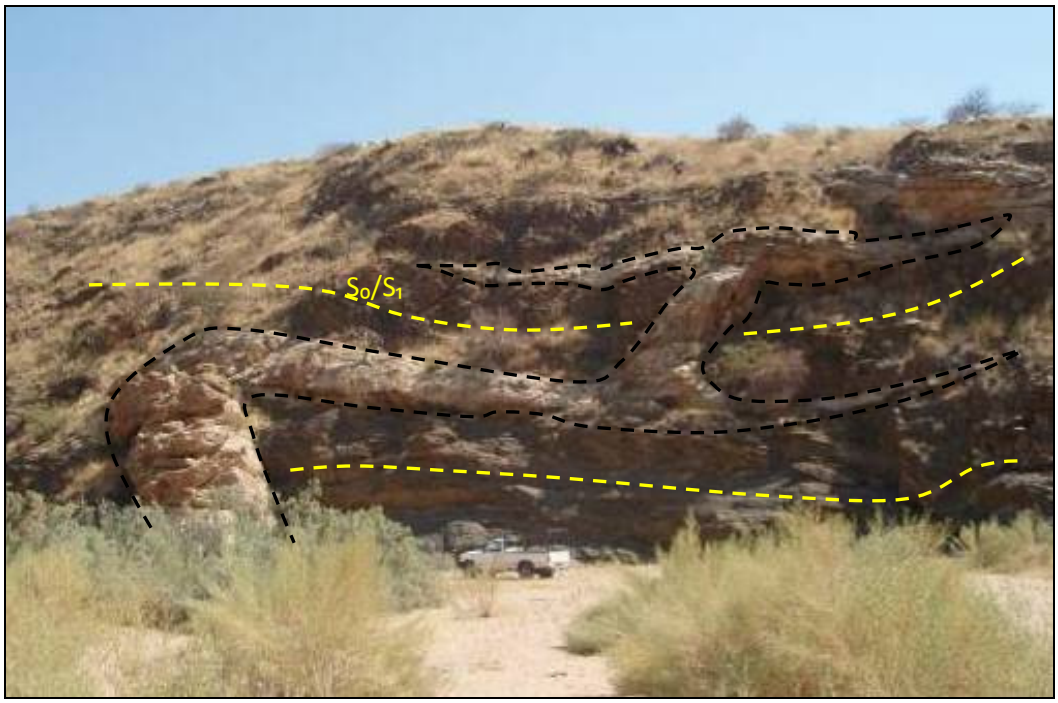

Fig 4.5.17: Granite sheeting in the Tinkas Formation. This granite sheet intruded along an upright S_2 foliation and formed sill-like body along a shallow S_0/S_1. It's likely that such intrusive features introduced strength beams into the crust, shielding shallow bedding from further tight transposition. This photo was taken in the Audawib river at 22°18'24"S; 15°56'45"E looking SW. This is the only location in the Audawib river where open folding can be observed.

Granite sheets and dykes are occasionally folded, indicating at least late-tectonic emplacement of granites. Smaller granite sills are commonly tightly folded and even transposed, whereas larger (>3m

wide) sills and dykes show only open folding. In much of the Otjimbingwe domain and especially in the NW part of the domain, smaller granite sills up to 1m wide are often boudinaged (Fig 4.5.7).

Deformed and undeformed sills and dykes are often found adjacent to each other thus emphasising the syn- to late-tectonic (D2) emplacement. Fig 4.5.18 shows a xenolith of folded rocks of the Tinkas Formation within a 6-8 m wide sill. Wall rocks identical to the entrained xenolith adjacent the granite sill have been completely transposed into S_2. This suggests that the granite intrusion shielded the wall-rock xenolith from progressive deformation, preserving earlier fold geometries. (Fig 4.5.18). Such intrusive features suggest that granites must have played a significant role in strain partitioning in this domain during progressive deformation, either weakening the crust when in a molten state, or providing strength beams when granites were fully crystallized (Fig 4.5.17).

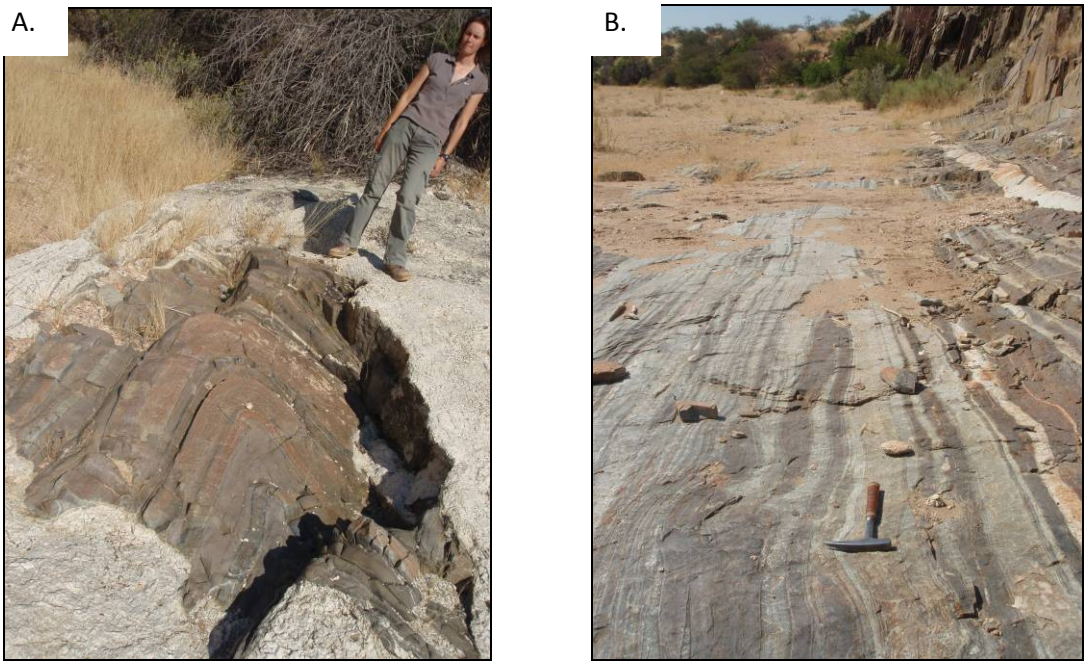

Fig 4.5.18: Granites shielding metasediments from deformation. **A.)** An isolated schist/calc-silicate fels xenolith in caught up in a granite intrusion show moderate to tight folding. **B.)** Similar rocks adjacent to the granite sill (A.) are completely transposed. The granite sill likely enveloped the metasedimentary xenolith during an earlier stage of folding. After crystallization of the granite sill, the metasedimentary xenolith was shielded from complete transposition. This photo was taken in the Audawib River at 22°18'3"S; 15°57'21"E, photo A was taken looking WSW, photo B lies just 15m S of the granite photo and was taken looking ENE.

Summary

The Otjimbingwe domain spans the boundary between the SCZ (sensu stricto) and the OLZ. This transition is characterized by marked structural changes as well as changes in the stratigraphy, from the marble dominated Karibib Formation in the north into the Tinkas Formation in the S.

From NW to SE and into the OLZ, there is a general increase in fabric and strain intensities. Upright, open folding in rocks of the Kuiseb Formation in the NW parts of the domain gives way to tight- to

isoclinal, upright to SE-verging folds and associated pervasive bedding transposition. Associated with this transposition folding is a very strong S_2 foliation that, for the most part, completely overprints earlier fabrics and bedding. Symmetrical folding and boudinage and conjugate shear bands all point to a subhorizontal NW-SE directed bulk shortening strain during fabric development. Non-coaxial fabrics are conspicuous by their absence and only developed in a few isolated locations close to folds. Flattening type strain recorded in the NE sector of the OLZ is succeeded by steep- to moderately NE plunging prolate fabrics around the Palmental diorite. Coaxial linear fabrics in both the Palmental diorite and DSG, suggest syn-tectonic intrusion of Palmental granite sills.

Numerous syn- and late-tectonic granites have been intruded into the OHL zone. Granite and pegmatite sills are intruded primary parallel to the subvertical S_2 foliation. The progressive deformation of sills indicates syn- to late- and post-tectonic emplacement.

Chapter 5 Discussion

The 40 km long traverse through the southern parts of the SCZ studied here represents a section through the forearc region of a convergent and, eventually, collisional Pan-African plate boundary, recording convergence from ca. 600-580Ma and the final collisional stages at ca. 540-510Ma (Miller, 2008). The following discussion aims to (1) characterize the structural evolution of each of the mapping domains described in the previous chapters, (2) integrate the structural and lithological characteristics of each domain in order to develop a possible geodynamic setting and evolution of this part of the SCZ, and (3) compare the structural inventory of this ancient plate margin with structurally similar, more modern fore-arc regions. This chapter discusses the data across the study area from SE to NW and from the presumably leading edge of the overriding plate into the retro-arc region and continental interior of the Congo craton.

5.1 The Otjimbingwe domain and Okahandja Lineament Zone

5.1.1 The Okahandja Lineament Zone

The SE mapping domain encompasses the OLZ along its SE margin thought to represent the leading edge of the Congo Craton. The significance of the OLZ as a major crustal feature of the Damara belt has been noted by many previous workers based on lithological and facies variations across the zone (Blaine, 1977; Downing & Coward, 1981; Miller, 1983; De Kock, 1989; 2001), a sharp metamorphic break between the high-P, medium-T rocks of the SZ and the high-T, low-P rocks of the CZ (Puhan, 1983; Kasch, 1983b, Miller, 2008), differences in structural style and vergence direction of structures (Miller, 1983; Kukla & Stanistreet, 1991) and the prominent geophysical signature of this zone (e.g. Corner, 2000). In addition, the OLZ marks the northern margin of the massive Donkerhuk batholith (Smith, 1965; Sawyer, 1981; De Kock, 1989; Miller, 2008).

Lithologically, basement rocks and the lower formations of the DSG (e.g. Nosib Group and Etusis Formation) are not exposed along the OLZ, whereas the marble succession of the Karibib Formation is replaced by the heterogenous Tinkas Formation. The Tinkas Formation is thought to represent basin-slope type turbidite deposits (Miller, 1979; Porada & Wittig, 1983; Kukla et al. 1990) along the transition from the passive continental margin of the Congo Craton, showing shelf-type carbonate sedimention of the Karibib Formation, into the deeper marine environment of the Khomas Sea to the S, characterized by turbidites (Fig 2.4).

A prominent unit of thinly bedded calc-silicates and marbles characterised by transposed bedding (Fig 5.1, Appendix V) corresponds to what De Kock (2001) has termed the Lievental Member of the Tinkas Formation. The Lievental Member seems to occupy a central stratigraphic position within the

Tinkas Formation in this domain. It is both over- and underlain to the NW and SE by the Tinkas Formation sensu stricto, (i.e. dominantly biotite-quartz schist and lesser marble and calcsilicate units) grading into the entirely siliciclastic units of the Kuiseb Formation away from the central Lievental Member. This map pattern suggests the presence of a large, antiformal structure developed along the OLZ (Fig 5.1).

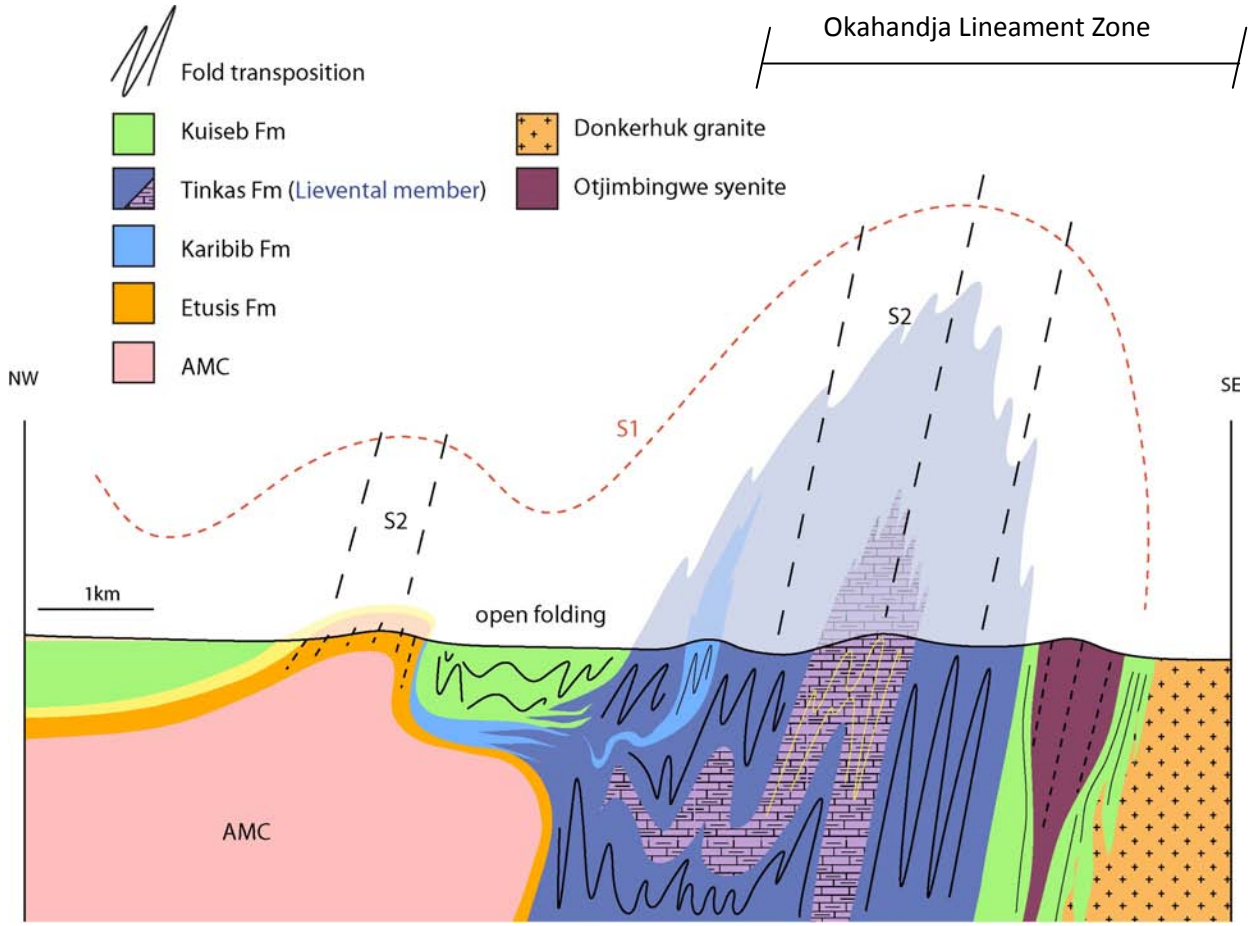

Fig 5.1: Cross-section through the Otjimbingwe mapping domain. The SE part of the domain shows tight-isoclinal upright SE-vergent folding, and a structure cored by De Kock's (2001) Lievental Member implies a larger scale antiform. F2 fold transposition has largely overprinted S_1 in the SE part of this mapping domain. From the NW the Karibib Formation grades into the Tinkas Formation which has been significantly thickened. (The location of this figure is annotated in map no.4)

Upright, isoclinal folding and associated bedding transposition into the steep and pervasively developed S_2 fabric characterize the structural geology of the OLZ over a width of 4.5 km. Isoclinal folding and bedding transposition also indicate significant telescoping of lithologic units. Overall shortening strains are difficult to determine, but the folding of e.g. granitic apophyses in schists or marble units in individual outcrops indicate a minimum shortening strain of 70-80%. Predominantly chocolate-tablet type boudinage of competent units and/or granite apophyses, the symmetrical folding of units as well as a L_2 mineral and stretching lineation are all developed in the S_2 plane. Fold plunges of isoclinal folds range from vertical to horizontal. Mineral stretching lineations show moderate- to steep plunges to the NE. Importantly, non-coaxial fabrics and shear-sense asymmetry

are rare and inconsistent, and mostly related to localized structures as part of e.g. conjugate shear zones (Fig 4.5.8.B) that accommodate the otherwise D2 coaxial layer flattening normal to S2. The, in places, steep fold plunges together with steeply plunging stretching lineations also indicate that the penetrative D2 flattening strains are associated with a steep stretch. This stretch becomes more prominent to the SW along strike of the OLZ centred around the intrusions of the Palmental diorite and, to a lesser extent, the Otjimbingwe syenite. The gradual transition from flattening to constrictional-type fabrics towards the intrusions suggests a spatial and temporal relationship between fabric development and the emplacement of the plutons. Both intrusive units show pervasive magmatic and solid-state prolate fabrics parallel to D2 fabrics developed in the wall-rocks (Fig 4.5.9 & Fig 4.5.13). The presence of L_2-parallel magmatic and solid-state fabrics implies a syn-D2 emplacement of the plutons and is consistent with the oblique extrusion of the rocks during subhorizontal D2 co-axial shortening. The localized extrusion may record a rheological weakening of the rocks around the plutons, at least during their emplacement and in the presence of a melt phase. Though no robust age exists for the Palmental diorite the Otjimbinge syenite is estimated to have intruded at ca. 520±9 Ma (Jung et al. 1998) and the Donkerhuk granite between 532 Ma and 527 Ma (Blaxland et al., 1979; Haack & Gohn, 1988; Miller, 2008). This suggests that D2 tectonism was still active along the OLZ between 530 Ma and 520 Ma.

The lack of non-coaxial fabrics in the high-strain rocks is somewhat surprising and contrasts with previous models that suggested a significant lateral component of movement along the OLZ displacement and, hence, oblique convergence and collisional tectonics. Blaine (1977), Stanistreet et al. (1991), Kukla (1992) and De Kock (1992) all suggested a dextral, oblique-slip displacement along the OLZ. In contrast, Oliver (1994), Downing & Coward (1981), and Tack & Bowden (1999) postulated sinistral displacement interpreted to record oblique convergence and collision between the two cratons. Numerical and experimental studies of transpressional systems have emphasized that finite strains and strain analysis are only of limited use to infer bulk kinematics of e.g. obliquely convergent margins (e.g. Fossen and Tikoff, 1993; Tikoff and Peterson, 1998; Merle and Gapais, 1997). During oblique convergence and/or collision, combinations of pure shear normal and simple shear parallel to the deformation zone depend on a number of factors, most importantly the angle of convergence. Even at relatively low angles of convergence of > 20-25° (0° - parallel, and 90° - normal to convergent margin), most models indicate that finite strains in rocks should record a predominantly co-axial flattening component. In natural and lithological and structurally heterogeneous successions, however, the bulk strain is commonly partitioned into pure- and a simple-shear components. The simple-shear component is preferentially partitioned into rheologically weaker units (e.g. Saint de Blanquat et al., 1998) such as (warm, partially-molten) intrusions or relatively incompetent

lithological packages. These units may then localize planar or anastomosing, margin-parallel, mainly steeply-dipping, strike-slip dominated shear zones. The pure-shear component is accommodated in the intervening areas through e.g. folding and axial planar foliation development. In the case of the OLZ, strain is dominated by subvertical co-axial flattening-type fabrics. Strike-slip shear zones and non-coaxial fabrics that would indicate a strike-slip component of the bulk D2 strain are not observed, despite the good outcrop in large parts of the OLZ. Strike-slip shearing is also not recorded in the various granitoid intrusions that, based on their progressive deformation, have intruded during D2 deformation. Similarly, the rheologically weak marble horizons show pervasive fabrics and high finite strains, but non-coaxial fabrics are not recorded. This lack of non-coaxial fabrics is here interpreted to indicate the OLZ is a zone of flattening related to high-angle convergence and subsequent collision between the Congo and Kalahari Cratons.

Subhorizontal, co-axial shortening strains, the formation of pervasive bedding transposition and development of regional-scale upright antiformal folds have also been described from recent forearc settings, such as the Kodiak Islands, off the Alaskan coast (e.g. Sample and Moore, 1987; Fisher and Byrne, 1992). The Kodiak Islands are underlain by an accretionary prism overlying the Aleutian trench that records tectonic underplating of marine sediments due to NW-ward subduction of the Pacific Plate below SW Alaska since the Late Cretaceous. Seaward (SE-directed) thrusting and imbrication is recorded in a several tens of kilometer wide complex overlying the trench, corresponding to the accretionary wedge complex. Shallow NW-dipping, predominantly non-coaxial fabrics dominate this zone of thrust imbrication that accommodates the movement of the accretionary wedge over the underlying detachment above the downgoing plate. Shallowly-dipping, non-coaxial fabrics, grade upwards into steeply dipping fabrics that record a largely layer- (foliation-) normal co-axial shortening strain. The steepening of fabrics is thought to have been the result of progressive underplating of sediments at the base of the accretionary wedge and the upward translation of rocks relative to the basal detachment as younger units are underplated. As a consequence, the rocks are undergoing a composite strain path from earlier non-coaxial strain, closer to the detachment, to subsequent subhorizontal co-axial shortening as rocks are rotated to steeper attitudes and, hence, orientated at high angles to the crustal convergence (e.g. Fisher and Byrne, 1992; Kusky et al., 1997).

In case of the Damara Belt, SE-verging thrusting and associated NW-dipping non-coaxial fabrics characterize large parts of the SZ, immediately south of the OLZ, and are interpreted to represent the accretionary prism complex of the Damara Belt (e.g. Kukla & Stanistreet, 1991). Large-scale upright folding and pervasively developed co-axial flattening strains in the OLZ may then correspond

to the structurally higher levels, close to the backstop of the accretionary prism. The steep stretch recorded in rocks of the OLZ is consistent with the upward translation of rocks. This may also account for the prominent metamorphic break along the OLZ, forming the boundary between the high-T, low- to medium P rocks of the SCZ in the NW to the low- to medium T, high P rocks characteristic of the SZ (Kukla & Stanistreet, 1991). The expected earlier history of non-coaxial shearing is, however, not evident in rocks of the OLZ. It is conceivable that these earlier fabrics may have been overprinted by the later shortening fabrics. However, xenoliths of folded Kuiseb Formation in synkinematic granite apophyses seem to preserve the earlier phases of deformation in the OLZ (Fig 4.5.18) and the open- to close, symmetrical folds also point to a co-axial strain history rather than non-coaxial shearing along low-angle fabrics.

5.1.2 The northern Otjimbingwe domain

To the N of the upright transposition zone that characterizes the OLZ, folding is still dominated by D2 strains, i.e. NE-trending, upright to slightly SE-verging folds and an associated axial planar S_2 foliation. However, fold geometries are more open, bedding transposition is subordinate and confined to narrow, commonly < 100 m wide corridors, fabric intensities are lower, pointing to overall lower strain intensities. This transition occurs (over an across-strike distance) of less than 1-2 km. Moreover, rocks of the lower DSG are exposed in the northern Otjimbingwe domain, including the continental rift-type sedimentary sequence of the Etusis Formation. The occurrence of the rift related Etusis Formation also points to the presence of underlying basement rocks, being the southernmost indication of the leading edge of the Congo Craton. The spatial correlation between the presence of basement rocks and a rapid change in structural style is unlikely to be coincidental. It probably indicates that thick, rigid continental crust of the Congo Craton protected the overlying supracrustals from pervasive strain during the D2 event of the Damara orogeny.

Overall, the OLZ and northern Otjimbingwe domain along the leading edge of the Congo Craton mark an important divide in structural style and vergence direction in this part of the Damara Belt. This zone of upright folding and subhorizontal shortening strains is the link or transition between the predominantly SE-verging fold-and-thrust belt of the SZ in the forearc region to the S and the predominantly NW-verging fold-and thrust belt of the retroarc region to the NW (Appendix V).

5.2 Audawib domain

The geology of the Audawib domain is dominated by the Audawib fold complex and the Salem-type granite. The series of SW-NE trending km-scale F2 folds refolds gneisses of AMC, and rocks of the Etusis, Karibib and Kuiseb Formations, resulting in a type 3 fold interference pattern of refolded folds (Fig 5.2). Importantly, in all of these either NW- or SE-verging F2 folds, the stratigraphy is consistently inverted with gneisses of the AMC overlying rocks of the DSG. The foliation in gneisses of the AMC is parallel to the bedding-parallel foliation (S_1) in the overlying DSG indicating the development of a overprinting foliation in basement and the overlying supracrustal rocks. The stratigraphic inversion is most likely explained by the presence of a recumbent, basement-cored fold nappe in which the present level of erosion exposes the overturned limb of the fold (Fig 5.2). Regional-scale recumbent folds have been described to be typical of the D1 deformation in the Damara belt (Blaine, 1977; Downing & Coward, 1981; Miller, 1983) such as the Rooi-Kuiseb anticline found some 50 km SW along strike of the Audawib fold complex that has been described by Downing & Coward (1981) as a refolded F1 nappe structure. The inversion of the stratigraphy, orientation of fabric elements and refolding of the first-order fold all point to the fact that the Audawib fold complex represents a km-scale F1 nappe that has been refolded by F2 folds.

The lithological succession exposed in the Audawib fold complex is typical for this part of the SCZ, including the Etusis Formation, highly recrystallized and thin units of the Karibib Formation and the overlying Kuiseb Formation. This would argue against the completely allochtonous nature of the rocks and a far-field transport of the nappe, which seems rather para-autochtonous. If a root zone of the nappe were to be identified, it would have to be located in the SW of the Audawib fold complex. This zone is characterized by a shear zone that extends along the contact between the Salem-type granites to the SE of the Audawib fold complex and AMC gneisses in the NW. Numerous, highly sheared and exotic blocks of the DSG along this contact also suggest the presence of a shear zone. The trend of the shear zone and allochthonous blocks contained within it is parallel to the F2 folds and foliations in the Salem granite surrounding the Audawib fold complex. This implies roughly synchronous F2 folding, granite intrusion, and shearing along the AMC/Salem suite margin. If the root zone of the Audawib fold complex is located along the SE shear zone, the F1 nappe structure would close to the NW (Fig 5.2).

The sheet-like Salem granite structurally underlies the Audawib fold complex. Given the syn-D2 timing of the granite, the granite sheet may have effectively decoupled the F1 nappe from the underlying rocks.

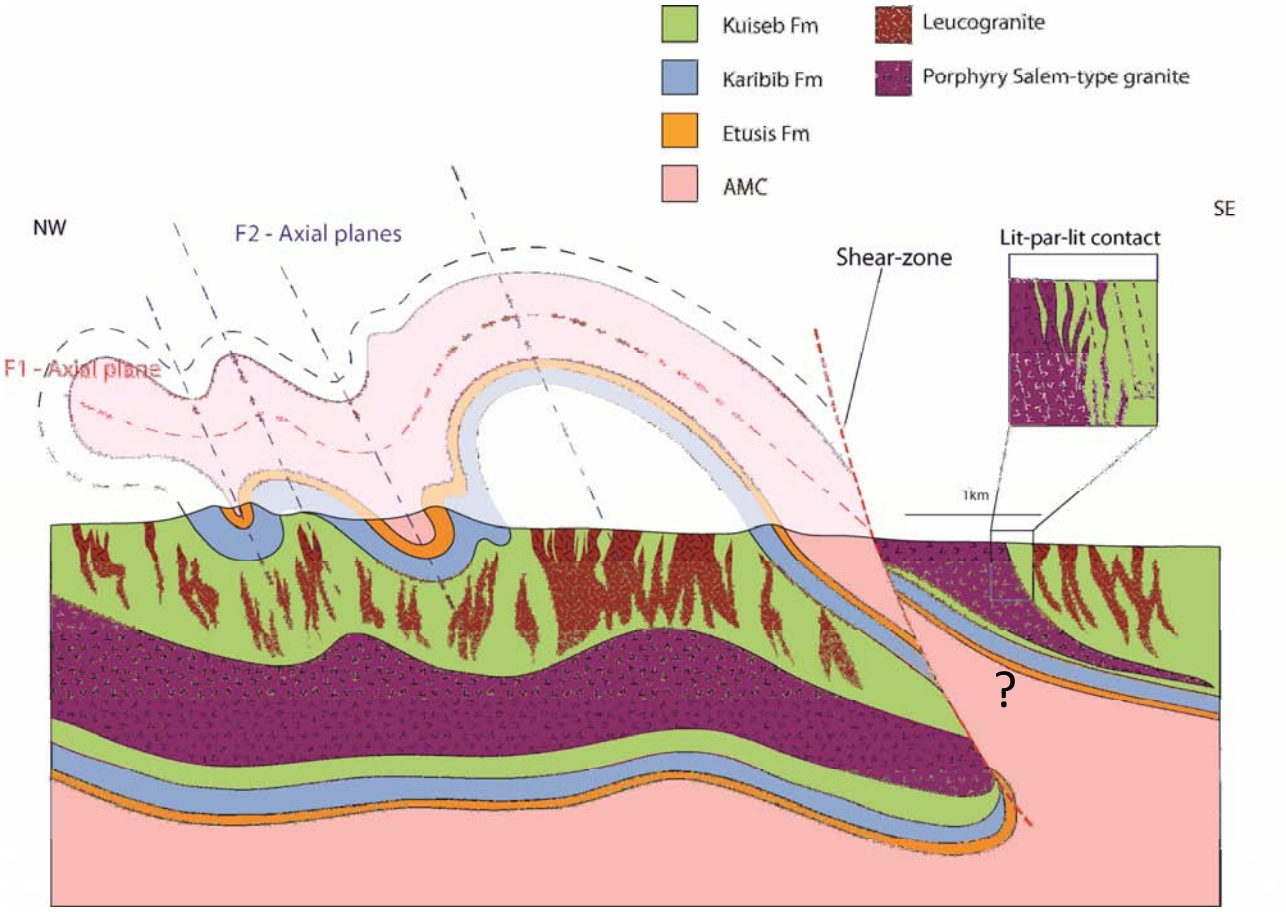

Fig 5.2: A cross-section of the basement cored nappe that forms the Audawib fold complex. The shear zone at the SE boundary of the fold complex is interpreted to be the root of the F1 recumbent nappe, refolded during D2 to form smaller NW-verging 2nd order F2 folds. The Salem-type granite below the nappe helped to accomodate shearing and progressive D2 deformation.

The recumbent (F1), refolded (F2) Audawib fold complex is inferred to close towards the NW, implying a NW vergence and transport (D1) direction of the nappe complex. NW transportation is also suggested by the strongly doubly plunging geometry of the F1 nappe, resulting in a sheath-like geometry. Similar km-scale crystalline nappes that indicate transport away from the trench and onto the retroarc region are widely documented from e.g. the Swiss and Austrian Alps (Froitzheim, 1992; Escher & Beaumont, 1997; Schmid et al., 2004). The formation of these nappe structures along retroshears has also been modeled in numerical and analogue models of collision zones (e.g. Pfiffner et al., 2000). These works show that crystalline nappes verging towards the retroarc form preferentially under conditions of (1) a rheologically weakened overriding plate. This weakening may be the result of e.g. heat advection due to the emplacement of granitoids in the magmatic arc or a weak inherited structure as the result of previous terrane accretion to the overriding plate, and (2) relatively low-angle subduction, causing the formation of a contractional back-arc and, thus, thick-skinned thrusting towards the retroarc region. This is also observed in parts of the Andes, where

basement uplifts and thick-skinned thrusting are recorded in regions of shallow subduction (e.g. Kley, 1996; Kley & Monaldi 1998).

Both prerequisites for the formation of retroarc-verging nappes seem to be present in the SCZ during the D1 and D2 deformation. The regional high-T low-P metamorphism and early dioritic plutonism are likely to have weakened the leading edge of the Congo crust. Indeed, the pervasive refoliation of rocks of the AMC parallel to the DSG illustrate that temperatures during deformation were above the onset of feldspar plasticity. Moreover, given that ocean-floor formation in the Khomas Sea is believed to have occurred at only ca. 625 Ma (Miller, 2008), the subsequent reversal of spreading and onset of convergence at ca. 600 Ma must have involved young and, thereby, relatively buoyant oceanic crust in the subduction. Hence, the closure of the Khomas Sea was most likely associated with shallow subduction, so that stresses during the convergence and collision could be transmitted into the retroarc region of the collisional orogen.

The timing, orientation, NW-facing direction and progressive deformation of the Audawib fold complex is consistent with its origin along a retroshear (i.e. vergence is towards the retroarc and away from the collisional suture in the S) situated on the overriding plate of the Congo Craton. Early low-angle shearing and nappe formation involving both basement gneisses and the overlying DSG during the early stages of collision (D1) illustrate the thick-skinned nature of deformation close to (within ca. 10-15km) the leading edge of the overriding craton. Similar to the Otjimbingwe domain in the immediate S, the subsequent D2 strains record a subhorizontal, NW-SE directed shortening. The upright- to bivergent F2 refolding of the earlier recumbent fold indicates that lateral translation and low-angle thrusting that dominated the D1 deformation were no longer possible during D2. Importantly, the F1/F2 fold interference pattern displayed by both the regional-scale Audawib fold complex and also the Rooi-Kuiseb antiform suggest that D1 and D2 can be regarded as a progressive deformation event. This would explain the often co-axial nature of D1 and D2 fabrics and structures that are, in places, only distinguished with difficulty.

5.3 Salem-type granites of the Dorneb domain

The Dorneb domain is almost entirely underlain by Salem-type granites. These granites have intruded into SE-dipping rocks of the Kuiseb Formation. On a regional scale, cross-cutting relationships suggest a post-D1, syn-D2 timing of emplacement of the Salem-type granites (Jacob, 1974; Miller, 1983, 2008) and the granites in the Dorneb domain are no exception. Radiometric ages of Salem-type granites suggest a emplacement of ca. 550-540 Ma (Haack et al., 1983; Johnson et al., 2006; Miller, 2008).

Moreover, the Salem granite in the Dorneb domain shows a number of characteristics commonly described for Salem granites by previous authors (e.g. Jacob, 1974; Miller, 1965; Miller, 1983). This includes its location in a regional-scale synclinal structure cored by schists of the Kuiseb Formation, its sheeted nature with upper biotite-rich, megacrystic granites underlain by leucogranites and the variable degrees of wall-rock assimilation (summarized in Miller, 2008).

Salem-type granite typically intrude in a lit-par-lit fashion into the Kuiseb Formation. D2 deformation of previously shallowly dipping schist (as is seen NW of the Salem granite pluton) accompanied with Salem-type granite intrusion (causing crustal weakening), led to the re-orientation of fabrics in schist of the Kuiseb Formations, resulting in steeply SE dipping fabrics in both schist and Salem-type granites that are (parallel to the trend of D2 structures across the Damara belt).

Shallow contacts between the leucogranites (Salem-type) and the porphyritic Salem-type granite imply a shallow S-dipping sheeted intrusion of the Salem "batholith" in this domain. This intrusive unit likely provided a strength beam in the crust after crystallization, shielding the central portion of this domain from any further fold amplification and tightening. As such this 1st order syncline is developed as a broad, large-wavelength, low amplitude synclinal structure (Fig 5.3).

Isolated masses of leuco-granites in schists of the Kuiseb Formation do not seem to represent intrusive sheets, and migmatic textures associated with these suggests that these are granites formed by the partial melting of the Kuiseb Formations due to Salem granite intrusion as described by Miller (2008).

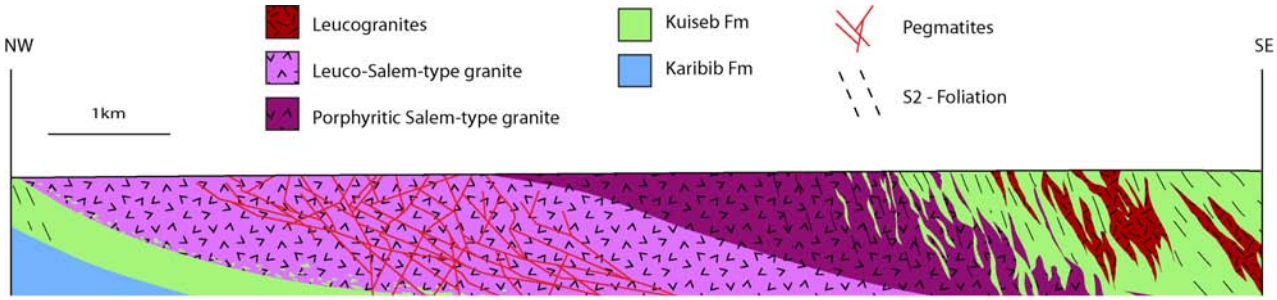

Fig 5.3: The Dorneb mapping domain is cored relatively shallowly intruded D2 Salem-type granites intruded into schist of the Kuiseb Formation. This intrusive body must have provided a strength beam in the crust shielding the middle of the traverse from forther defromation.

5.4 The Etusis mapping domain

Lithologically, this is the most heterogeneous domain. It represents the transition from the southern parts of the SCZ, dominated by the Kuiseb Formation and only sporadic outcrops of other formations, such as the Etusis and Karibib Formations, to the northern parts of the SCZ, where the central parts of the DSG are well developed, reaching a thickness of several thousand meters, in places (Jacob, 1974; Badenhorst, 1992; Miller, 2008). In addition a variety of Pan-African granitoids occur in this domain that straddles the central basement window of the AMC (sensu stricto) (Brand, 1987; Steven 1993).

Rocks of the Nosib and lower Swakop Groups are not developed throughout the Etusis domain, but are rather preserved as a wedge-shaped sequence (in plan view) in the SW parts of the domain, showing a substantial thickening to the SW. Unconformable contacts between the Etusis Formation and the basement gneisses are well preserved and both angular unconformities as well as basal conglomerates in the Etusis Formation can be demonstrated for the basement-cover contacts. This contrasts with basement-cover relationships further S in e.g. the Audawib domain, where the presumably originally unconformable contacts have been completely obliterated by later strains and where the basement rocks have been pervasively refoliated. The wedge-shaped geometry of the sedimentary package together with the coarse conglomeratic development of particularly the Etusis, Okawayo and Ghaub Formations may indicate their deposition in a repeatedly reactivated half-graben structure and that the deposition of these rocks was controlled by basement topography created during normal faulting. Rapid facies and thickness variations are, indeed, invoked by a number of authors across the Damara belt as being the result of heterogeneous basement topography and graben fills, particularly during the early rift-type sedimentation (Smith, 1965; Jacob, 1974; Hoffmann, 1990; Stanistreet et al., 1991; De Kock, 2001; Miller, 2008). Despite this, the pinching and disappearance of most of these formations over an along-strike distance of merely 2km is difficult to explain by facies variations only. Layers do not gradually pinch out northward, but appear truncated, particularly against the highly-recrystallized marbles of the lower Karibib Formation. In general, the progressive obliteration of primary sedimentary structures and features recorded from the upper parts into the lower, pervasively recrystallized and seemingly homogeneous parts of the Karibib Formation indicates a strain gradient towards the base of the marble unit. High-strain textures or kinematic indicators that can be expected in e.g. mylonites developed in siliclastic rocks are absent from the marble units that readily recrystallize under the high-grade metamorphic conditions. However, where stratigraphic relationships can be shown, pervasively recrystrallized marbles can be demonstrated to be developed in e.g. thrust zones or high-strain zones (e.g. Kisters et al., 2004; Johnson et al., 2006). In the Etusis domain, the role of the

basal, strongly recrystallized marbles as high-strain zones is indicated by, at least, three aspects. These includes (1) the aforementioned truncation of units against the marbles, (2) the seemingly transgressive nature of the basal parts of the Karibib Formation (In the SW, the marbles overlie rocks of the Ghaub Formation, but cut down in the sequence to the contact with the Habis granite in the E), and (3) the development of mylonitic fabrics in the marginal zones of the Habis granite, where the granite is in contact with the marbles. The sum of these observations suggest, that the basal parts of the Karibib Formation represent a low-angle shear zone, probably accommodating top-to-the-NW thrusting, although shear sense indicators are rare.

In the central and northern portion of the Etusis domain, predominantly marbles of the Karibib Formation are developed. These are in direct contact with basement gneisses and rocks of the Ghaub Formation, in the northern and central parts of the domain, or rocks of the Mon Repos diorite suite in the N of the domain. The contact between the Ghaub and/or Karibib Formations and AMC gneisses in these N parts of the Etusis domain often contains slivers of diorite. The isolated diorite pods and slivers thicken and amalgamate to form a more continuous diorite sheet of up to 30m thickness sandwiched between recrystallized marbles of the Karibib Formation and the AMC at the NW-most part of this mapping domain. This field evidence again suggests that this contact (AMC/DSG) is tectonic in nature. Diorites preserved between the AMC and DSG suggest that the diorites intruded as very thin sheets into and along this shear zone localized in the basal parts of the Karibib Formation. Indeed, geophysical data show that the two, in plan view, round- to oval- shaped plutons of the Mon Repos diorite suite represent shallow SE-dipping sheets (Ameglio, 2000). The erosional klippe at the centre of the Etusis mapping domain is all that remains of diorites SE of Mon Repos diorite. A crystallization age of between 564 ± 5 and 558 ± 5 Ma for the Mon Repos diorite (Jacob et al., 2000) implies that intrusion of diorites and shearing along the shallow thrust occurred at a relatively early point in the deformational history. The intrusion of the post-tectonic Rote Kuppe granite NE of Mon Repos suggests that deformation ceased by ca. 540 Ma (Jacob et al., 2000). Moderate to steep NE trending S_2 fabrics in the DSG and Mon Repos diorite (solid state) indicate a D2 tectonic overprint.

In summary, the Etusis domain is characterized by thin-skinned tectonics. Originally unconformable basement-cover contacts are largely preserved and the basement has not been affected by pervasive strains typical of the DSG in this part of the SCZ. Shearing seems to be localized close to the basement-cover contact, but is controlled by the presence of the highly ductile, thick marble sequence of the Karibib Formation and, particularly, the lower parts of the marble succession. Pan-African intrusions include the early (D1) Mon Repos granodiorites and the Habis granite, both of which seem to exploit the high-strain zone close to the basement-cover contact. Notably, despite

the large areal extent of the granitoids, the exposure of both hanging and footwall contacts of e.g. the Mon Repos diorites indicate their thin, sheet-like nature. A condensed sequence of the central stratigraphy of the DSG seems to have been preserved in an original topographic basement low, probably provided by normal faulting, and was truncated by the shear zone developed in the overlying Karibib Formation. The low-angle shearing demonstrated here for the Etusis domain probably continues in well-developed top-to-the-NW thrusting and folding to the NW in the Karibib region (Kisters et al., 2004).

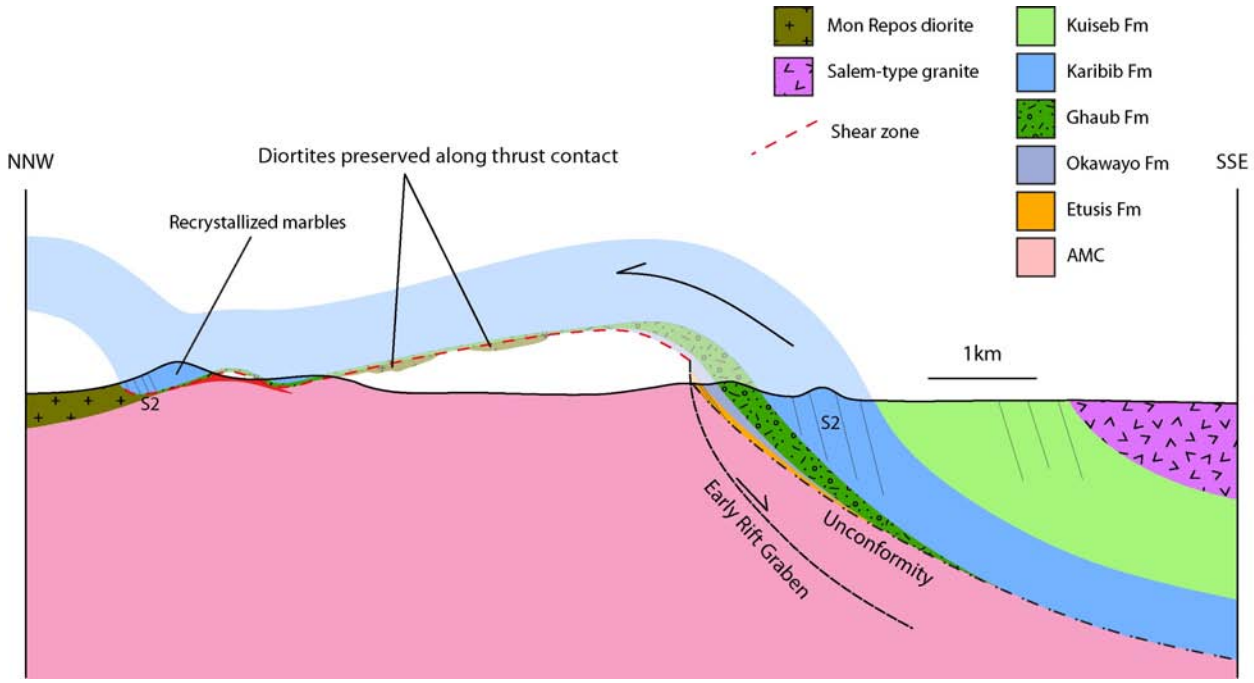

Fig 5.4: A cross-section of the Etusis domain suggests thin-skinned tectonics, with strain being localised at the base of the Karibib Formation. A well developed sequence of coarse clastic metasedimentary rocks of the DSG indicates the presence of a earlier rift graben in the rocks of the AMC, that unconformably underlie the DSG. Recrystallized marble and the presence of diorite slithers give just some indication of the shear zone developed between the Karibib Formation and the underlying rocks of the AMC and Habis granite (developed further E). Continuation of deformation led to a somewhat steeper (than S_1) S_2 foliation bieng developed in both the DSG and the Mon Repos diorite in the NNW of this section.

6. Conclusions

The transect through mid-crustally deformed rocks of the south Central Zone between Otjimbingwe in the S and Karibib in the N shows many features that are consistent with deformation across a collisional forearc region. Systematic variations in strain, strain intensity and structural styles correspond to the position of the forearc relative to the leading edge of the Congo Craton. The following systematic changes can be recognised:

1. Upright folding and pervasive transposition of fabrics (D2) in the OLZ record bulk NW-SE subhorizontal shortening and associated steep extrusion of the high-metamorphic-grade rocks. Non-coaxial fabrics are conspicuous by their absence. In contrast to previous studies, the predominance of co-axial shortening strains is here interpreted to record the high-angle collision between the Congo and Kalahari Cratons. Deformation is recorded until at least ca. 520 Ma, the timing of the synkinematic Otjimbingwe syenite that records pervasive D2 strains. D2 strain intensities decrease markedly over a distance of a few kilometres to the NW. This, together with the presence of rocks of the basal Nosib Group, indicate the existence and position of the underlying basement of the Congo Craton in this area. Pervasive transposition, steep extrusion of the DSG and the sharp metamorphic gradient across this zone indicate that the OLZ (sensu stricto) is located off the margin of the underlying craton.

2. The NW-verging, kilometre-scale, basement-cored, refolded (F2) F1 nappe of the Audawib fold complex is interpreted to record thick-skinned thrusting along an early (syn-D1, early-D2) retroshear. The closure of the fold to the NW and sheath-fold like geometry suggested by the hinge-line curvature of the F1 hinges point to the NW-vergent nappe transport onto the retroarc region. The refoliation and co-axial deformation of basement gneisses and the overlying DSG during D2 imply a relatively weakened basement rheology close to the leading edge of the Congo Craton.

3. The areally extensive Salem granites associated with the Audawib fold complex form large, shallowly-dipping sheets underlying the nappe and possibly detaching the nappe from its base. Co-axial fabrics within the granites and the folded DSG suggest a syn- to late-kinematic (D2) emplacement of the granites.

4. Thin-skinned tectonics dominate in the northernmost section of the transect in the Etusis domain. It is particularly the highly-ductile marbles of the, in this part, very thick Karibib Formation that seem to localize strain and shearing. Large, in plan view, oval- shaped

plutons of e.g. the Goas Dioritic Suite or the Habis granite in the Etusis domain can be shown to be thin (< 40-50 m) sheet-like intrusions that intrude below the high-strain basal parts of the marbles and above the basement. Strain localization in the marble units and the widespread preservation of unconformable basement-cover contacts indicate that the basement has not been involved in Damara deformation in this part of the belt. This suggests a significantly more rigid rheology of the basement in the N compared to the S (e.g. the Audawib domain). D1 and D2 strains are recorded between ca. 550 Ma, the emplacement age of the Mon Repos diorites, and ca. 540 Ma, the crystallization age of the post-tectonic Rote Kuppe Granite to the immediate N of the transect (Jacob et al., 2000).

5. The seemingly diachronous timing of tectonism (520 Ma in S, 540 Ma in N) is interpreted to reflect the different basement rheology at the leading edge of the Congo Craton compared to its interior, some 40 km to the NW. Thermally weakened basement in the S allowed the deformation to continue and residual strain to be accommodated by the weaker basement. The multitude of granite dykes and sills related to the large Donkerhuk batholith that intruded at ca. 525 Ma in this area are likely to have contributed to this thermal and mechanical weakening. In contrast, colder and, thus, stronger basement rocks in the N may have effectively locked/stopped the D2 deformation at ca. 540 Ma.

6. Strain localization into the abundant granitoid phases along this transect that has influenced the regional deformation pattern is observed in a number of places. In and around the syn-D2 Palmental diorite and Otjimbingwe syenite, pervasive prolate fabric development implies that the steep extrusion of the rocks during subhorizontal shortening in the OLZ was localized around the synkinematic melts. Similarly, the sheet-like Mon-Repos diorites and the Habis granite in the northern Etusis domain intrude into the sheared basement-cover contact. Fabric development in both plutonic rock suites suggest that the plutons have contributed to the thin-skinned nature of deformation, detaching cover rocks from basement. In contrast, the rather open, high-wavelength, low-amplitude fold shapes around the mainly sheet-like granitoids of, in particular, the Salem-type granites suggest that when crystallized, the competent granite sheets hindered fold amplification. This would indicate a role for the sheet-like, subhorizontal granites as a type of “strength beams” in the deforming crustal column.

Acknowledgements

- Thanks go to Professor Alex Kisters for his continuous support throughout this project, for inspiring me and keeping me motivated all the way to the end. It has been a great honour to work with such a brilliant geologist, without whose knowledge, wisdom and enthusiasm I would have been utterly and completely lost.

- Many thanks to the people at the Navachab gold mine, for the financial and logistical support that was needed to keep this project afloat.

  Specifically Frik Badenhorst who made this project feasable by securing the funds and a verhicle for such a lengthy undertaking.

  Shaun Kitt for showing me the ropes and for making me feel truly at home in Karibib.

  Graham Bell for helping to get through all the annoying paperwork.

  Nick Steven who always showed a keen interest in the project and a willingness to share his expertise.

- Thanks to Professor Gary Stevens and the NRF without whose support the study would have been impossible.

- Charlie Hoffmann and Ewereth Muvango at the Namibian Geological Survey for helping us organise maps, aerial photos and access.

- To the fellow students in the M.Sc lab at Stellenbosch, for keeping me entertained and often enough out of work.

- To my family and friends, especially those in Huis Div. Cheers for your support and for providing some very necessary distractions throughout the year.

- Thanks also to Martin Vietze, for the beers, the Kegel and for also getting the university bakkie stuck in the sand...often. CHEERS, co-worker!

References:

Allsopp, H., Barton, E.S., Kröner, A., Welke, H.J. Burger, A.J. (1983) Emplacement versus inherited isotopic age patterns: A Rb-Sr and U-Pb study of Salem-type granites in the central Damara belt. In: Miller, R.McG. (Ed), Evolution of the Damara Orogen of South West Africa. *Special Publication of the Geological Society of South Africa* 11, 281-287.

Ameglio, L., Page, P., Jacob, R.E. (2000) 3D-geometry of the Mon Repos granodiorite (Goas dioritic suite, Damara Belt, Namibia) inferred from gravity data. *Journal of African Earth Sciences*, 31, 2.

Anderson, H.F. Nash, C.R. (1997) Integrated lithostructural mapping of the Rössing area, Namibia, using high resolution aeromagnetic, radiometric, Landsat data and aerial photographs. *Exploration geophysics* 28, 185-191.

Badenhorst, F.P. (1987) Lithostratigraphy of the Damara Sequence in the Omaruru Area of the northern Central Zone of the Damaran Orogen and a proposed correlation across the Omaruru Lineament. *Communications of the Geological Survey of South West Africa* 3, 3-8.

Badenhorst, F.P. (1992). The Lithostratigraphy of area 2115B and D in the Central Zone of the Damara Orogen in Namibia: with emphasis on facies changes and correlation. Unpublished MSc thesis, University of Port Elizabeth, 124p.

Barnes, J.F.H., Downing, K.N. (1979) Origin of domes in the central Damara belt, Namibia. *Revue de Geologie Dynamique et de Geographie Physique* 21, 383-386.

Barnes, S.J., Sawyer, E.W. (1980) An alternative model for continental convergence. *Precambrian Research* 13, 297-336.

Blaine, J.L. (1977) Tectonic evolution of the Waldua ridge and the Okahandja lineament in part of the Central Damara orogen, west Okahandja South West Africa. *Bulletin of the Precambrian research unit 21*, 99p. University of Capetown, Cape Town, South Africa.

Blaxland, A., Gohn, E., Haack, U., Hoffer, E. (1979) Rb/Sr ages of late-tectonic granites in the Damara orogen, South West Africa/Namibia. *Neues Jahrbuch für Mineralogie, Monatshefte* 11, 498.

Bowden, P., Tack, L., Williams, I.S., Deblond, A. (1999) Transpressional and transtensional magmatism in the Central Damaran (Pan-African) orogenic belt, Western Namibia. Abstracts, GSA 11: Earth Resources for Africa. *Journal of African Earth Sciences* 28, 13.

Brandt, R. (1985) Preliminary report on the stratigraphy of the Damara Sequence and the geology and geochemistry of Damaran granites in an area between Walvis Bay and Karibib. *Communications of the Geological Survey of Namibia* 1, 31-43.

Brandt, R. (1987) A revised stratigraphy for the Abbabis Complex in the Abbabis inlier Namibia. *South African Journal of Geology* 90, 314-323.

Brown, M. (2007)Crustal melting and melt extraction, ascent and emplacement in orogens: mechanisms and consequences. *Journal of the Geological Society, London* 164, 709–730.

Brown, M., Solar, G.S. (1999) The mechanism of ascent and emplacement of granite magma during transpression: a syntectonic granite paradigm. *Tectonophysics* 312, 1–33.

Corner, B. (2000) Crustal framework of Namibia derived from magnetic and gravity data. *Communications of the Geological Survey of Namibia* 12, 13-20.

Corner, B. (1983) An interpretation of the aeromagnetic data covering the western portion of the Damara Orogen in South West Africa/Namibia. In: Miller, R. McG. (Ed.), Evolution of the Damara Orogen of South West Africa/Namibia. *Special Publications of the Geological Society of South Africa* 11, 339–354.

Coward, M.P. (1983) The tectonic history of the Damaran Belt. In: Miller, R.McG. (Ed), Evolution of the Damara Orogen of South West Africa. *Special Publication of the Geological Society of South Africa* 11, 409-421.

Davidson, C., Schmid, S.M., Hollister, L.S. (1994) Role of melt during deformation in the deep crust. *Terra Nova* 6, 133-142.

De Kock, G.S. (1989) A geotectonic study of the Damara orogen in an area southeast of Karibib, South-West Africa. Ph.D.-thesis (unpublished), University of the Orange Free State, Bloemfontein, South Africa. 438p.

De Kock, G.S., (1992) Forearc basin evolution of the Panafrican Damara belt, central Namibia: The Hureb Formation of the Khomas zone. *Precambrain research* 57, 169-194.

De Kock, G.S. (2001) A reappraisal of the Namibian Damara stratigraphy in part of the Southern Swakop Terrane and its implications to basin evolution. *South African Journal of Geology* 104, 115-136.

De Kock, G.S., Walraven, F. (1995) New Pb–Pb zircon ages for the post-tectonic Donkerhuk granite in the Damara Orogen. *Centennial Geocongress, Extended abstracts.* Geological society of South Africa, Rand Afrikaans University, Johannesburg, South Africa. 1109-1112.

De Kock, G.S., Eglington, B., Armstrong, R.A., Harmer, R.E., Walraven, F. (2000) U-Pb and Pb-Pb ages on the Naaupoort rhyolite, Kawakeup leptite and Okangava Diorite: implication for the onset of rifting and orogenesis in the Damara belt Namibia. *Communications of the Geological Survey of Namibia* 12, 81-88.

Downing, K.N. (1983) The stratigraphy and palaeoenvironment of the Damara sequence in the Okahandja lineament area. In: Miller, R.McG. (Ed), Evolution of the Damara Orogen of South West Africa. *Special Publication of the Geological Society of South Africa* 11, 37-64.

Downing, K.N., Coward, M.P. (1981) The Okahandja Linearment and its significance for Damaran Tectonics in South West Africa. *Geologische Rundschau* 70, 972-1000.

Escher, A., Beaumont, C. (1997) Formation, burial and exhumation of basement nappes at a crustal scale: a geometric model based on the Western Swiss-Italian Alps. *Journal of Structural geology* 19, 955-975.

Fisher, D.M., Byrne, T. (1992) Strain variations in an ancient accretionary complex: implications for forearc evolution. *Tectonics* 11, 330–347.

Froitzheim, N. (1992) Formation of recumbent folds during synorogenic crustal extension (Austroalpine nappes, Switzerland) *Geology* 20, 923-926.

Fossen, H., Tikoff, B. (1993). The deformation matrix for simultaneous simple shearing, pure shearing, and volume change, and its application to transpression/transtension tectonics. *Journal of Structural Geology* 15, 413-422.

Gevers, T.W. (1931) Fundamental Complex of Western Damaraland, South West Africa- Unpublished. Phd. thesis, University of Cape Town, 163p.

Gevers, T.W. (1963) Geology along the north-western margin of the Khomas Highlands between Otjimbingwe-Karabib and Okahandja, South West Africa. *Transactions Geological Society South Africa* 66, 199-251.

Goscombe, B., Hand, M., Gray, D. (2003) Structure of the Kaoko belt Namibia: progressive evolution of a classic transpressional orogen. *Journal of Structural Geology* 25, 1049-1081.

Gray, D.R., Foster, D.A., Goscombe, B.D., Passchier, C.W., Trouw, R.A.J. (2006) 40Ar/39Ar thermochronology of the Pan-African Damara Orogen, Namibia, with implications for tectonothermal and geodynamic evolution. *Precambrian Research* 150, 49–72.

Gray, D.R., Foster, D.A., Meert, J.G., Goscombe, B.D., Armstrong, R., Trouw, R.A.J., Passchier, C.W. (2008) A Damara orogen perspective on the assembly of southwestern Gondwana. *Geological society of London, Special publications* 294, 257-278.

Haack, U. and Martin, H. (1983) Geochronology of the Damara orogen – a review. *In:* H. Martin and F, Eder (Editors*), Intracontinenial fold belts*. *Springer. Berlin, Germany.* 839-845.

Haack, U. Gohn, E. (1988) Rb-Sr data of some pegmatites in the Damara orogen, Namibia. *Communications of the geological Survey of South West Africa/Namibia* 4, 13-17.

Haack, U., Hoefs, J., Gohn, E. (1982) Constraints on the origin of Damaran granites by Rb/Sr and $\delta^{18}O$ data. *Contributions to Mineralogy and Petrology* 79, 279–289.

Haack, U., Gohn, E., Hartmann, O. (1983) Radiogenic heat generation in Damaran rocks. In: Miller, R.McG. (Ed), Evolution of the Damara Orogen of South West Africa. *Special Publication of the Geological Society of South Africa* 11**,** 225-232.

Haack, U., Gohn, E., Brand, R., Feldmann, H. (1988) Rb-Sr data on the Otjimbingwe Alkali complex in the Damara Orogen, Namibia. *Chemie Erde* 48, 131-140.

Hawkesworth, C.J., Marlow, A.G. (1983) Isotope Evolution of the Damara orogenic belt. In: Miller, R.McG. (Ed), Evolution of the Damara Orogen of South West Africa. *Special Publication of the Geological Society of South Africa* 11, 397-408.

Hawkesworth, C.J., Geldhill, A.R., Roddick. J.C., Miller, R.McG., Kröner, A. (1983) Rb-Sr and K-Ar studies bearing on models for the thermal evolution of the Damara belt, Namibia. In: Miller, R.McG. (Ed), Evolution of the Damara Orogen of South West Africa. *Special Publication of the Geological Society of South Africa* 11**,** 323-338.

Henry, G. (1992) The sedimentary evolution of the Damara Sequence in the lower Khan River valley, Namibia. PhD thesis, University of the Witwatersrand, Johannesburg, South Africa.

Henry, G., Clendenin, C.W., Stanistreet, I.G., Maiden, K.J. (1990) A multiple detachment model for the early rifting stage of the Late Proterozoic Damara orogen in Namibia. *Geology* 18, 67-71.

Hoffer, E. (1977) Mineralparageneses und Reaktionen in den Al-reichen Metapeliten des zentralen Damara-Orogen. *Ber. SondForschBers 48, Univ Göttingen(unpubl.), 149-153.*

Hoffmann, C., (1976) Granites and migmatites of the Damara belt, South West Africa. Petrography and melting experiments*. International journal of Earth sciences* 65, p939-966.

Hoffmann, K-H. (1983) Lithostratigraphy and facies of the Swakop Group of the southern Damara belt, SWA/ Namibia. In: Miller, R.McG. (Ed), Evolution of the Damara Orogen of South West Africa. *Special Publication of the Geological Society of South Africa* 11, 43-63.

Hoffmann, K-H., (1990) Sedimentary depsoitional history of the Damara belt related to continental breakup, passive to active margin transition and foreland basin development*. Abstracts. Geocongress 90', Geological society of South Africa*, Cape Town, South Africa. 250-253.

Hoffmann, K.-H., Condon, D.J., Bowring, S.A., Crowley, J.L. (2004) U-Pb zircon date from the Neoproterozoic Ghaub Formation, Namibia: Constraints on Marinoan glaciation. *Geology* 32, 817-820.

Hoffman, P.F., Hawkins, D.P., Isachsen, C.E., Bowring, S.A. (1996). Precise U-Pb zircon ages for early Damaran magmatism in the Summas Mountains and Welwitschia inlier, northern Damara belt, Namibia. *Communications of the Geological Survey of Namibia* 11, 47-52.

Hoffman, P.F., Halverson, G.P., Schrag, D.P. (1998) A Neoproterozoic Snowball Earth**.** *Science* 281, 1342–1346.

Jacob, R.E. (1974) Geology and metamorphic petrology of part of the Damara Orogen along the lower Swakop River, South West Africa. *Bulletin op the Precambrian Research Unit*, Univ. Cape Town 17, 184p.

Jacob, R.E., Snowden, P.A., Bunting, F.J.L. (1983) Geology and structural development of the Tumas Basement Dome and its cover rocks. In: Miller, R.McG. (Ed), Evolution of the Damara Orogen of South West Africa. *Special Publication of the Geological Society of South Africa* 11, 157-172.

Jacob, R.E., Kröner, A., Burger, A.J. (1978) Areal extent and first U-Pb age of the Pre-Damaran Abbabis complex in the central Damara belt of South West Africa (Namibia). *Geologische Rundschau* 67, 1432-1149.

Jacob, R.E., Moore, J.M., Armstrong, R.A. (2000) Zircon and titanite age determinations from igneous rocks in the Karibib District, Namibia: implications for Navachab vein-style gold mineralization. *Communications of the Geological Survey of Namibia* 12, 157-166.

Johnson, S.D. (2005) Structural geology of the Usakos dome, Damara Belt, central Namibia. Unpublished MSc thesis, University of Stellenbosch, 159p.

Johnson, S.D., Poujol, M., Kisters, A.F.M. (2006) Constraining the timing and migration of collisional tectonics in the Damara Belt, Namibia: U-Pb zircon ages for the syntectonic Salem-type Stinkbank granite. *South African Journal of Geology* 109 427-440.

Jung, S., (2000) High-temperature, mid-pressure clockwise P–T paths and melting in the development of regional migmatites: the role of crustal thickening and repeated plutonism. *Geological Journal* 35,345-359.

Jung, S., Hellebrand, E. (1998) Textural, geochronological and chemical constraints from polygenetic titanite and monogenetic apatite from a mid-crustal shear zone: An integrated EPMA, SIMS, and TIMS study. *Chemical Geology*, 241, 88–107.

Jung, S., Mezger, K. (2003) Petrology of basement-dominated terranes: I Regional metamorphic T-t path from U-Pb monazite and Sm-Nd garnet geochronology (Central Damara orogen, Namibia). *Chemical Geology* 198, 223-247.

Jung, S., Mezger, K., Hoernes, S. (1998) Geochemical and isotopic studies of syenites from the Proterozoic Damara belt (Namibia): implications for the origin of syenites. *Mineralogical Magazine* 62A (Part II), 729–730.

Jung, S., Hoernes, S., Mezger, K. (2000) Geochronology and petrogenesis of Pan-African, "syn-tectonlc S-type and post-tectonic A-type granite; (Namibia): products of melting of crustal sources, factional crystallization and wall-rock entrainment. *Lithos* 50, 259-287.

Jung, S., Hoernes, S., Mezger, K. (2001) Trace element and isotopic (Sr, Nd, Pb, O) arguments for a mid-crustal origin of Pan-African garnet-bearing S-type granites from the Damara orogen (Namibia). *Precambrian Research* 110, 325-355.

Jung, S., Hoernes, S., Mezger, K. (2002) Synorogenic melting of mafic lower crust: constraints from geochronology, petrology and Sr, Nd, Pb and O isotope geochemistry of quartz diorites (Damara orogen, Namibia). *Contributions to Mineral Petrology* 143, 551-566.

Jung, S., Mezger, K., Hoernes, S. (2004) Shear zone-related syenites in the Damara belt (Namibia): the role of crustal contamination and source composition. *Contributions to Mineral Petrology* 148, 104–121.

Jung, S., Hoernes, S., Masberg, P., Hoffer, E. (1999) The petrogenesis of some migmatites and granites (Central Damara orogen, Namibia): Evidence for disequilibrium melting, Wall rock contamination and crystal fractionation. *Journal of petrology* 40, 1241-1269.

Kasch, K.W. (1983a) Continental Collision, Suture Progradation and Thermal Relaxation: A Plate Tectonic Model for the Damara Orogen in Central Namibia. In: Miller, R.McG. (Ed.), Evolution of the Damara Orogen of South West Africa. *Geological Society of South Africa, Special Publication* 11, 423-429.

Kasch, K.W. (1983b) Regional P-T variations in the Damara orogen with particular reference to early high pressure metamorphism along the Southern margin. In: Miller, R.McG. (Ed.), Evolution of the Damara Orogen of South West Africa. *Geological Society of South Africa, Special Publication* 11, 243-253.

Kisters, A.F.M., Jordaan, L.S., Neumaier, K. (2004) Thrust-related dome structures in the Karibib district and the origin of orthogonal fabric domains in the south Central Zone of the Pan-African Damara belt, Namibia. *Precambrian Research* 133, 283-303.

Kisters, A.F.M., Hoffman, K.H., Ward, R.A. (2007) Pan African granites of the Damara belt, Namibia. *Field guide for the 6th International Hutton symposium on the origin of granites and related rocks*. 51p.

Kitt, S.L. (2008) Structural controls of auriferous quartz veins in the Karibib area, Southern Central Zone of the Pan-African Damara belt, Namibia. Unpublished MSc thesis, University of Stellenbosch, 108p.

Kley, J. (1996) Transition from basement-involved to thin-skinned thrusting in the Cordillera Oriental of southern Bolivia. *Tectonics* 15 ,763–775.

Kley, J., Monaldi, C.R. (1998) Tectonic shortening and crustal thickness in the Central Andes: How good is the correlation. *Geology* 26, 723-726.

Kröner, A. (1982) Rb-Sr geochronology and tectonic evolution of the Pan-African Damara belt of Namibia, southwestern Africa. *American journal of Science* 282, 1471-1507.

Kröner, A. (1984) Dome structures and basement reactivation in the Pan-African Damara belt of Namibia, South West Africa. In: Kröner, A., Greiling, R. (Eds.), Precambrian Tectonics Illustrated. Nagele u Obermiller, Stuttgart, Germany, 191-206.

Kröner, A., Retief, E.A., Compston, W., Jacob, R.E. Burger, A.J. (1991) Single-grain and conventional zircon dating of remobilized basement gneisses in the central Damara Belt of Namibia. *South African Journal of Geology* 94, 279-387.

Kukla, P.A., Opitz, C., Stanistreet, I.G., Charlesworth, E.G. (1988) New aspects of the sedimentology and structure of the Kuiseb Formation in the western Khomas Trough, Damara Orogen, SWA/Namibia. *Communications of the geological survey of Namibia* 4, 33-42.

Kukla, P.A., Stanistreet, I.G. (1991) Record of the Damaran Khomas Hochland accretionary prism in central Namibia: refutation of an ensialic origin of the late Proterozoic orogenic belt. Geology 19, 473–476.

Kukla, P.A. (1992) Tectonics and sedimentation of a late Proterozoic Damaran convergent continental margin, Khomas Hochland, central Namibia. *Geological survey of Namibia Memoir* 12, 95p.

Kukla, C. (1993) Sr-isotope heterogeneities in amphibolites facies, banded metasediments- a case study from the Late Protorezoic Kuiseb Formation of the southern Damara Orogen, Central Namibia. *Geological survey of Namibia Memoir* 15, 139p.

Kukla, P.A., Kukla, C., Stanistreet, I.G., Okrusch, M. (1990) Unusual Preservation of Sedimentary Structures in Sillimanite-Bearing Metaturbidites of the Damara Orogen. *The Journal of Geology* 98, 91-99.

Kusky, T.M., Bradley, D.C., Haeussler, P.J., Karl, S. (1997) Controls on accretion of flysch and mélange belts at convergent margins: evidence from the Chugach Bay thrust and Iceworm mélange, Chugach accretionary wedge, Alaska. *Tectonics* 16, 855–878.

Lehtonen, M.I., Manninen, T.E.T., Schreiber, U.M. (1995) Geological map sheet 2214 – Walvis Bay, 1:250 000. Geological survey of Namibia.

Marlow, A.G., (1983) Geology and geochronology of mineralised and anomalous granites and alaskites, Namibia. In: Miller, R.McG. (Ed.), Evolution of the Damara Orogen of South West Africa. *Geological Society of South Africa, Special Publication* 11, 289-298.

Martin, H., (1965) The Precambrian geology of South West Africa and Namaqualand. *Bulletin of the Precambrian research unit*, University of Cape Town, 4, 1-159.

Martin, H., Porada, H. (1977) The intracratonic branch of the Damara orogen in South West Africa. I. Discussions of geodynamic models. *Precambrian Research* 5, 311-338.

Masberg, H.P. (2000) Garnet growth in medium pressure granulite-facies metapelites from the central Damara Orogen: igneous versus metamorphic history. *Communications of the Geological Survey of Namibia* 12, 115-124.

Merle, O., Gapais, D. (1997) Strains within thrust-wrench zones. *Journal of Structural Geology* 19, 1011-1014.

Mcdermott, F. (1986) Granite petrogenesis and crustal evolution studies in the Damara Pan-African Orogenic Belt, Namibia. Unpubl. Ph.D Thesis, Open University, Milton Keynes, England. 303p.

Mcdermott, F., Harris, N.B.W., Hawkesworth, C.J. (1996) Geochemical constraints on crustal anatexis: a case study for the Pan-African Damara granatoids of Namibia. *Contributions to Mineral Petrology* 123, 406-423.

Miller, R.McG. Hoffmann, K-H. (1981) Guide to the excursion through the Damara orogen. Geological Society of South Africa, Geocongress '81, 115p.

Miller, R.McG. (1983) The Pan-African Damara Orogen of South West Africa/Namibia. In: Miller, R.McG. (Ed.), Evolution of the Damara Orogen of South West Africa. *Geological Society of South Africa, Special Publication* 11, 431-515.

Miller, R.McG. (1979) The Okahandja Lineament a fundamental tectonic boundary in the Damara orogen of South West Africa/Namibia. *Transations of the Geological Society of South Africa* 82, 349-361.

Miller, R.McG. (2008) The Geology of Namibia. Windhoek, Namibia: Ministry of Mines and Energy, Geological survey.

Nash, C.R. (1971) Metamorphic petrology of the SJ area, Swakopmund district, South West Africa. *Bulletin of the Precambrian Research Unit.* University of Cape Town, 159p.

Nex, P.A.M., Oliver, G.J.H. Kinnaird, J. (2001) Spinel-bearing assemblages and P-T-t evolution of the Central Zone of the Damara Orogen, Namibia. *Journal of African Earth Sciences* 32, 471-489.

Oliver, G.J.H., (1994) Mid-crustal detachments zones in the central zone of the Damara orogen. Namibia. *Journal of African Earth Sciences* 19, 331-344.

Pfiffner, O.A., Ellis, S., Beaumont, C. (2000) Collision tectonics in the swiss alps: Insight from geodynamic modelling. *Tectonics* 19, 1065-1094.

Poli, L.C., Oliver, G.J.H. (2001) Constrictional deformation in the Central Zone of the Damara Orogen Namibia. *Journal of African Earth Sciences* 33, 303–312.

Porada, H. (1989) Pan-African rifting and orogenesis in southern to equatorial Africa and eastern Brazil, *Precambrian Research* 44, 103-138.

Porada, H., Wittig, R. (1983) Turbidites and their significance for the geosynclinals evolution of the Damara orogen, South West Africa/Namibia. In: Miller, R.McG. (Ed.), Evolution of the Damara Orogen of South West Africa. *Geological Society of South Africa, Special Publication* 11, 21-36.

Roering, C. (1966) Aspects of the genesis and crystallization sequence of the Karibib pegmatites, South West Africa. *Economic geology* 61, 1064-1089.

Prave, A.R. (1996) Tale of three cratons: Tectonostratigraphic anatomy of the Damara orogen in northwestern Namibia and the assembly of Gondwana. *Geology* 24, 1115-1118.

Puhan, D., (1983) Temperature and pressure of metamorphism in the central Damara orogen. In: Miller, R. McG. (Ed.), Evolution of the Damara Orogen of South West Africa. *Geological Society of South Africa, Special Publication* 11, 219-224.

Saint de Blanquat, M., Tikoff, B., Teyssier, C., Vigneresse, J.-L. (1998) Transpressional kinematics and magmatic arcs. In: Holdsworth, R.E., Strachan, R.A., Dewey, J.F. (Eds.), Continental Transpression and Transtension Tectonics. *Geological Society of London, Special publications* 135, 327–340.

Sample, J.C., Moore, J.C. (1987) Structural style and kinematics of an underplated slate belt, Kodiak and adjacent islands, Alaska. *Bulletin of the Geological Society of America* 99**, 7-20.**

Sawyer, E.W. (1981) Damaran structural and metamorphic geology of an area south-east of Walvis Bay, SWA/Namibia. *Memoir of the Geological Survey of South West Africa/Namibia* 7, 94p.

Sawyer, E.W. (1983) Structures in the strain Aureole of the Donkerhuk granite, Gross Barmen area, South West Africa/Namibia. In: Miller, R.McG. (Ed.), Evolution of the Damara Orogen of South West Africa, *Geological Society of South Africa, Special Publication* 11, 209-217.

Schmid, S. M., Fügenschuh, B., Kissling, E, Schuster, R. (2004) Tectonic Map and Overall Architecture of the Alpine Orogen. *Eclogae geologicae Helvetiae* v. 97, Basel: Birkhäuser Verlag, 93–117.

Smith, D.A.M. (1965) The geology of an area around the Khan and Swakop Rivers in South West Africa. *Memoir of the Geological Society of South Africa, South West Africa Series* 3, 113p.

Smith, D.A.M. (1966) Geological Map of area 2215B-Usakos, Geological Survey, Windhoek, South West Africa.

Stanistreet, I.G., Kukla, P.A., Henry, G. (1991). Sedimentary basinal responses to a Late Precambrian Wilson Cycle: The Damara Orogen and Nama Foreland, Namibia. *Journal of African Earth Science* 13, 141-156.

Steven, N.M. (1993) A study of Epigenetic Mineralization in the Central Zone of the Damara Orogen, Namibia, with special reference to gold, tungsten, tin and rare elements. *Memoirs of the Geological Survey of Namibia* 16, 166p.

Tack, L., Bowden, P. (1999) Post-collisional granite magmatism in the central Damara (Pan-African) Orogenic belt, western Namibia. *Journal of African Earth Science* 28, 653–674.

Tikoff B., Peterson K. (1998) Physical Experiments of Transpression Folding. *Journal of Structural Geology* 20, 661-672.

Trompette, R. (2000) Gondwana evolution: its assembly at around 600Ma. *Earth and planetary sciences* 330, 305-315.

Ward, R.A., Stevens, G., Kisters, A.F.M. (2008) Fluid and deformation induced partial melting and melt volumes in low-temperature granulite-facies metasediments, Damara Belt, Namibia. *Lithos* 105, 253-271 .